NOTE TO USERS

DISSERTATION

STRUCTURAL AND FUNCTIONAL STUDY OF YEAST NUCLEOSOME ASSEMBLY PROTEIN 1

Submitted by

Young jun Park

Department of Biochemistry and Molecular Biology

In partial fulfillment of the requirements

for the Degree of Doctor of Philosophy

Colorado State University

Fort Collins, CO

Spring 2005

COLORADO STATE UNIVERSITY

March 7, 2004

WE HEREBY RECOMMEND THAT THE DISSERTATION PREPARED UNDER OUR SUPERVISION BY YOUNG JUN PARK ENTITLED "STRUCTURAL AND FUNCTIONAL STUDY OF YEAST NUCLEOSOME ASSEMBLY PROTEIN 1" BE ACCEPTED AS FULFILLING IN PART THE REQUIREMENT FOR THE DEGREE OF DOCTOR OF PHILOSOPHY.

Committee on Graduate Work

Olve Peersen

Paul Laybourn

Oren Andersen

Robert W. Woody

Kanlin Lujen

Advisor

Marvin Paule

Department Head

ABSTRACT OF DISSERTATION

STRUCTURAL AND FUNCTIONAL STUDY OF YEAST NUCLEOSOME ASSEMBLY PROTEIN 1

At one time nucleosome was considered a very static structure that packs DNA into the nucleus. However, the data in the last 15 years suggest that nucleosomes are highly dynamic macromolecular complexes that are assembled and disassembled by various factors. One important way in which this dynamic process can be modulated is by the replacement of major histones with their variants, thereby affecting nucleosome structure and function. One of the essential histone H2A variants is H2A.Z that is conserved from yeast to humans. The early observation suggested that H2A.Z is associated with the transcriptionally active genes. However, the mechanism of histone variant exchange and the effect in nucleosome is not clearly understood.

We measured the stability of major H2A or histone variant H2A.Z containing nucleosome using Fluorescence resonance energy transfer (FRET). We found that variant H2A.Z containing nucleosomes are more stabile than canonical H2A nucleosomes. Another observation was that the nucleosome assembly protein 1 (NAP-1) from yeast facilitates the exchange of H2A-H2B or histone variant H2A.Z-H2B dimers into assembled nucleosomes. We also showed that transient

removal of H2A-H2B dimers facilitates nucleosome sliding along the DNA to a thermodynamically favorable position. Histone exchange as well as nucleosome sliding is independent of ATP and rely on the presence of the C-terminal acidic domain of yeast NAP-1. Our results suggest a novel role for NAP-1 in mediating chromatin fluidity by incorporating histone variants and assisting nucleosome sliding.

In the X-ray crystallography study, we found that the NAP-1forms a homodimer with α-helix dimerization motif and concave β-sheet. In the NAP-1 structure, loop domains wrapping around adjacent α-helix stabilize the dimer structure. This helix loop - helix loop (HL-HL) dimer conformation may provide the strong stability of dimer structure. The conservation of concave β-sheet domain between yNAP-1 and other chaperones suggests that the histone chaperons share the similar structural motif, four-antiparalle strand motif. X-ray crystallography study of nucleosome assembly protein provides other insights into structure and function relationships.

Young jun Park
Department of Biochemistry and Molecular Biology
Colorado State University
Fort Collins, CO 80523
Spring 2005

ACKNOWLEDGEMENTS

I would like to thank Dr. Karolin Luger for being an outstanding advisor. She has given me lot of support and encouragement. She has been a constant driving force in my graduate research career. She has always support my idea and given valuable suggestions. I also thank my committee members; Dr. Oren Andersen, Dr. Olve Peersen, Dr. Paul Laybourn, and Dr. Robort Woody for their guidance and criticism in my research career. My committee has always been there to help me with my projects and any problems that I have had.

I would like to thank all the member of the Luger lab past and present who have been extremely supportive. In particular, I would like to mention Pam, Uma, Cindy, Raji, Cheenu, Jay, and Yunhe for their constant support and friendship.

Finally, I would like to thank my family, all of my friends, department members, all of department faculty members and Colorado state university. I am deeply grateful to everyone who has contributed to my success as a graduate student.

Table of contents

Chapter 1

Review of the Literature

1.1 Chromatin structure and function

A key problem for eukaryotic cells is the packaging of ~2m long DNA into a nucleus just around 10^{-5} m. This is achieved by organizing the DNA around core histones to form nucleosomes, which are further organized into higher order structure (reviewed in [Workman and Kingston, 1998]). Micrococcal nuclease experiments have shown that the histone octamer protects 146bp of DNA from digestion, thus defining the lowest structural entity of chromatin, the nucleosome core particle (NCP). The NCP is composed of an octamer of four folded proteins, H2A, H2B, H3 and H4, and of 146 base pairs of DNA wrapped around the octamer. DNA is wrapped in 1.65 left-handed superhelical turns around the histone octamer [Luger et al., 1997a]. The histone octamer is composed of a tetramer of two copies each of histone H3 and H4 flanked by two H2A-H2B heterodimers. The H3-H4 tetramer, which organizes the central 60 base pairs of the nucleosomal DNA, is assembled by the association of hetero dimers of H3 and H4. This histone fold formed by the dimerization of histones via a handshake motif provides sites for histone - DNA interaction [Arents and Moudrianakis, 1995]. The interaction between each H4 of the tetramer with H2B of an H2A-H2B

dimer drives the formation of an octamer. This interaction is only stable in the presence of DNA because the H4-H2B interface is considerably more hydrophobic than the H3-H3 interfaces [Luger and Richmond, 1998a]. More than 116 direct and 358 water mediated hydrogen-bond bridges generate stable DNA-histone interactions [Davey et al., 2002]. Bridging water molecules may not only provide stability to direct protein–DNA interactions, but also form many additional interactions between more distantly related elements. Water structure at the interface of the histones and DNA, without directly interacting between DNA base and histone protein provides a means of accommodating intrinsic DNA conformational variation, thus limiting the sequence dependency of nucleosome positioning while enhancing mobility [Davey et al., 2002; Luger et al., 1997a]. These properties reveal that chromatin has a dynamic structure, which stems from the structural design of the nucleosome.

Chromatin reconstituted with purified components is greatly repressed for transcription relative to DNA. This is because of the decreased accessibility of regulatory proteins and RNA polymerase initiation complex for their binding sites within nucleosomes. This raises the important issue of how chromatin structure can be modulated to generate a transcriptionally active configuration. There are three distinct categories to modulate the chromatin structure: histone-modifying enzymes which covalently acetylate, phosphorylate, ubiquitinate, or methylate histones; ATP-dependent chromatin remodeling complexes which can disrupt nucleosome structure; and histone variant incorporation (reviewed in [Workman and Kingston, 1998]). A discussion of these classes is given below.

1.2 Chromatin and Transcription regulation

Histone modifications - The N-terminal tails of the core histones and the C-terminal tail of histone H2A protrude on the outside of the nucleosome [Luger and Richmond, 1998a] , where they can potentially contact other nucleoprotein complexes, leading to activation or repression of transcription in a protomer-specific manner. The N- and C-terminal tails of histones contain several conserved residues that can be post-translationally modified; acetylation, methylation, phosphorylation, ubiquitination, and ADP-ribosylation are some of the modifications that have been closely linked to the control of many cellular activities [Grant, 2001].

Specific lysines in particular histones are functional targets for acetyltransferases and deacetylases [Rundlett et al., 1998]. Rundlett and Grunstein reported that the histone deacetylase RPD3 could be targeted to certain genes through its interaction with DNA-binding regulatory proteins and then repress gene transcription [Rundlett et al., 1998]. It is clear that acetylation or deacetylation of the core histone N-termini affects the transcriptional properties of chromatin. Acetylation facilitates access to RNA polymerase and transcription from nucleosomal arrays by inhibiting higher-order folding of the completely compacted 30 nm fiber [Garcia Ramirez et al., 1995; Tse et al., 1998]. It is also likely that acetylation leads to the destabilization of long-range structures [Woodcock and Dimitrov, 2001].

Another modification involved in transcriptional activity is methylation [Bauer

et al., 2002; Feng et al., 2002]. Many histone methyltransferase enzymes have been identified. Methylation of lysine differs from acetylation in several important aspects. It does not remove the charge of the lysine, and uniquely, the ε-amino group of a targeted lysine residue can accept one, two, or three methyl groups. Recent findings suggest that di- and trimethylation have different functional role in transcription [He and Lehming, 2003].

Histone H3 is rapidly phosphorylated on serine residues within its basic N-terminal domain, when mitogen or MAP kinases stimulate quiescent cells to proliferate [Barratt et al., 1994; Clayton and Mahadevan, 2003]. Global phosphorylation of Ser10 in H3 occurs in pericentromeric chromatin in late G_2 phase, completely spreads throughout the chromosome just before prophase of mitosis, and is rapidly lost during anaphase [Hendzel et al., 1997]. It was also proposed that the singular phosphorylation of the amino-terminus of histone H3 might be involved in facilitating protein-protein interactions to promote binding. Several other studies have suggested a change in either nucleosomal conformation or higher order structure concomitant with phosphorylation of H3 within the chromatin [Van Hooser et al., 1998; Wei et al., 1998].

Ubiquitin is a 76-amino acid peptide that is attached to the C-terminal tail of histone H2A and perhaps H2B [Jason et al., 2002; Mueller et al., 1985; Robzyk et al., 2000]. Ubiquitinated H2A can be incorporated into nucleosomes without significant changes in the organization of nucleosome cores (reviewed in [Moore et al., 2002]). Ubiquitination of histone H2A is associated with transcriptional activity [Davie and Murphy, 1990; Nacheva et al., 1989]. ADP-ribosylation of core

histones may also lead to localized unfolding of the chromatin fiber [Moore et al., 2002].

ATP-dependent Chromatin Remodeling - The transcriptional control of the genome is maintained not only by histone modification but also by chromatin remodeling proteins. The purpose of the chromatin remodeling proteins is to alter the nucleosome architecture such that genes are exposed to or hidden from the transcriptional machinery. The movement of nucleosomes along DNA is carried out by ATP-dependent chromatin remodeling complexes: SWI/SNF, NURF, ISW1, INO80, and so on. A number of the ATP-dependent family of chromatin remodeling enzymes play key roles in the regulation of transcription, development, DNA repair and cell cycle [Peterson, 2002]. Each of these enzymes are multi-subunit assemblies that hydrolyze ATP in order to change nucleosome positions, disrupt DNA–histone interactions, and perhaps destabilize chromatin folding [Becker and Horz, 2002]. An example would be the member of the SWI2/SNF2 family of ATPases. The Swi2/Snf2 subfamily can be divided into four classes, according to their domain structures, Swi2, ISWI, CHD or INO80. ISWI complexes remodel chromatin by mediating nucleosome "sliding (or tracking)" the relative movement of a histone octamer without irretrievable displacement from DNA [Whitehouse et al., 1999]. The actions of the SWI/SNF or RSC complexes allow greater disruption of nucleosome architecture to increase the accessibility of the nucleosomal DNA to DNA-binding proteins [Cote et al., 1998].

In addition to chemical modification of histone and energy-dependent

alterations of chromatin structure, there is a third form of chromatin regulation that involves the replacement of canonical histone with histone variants. The next part discusses the role of histone variants in the transcriptional regulation.

1.3 Histone variants

In proliferating cells, the DNA synthesis-coupled histone synthesis occurs during the S phase of the cell cycle in order to assemble the chromatin on the newly replicated DNA. However, a lower level of histone synthesis also takes place outside of S phase, arising from a set of histone genes called the histone variants or replacement histones that include H3.3, CENP-A, H2A.X, H2A.Z, and, macro H2A (Table1). Based on the timing of their synthesis, it is believed that these variants can be deposited onto DNA independently of DNA synthesis. Histone variants have been known for decades. Although histone modifications and nucleosome remodeling have received the most attention, an alternative way of changing chromatin structure is the incorporation of variant histones. A brief summary of core histone and histone variants is given in Table1.

It is known that the histone H3 variant H3.3 in *Drosophila* can be incorporated into the genomic loci of highly transcribed regions of Drosophila chromatin through a replication-independent mechanism [Ahmad and Henikoff, 2002]. Furthermore, Janicki and coworkers characterized the dynamic loss of HP1α

Table 1 Histone varints with potential assembly manner [Henikoff et al., 2004]
(d) Drosophila, (sc) Saccharomyces cerevisiae, (h) Homo sapiens, (x) Xenopus laevis, (m) mouse, (tt)tetrahymena thermophila, (su)sea urchin, (sp)S. pombe
RI; Replication-independent assembly, RC: Replication-coupled assembly

Histones	Species specific name	Distributed location in the cell	Assembly manner
H2A, H2B, H3, and H4	(*d,x,m,h*) H2A, H2B, H3(H3.1), and H4	Widely distributed	RC
H2A.Z	(*m*)H2A.Z, (*su*)H2A.Z/F (*d*)H2AvD, (*tt*)hv1 (*sp*)Pht1, (*sc*)Htz1	Widely distributed	RI
MacroH2A	Vertebrate-specific H2A variant	Widely distributed, Highly condensed in Inactive X chromosome (macro chromatin body)	RI
H2A-Bbd	Vertebrate H2A variant (no data from other species)	Widely distributed, Deficient on the inactive X chromosome	RI
H2AX	(m)H2AX (*d*)H2AvD (*sc*)H2A	Widely distributed, Highly condensed in double-strand break sites	RI
CenH3	(*h, x*)CENPA, (*d*)CID, (*sc*)CSE4	Centromeres	RI
H3.3	H3.3 H3.2 (in plants)	Euchromatin	RC, RI

protein, increased RNA level and the recruitment of the histone variant H3.3 during the induction of transcription, suggesting that histone exchange is a mechanism through which heterochromatin is transformed into a transcriptionally active state [Janicki et al., 2004]. Centromere protein A (Cenpa for mouse, CENP-A for other species) is a histone H3-like protein that is thought to be involved in the nucleosomal packaging of centromeric DNA [Janicki et al., 2004]. The centromere activity is maintained by a chromatin assembly mechanism rather than by the primary DNA sequence [Janicki et al., 2004]. These histone variants might be used to mark specific regions.

Variants of histone H2A also play locus-specific roles. The histone-like domain macro H2A has only 64% identical amino acids to full-length histone H2A [Pehrson and Fried, 1992]. Immunofluorescence studies showed that macroH2A is concentrated in the inactive X chromosome in mammals [Costanzi and Pehrson, 1998]. Interestingly a novel H2A variant, H2A-Bbd, is markedly excluded from the inactive X chromosome and may be associated with transcriptional active region [Chadwick and Willard, 2001]. H2A.X is in sites of DNA damage [Paull et al., 2000]. The response of eukaryotic cells to the formation of a double-strand break (DSB) in chromosomal DNA is highly conserved. One of the earliest responses to DSB formation is phosphorylation of the C-terminal tail of H2A histones within nucleosomes near the break. Ionizing radiation inducing double strand breaks caused H2AX phosphorylation, but not oxidative or UV-induced double strand breaks. H2AX is uniformly distributed in chromatin, but phosphorylated H2AX is concentrated in the vicinity of a DSB

[Celeste et al., 2003; Redon et al., 2002]. In yeast, the SQ motif located in core histone H2A is phosphorylated, instead of histone H2AX variant. In *Drosophila melanogaster,* the DSB-induced phosphorylation is observed in histone variant H2Av. H2Av is a member of the H2A.Z family of histone variants. H2AV is a unique histone variant, providing in a single histone both the transcriptional function of H2A.Z variant and the DNA repair function of H2AX variant [Leach et al., 2000]. Ser137 within an SQ motif located near the C- terminus of H2Av was phosphorylated in response to ionizing-irradiation. From the C-terminal tail deletion test, Madigan and colleagues found that phosphorylation of H2Av or H2AX is important for repair of radiation-induced DSBs [Madigan et al., 2002].

Another histone H2A variant is H2A.Z (also known as H2A.Z/F, H2AvD, hv1, Pht1, or Htz1), which is conserved from yeast to humans. The early observation that H2A.Z is associated with the transcriptionally active macronucleus but not the quiescent micronucleus of the ciliated protozoan *Tetrahymena*, indicated a role for this histone variant in transcription [Allis et al., 1980]. Another line of evidence for the function of histone variants comes from the study of *Saccharomyces cerevisiae* histone. In *Saccharomyces cerevisiae* the deletion of HTZ1 encodes yeast H2A.Z results in a defective induction of the GAL1 and PHO5 genes in response to their respective inducing signals, particularly in the absence of the SWI/SNF ATP-dependent nucleosome remodeling complex [Santisteban et al., 2000]. H2A.Z has also been shown to promote gene silencing at reporter genes integrated at HMR and at a telomeric locus, leading to the proposale that it functions both in gene activation and gene silencing [Dhillon and

Kamakaka, 2000]. Using a whole-genome microarray, Meneghini and colleagues identified two hundred H2A.Z activated genes, supporting a role of H2A.Z in active transcription [Meneghini et al., 2003]. About 40% of those genes were found in the silent chromatin domains of telomeres and HMR. This finding suggested that Htz1 functions to protect genes from sir-dependent silencing at these telomeric locations and in regions flanking the HMR silent cassette.

H2A.Z has also been shown to make subtle changes in the nucleosome structure, which in turn has quite large effects on higher order chromatin structure [Fan et al., 2002b; Suto et al., 2003]. However, little is known about such histone-replacing mechanisms and stability changes of octamer structure after incorporation of histone variant H2A.Z into nucleosome. H2A.Z is estimated to be at only 10% of the level of H2A. So, how H2A.Z can be incorporated into specific regions of the genome remains a big question to be answered.

1.4 Chromatin assembly

1.4.A. Chromatin assembly

During DNA replication, not only the duplication of DNA, but chromatin assembly also takes place. It is generally agreed that the daughter strands of newly replicated DNA appear to be rapidly assembled into chromatin by the initial deposition of histone H3-H4 followed by incorporation of two histone H2A-H2B dimers to complete the nucleosome [Gasser et al., 1996]. Half of the histones is

provided by the parental chromatin, which is disassembled into H3-H4 tetramers and H2A-H2B dimers by an unknown mechanism. Interestingly, truncated histones were also efficiently transferred to the daughter DNA strands, suggesting that the structured domain (histone fold domain) of the histones may be recognized by assembly factors [Quintini et al., 1996]. The other half of the nucleosome complement is made from newly synthesized histones. Newly synthesized histones H3 and H4 differ from bulk histones in their post-translational modification: acetylation of lysine residues 5 and 12 of H4, and lysine residue 14 of H3 [Sobel et al., 1995]. This acetylation is transient. After chromatin assembly, this deposition-related acetylation is rapidly removed [Annunziato and Seale, 1983].

1.4.B. Nuclear import of core histone

During S-phase of the cell cycle, de novo chromatin assembly requires nuclear uptake of newly synthesized core histones. Generally, transport of proteins into and out of the nucleus is a signal-dependent, receptor-mediated process that proceeds through nuclear pore complexes. A number of signals in nuclear proteins have been identified which allow their selective access to the transport machinery. Nuclear localization signals (NLS) are recognized by members of a family of nuclear transport receptors referred to as importin α and importin β (or karyopherins) [Gorlich and Kutay, 1999]. These receptors are able to interact with the small GTPase Ran in its GTP-bound form. While binding of

RanGTP to importins facilitates import substrate release, exportins need to bind RanGTP for efficient loading of the export cargo [Gorlich and Kutay, 1999]. NPCs are characterized by an eight-fold rotational symmetry; the nuclear pore complexes (NPC) is believed to have an effective diameter of 9 nm. Individual core histones (less than 20kDa, less than 3nm diameter) are small enough to pass through NPCs without signal-mediated active transport mechanism. However, recent studies have analyzed sequence motifs involved in nuclear targeting of core histones. It has been demonstrated that both the basic N-terminal domains and the central structured domains of all four-core histones can serve as nuclear targeting signals [Baake et al., 2001]. Muhlhausser showed that histone import is an importin-mediated process, and several members of the importin family of transport receptors are able to interact with core histones [Muhlhausser et al., 2001]. They identified five importin proteins that can directly interact with individual core histones and support their import into the nuclei, suggesting that multiple pathways of import exist to provide efficient nuclear uptake of these essential proteins. Although there are several reports [Chang et al., 1997; Mosammaparast et al., 2001], whether the formation of histone heteromers (H2A-H2B or H3-H4) take place in the cytoplasm and/or in the nucleus is still not completely understood.

1.5 The histone chaperones

Chromatin assembly is a stepwise process involving the association of a

tetramer of histone $(H3\text{-}H4)_2$ with the DNA, followed by the incorporation of H2A-H2B dimers to form the nucleosome [Laskey et al., 1993; Nakagawa et al., 2001]. Biochemical analysis of the nucleosome assembly process has led to the identification of several histone-binding proteins, such as nucleoplasmin, *S.cerevisiae* antisilencing factor 1 (Asf1), histone regulator (HIR), Spt6, DF31, ATP-utilizing chromatin assembly and remodeling factor (ACF), REF, Nucleoplasmin/B23, chromatin assembly factor 1 (CAF-1), N1/N2, and nucleosome assembly factor 1 (NAP-1) (reviewed in [Krude, 1999]). Some of these proteins appear to function as histone transfer vehicles. Nucleoplasmin and NAP-1 are nucleosome assembly proteins that bind H2A and H2B histones, whereas N1/N2, CAF-1, ASF1, HIR protein can make a complex with H3 and H4 histones *in vivo* [Laskey et al., 1978] [Adams and Kamakaka, 1999] [Ito et al., 1997] [Haushalter and Kadonaga, 2003]. *In vitro*, nucleoplasmin, NAP-1, and HIR can bind both H2A-H2B dimer and H3-H4 tetramer (reviewed in [Haushalter and Kadonaga, 2003]). The N-terminal tails of the H2A-H2B dimer are dispensable for nuclear import but at least one tail is required for replication-dependent, active assembly of H2A-H2B dimers into chromatin *in vivo* [Thiriet and Hayes 2001]. In addition, the N-terminal domains of histones H3 and H4 are not necessary for CAF-1 (chromatin assembly factor) mediated nucleosome assembly [Shibahara et al., 2000]. Table 2 describes recent works that indicate histone chaperone complexes and their involvement in assembly mechanism.

Table 2 Chromatin assembly factors with potential assembly manner [Haushalter and Kadonaga, 2003; Loyola and Almouzni, 2004].
(d) Drosophila, (sc) Saccharomyces cerevisiae, (h) Homo sapiens, (x) Xenopus laevis, (m) mouse
RI; Replication-independent assembly, RC: Replication-coupled assembly

Histone chaperone	Complex and Species specific name	Interacting Histone	Interacting Histone variant	Associated factors	Related function
Nucleoplasmin	Homomultimer (*x*) Nucleoplasmin (*d*) dNLP	H2A/H2B, H3/H4 (low affinity)			Storage of histones, Chromatin decondensation
N1/N2	(*x*) N1/N2	H3/H4			Storage of histones
NAP (nucleosome assembly protein)	Homodimer (*sc,d,m,h*) NAP1	H2A/H2B, H3/H4	H2A.Z (In the presence of SWR1)	P300, Kap114p, SWR1	Histone transfer, RC and RI assembly
HIR (HIRa)	(*sc*) Hir1, Hir2 (*d,x,m,h*) HIRA	H2A/H2B H3/H4	H3.3	ASF1	RI assembly
CAF1 complex (Chromatin assembly factor)	Heterotrimeric protein (*d*) p150, p105, and p55 (*h*) p150, p60, and p48 (*sc*) Cac1, Cac2, and Cac3	Acetylated H3 and H4		PCNA, ASF1	RC assembly
ASF (ATP-utilizing chromatin assembly and remodeling factor)	RCAF (Replication coupling assembly factor) (*sc,d*) ASF1 (*m,h*) ASF1a and b	Acetylated H3 and H4		CAF1, Brahma, TAF250/CCG1, Rad53 SAS1, Hir1, Hir2	RC assembly
Nucleophosmin/B23		H3			Histone transfer
SPT6	FACT (*sc*) spt16/Cdc68,Pob3 (*d,x,h*) hSpt16, SSRP1	H3/H4 H2A/H2B (low affinity)		FACT	Histone transfer

CAF-1 (chromatin assembly factor-1) was initially identified from the fractionation of the human cell extract having an activity to promote incorporation of H3-H4 into nucleosomes [Gaillard et al., 1996]. The co-purified histones with CAF-1 have a similar pattern of lysine acetylation to that reported for newly synthesized H4. CAF-1 consists of three components. In humans, the subunits correspond to p150, p60, and p48, and in budding yeast to Cac1, Cac2, and Cac3 (Table 2). In humans, p150, the largest subunit of CAF-1, interacts directly with proliferating cell nuclear antigen (PCNA), an accessory factor of the DNA polymerase complex [Shibahara and Stillman, 1999]. The smallest subunit p48, conserved from yeast to human, can bind to histones in the absence of the other subunits of CAF-1 (p150 and p60) [Gaillard et al., 1996]. Also p48 (p55 in Drosophila) possesses seven WD repeat interacts with histone deacetylases (chHDAC-1 and -2) *in vivo* [Tyler et al., 1996; Verreault et al., 1996; Verreault, 1998]. Interestingly, one of the Drosophila nucleosome remodeling factor (NURF) subunits is predicted to be a WD repeat protein that is identical with the p55 subunit of the Drosophila CAF-1 [Martinez-Balbas et al., 1998]. The seven WD-repeat cluster is also conserved between yeast and man in the HIR proteins [Kirov et al., 1998; Lorain et al., 1996; Scamps et al., 1996]. These seven copies of the antiparallel beta-sheet of Hir1p are required to repress transcription and functionally interact with different protein complexes: the SPT4, SPT5, and SPT6 gene products. HIRA binds to CAF-1p48 and HDAC-1 and -2 *in vitro*, and seven WD motifs in HIRA are required for the *in vitro* interaction with CAF-1p48 [Ahmad

et al., 2003; DeSilva et al., 1998]. WD repeats might serve as a binding site of multi-protein complexes [Kirov et al., 1998; Martínez-Balbás et al., 1998].

Replication-coupling assembly factor (RCAF) was identified by its ability to facilitate CAF-1-mediated assembly of nucleosomes onto newly replicated DNA *in vitro* [Tyler et al., 1999]. RCAF is a complex of the *Drosophila* homologue of the yeast antisilencing function 1 (ASF1) protein and acetylated histones H3 and H4 having the characteristics of newly synthesized histones. It appears therefore, that ASF1 and CAF-1 are the histone chaperones for newly synthesized histones H3 and H4 *in vitro*. However, ASF1 does not have a preference for assembling newly replicated DNA into chromatin *in vitro* in the absence of CAF-1 [Tyler et al., 2001]. The function of Hir (or Hira) overlaps with an assembly pathway that involves CAF-1 and PCNA. CAF-1 and HIRA are identified from histone H3.1 and H3.3 complexes. Deposition of the major histone H3 (H3.1) is coupled to DNA synthesis during DNA replication and possibly DNA repair, whereas histone variant H3.3 serves as the replacement variant for the DNA-synthesis-independent deposition pathway. Thus, it is believed that a role for the *HIR (HIRA)* gene products may be involvement in the DNA synthesis-independent assembly reaction, for example histone turnover or histone-variant exchange.

CIA, which interacted with the TAF1 histone acetyltransferase subunit of TFIID, was identified as a human histone chaperone [Umehara and Horikoshi, 2003]. CIA was found to be a histone chaperone that modulates the formation of nucleosomes: the purified recombinant GST-CIA converts the topology of the relaxed form of a plasmid into the supercoiled form in the presence of

topoisomerase I and core histones in an apparently ATP-independent manner. The CIA counterpart in *Saccharomyces cerevisiae* was shown to be anti-silencing function-1 (Asf1p), the over-expression of which causes de-repression of the silent mating type, telomere proximal, and rDNA loci [Umehara et al., 2002]. *In vivo* and *in vitro* analyses showed that the acidic stretch of the histone chaperone Asf1p is not necessary for the complementation of *cia1*, telomeric de-repression, and nucleosome assembly activity. Although the acidic stretch of Asf1p does not play an essential role in nucleosome-modulating processes, the function of acidic stretches in histone chaperones remains unclear.

Nucleoplasmin was the first identified histone chaperone due to its ability to mediate nucleosome assembly. This acidic protein is complexed with the histones H2A-H2B, whereas N1/N2, another histone chaperone, is associated with histones H3-H4 [Kleinschmidt et al., 1985; Kleinschmidt et al., 1990]. Crystallographic studies of the nucleoplasmin core show that a pentamer of nucleoplasmin dimerizes to form a decamer that is competent for the association of five H2A-H2B dimers or five histone octamers, ideal for such a storage role [Dutta et al., 2001]. It is believed that nucleoplasmin also participates in the decondensation process that the highly compacted sperm chromatin undergoes after fertilization. C-terminal deletion experiments showed that the C-terminal domain of nucleoplasmin, containing the positively charged nuclear localization sequence and negatively charged poly (glutamic acid) tract, activates its chromatin decondensation ability. Also, electrostatic interactions between the positive nuclear localization sequence and the poly (glutamic acid) tract can

modulate protein activity and stability.

1.6 Nucleosome assembly protein 1 (NAP-1)

Nucleosome assembly protein1 (NAP-1) was originally identified in HeLa cell extracts as an activity that facilitates nucleosomes reconstitution. A family of NAP-1 proteins has been identified based on sequence homology, without identifying functions. Biochemical analysis of the yeast NAP gene product has led to the proposal that it functions in a manner similar to that of nucleoplasmin and N1/N2 to deposit histone onto DNA [Ishimi et al., 1983]. yNAP-1 is a 48 kDa polypeptide that has a binding affinity for H2A-H2B and for H3-H4, and can mediate nucleosome assembly *in vitro* [Ishimi and Kikuchi, 1991; McBryant et al., 2003].

In *S. cerevisiae,* a genome-wide analysis showed that the expression of about 10% of all genes were affected in a *nap-1*-deficient yeast strain, with some genes being up-regulated and others down-regulated. A detailed analysis of chromosome IV showed that 35% of the genes affected were clustered together, suggesting that NAP-1 might function in large chromosomal domains rather than at local restricted sites [Ohkuni et al., 2003].

Examination of the primary amino acid sequence of yNAP-1 revealed that there is 31% identity between yNAP-1 and hNAP2, 47% identity between hNAP-1 and dNAP-1 and 31% identity between yNAP-1and hNAP-1. There are three

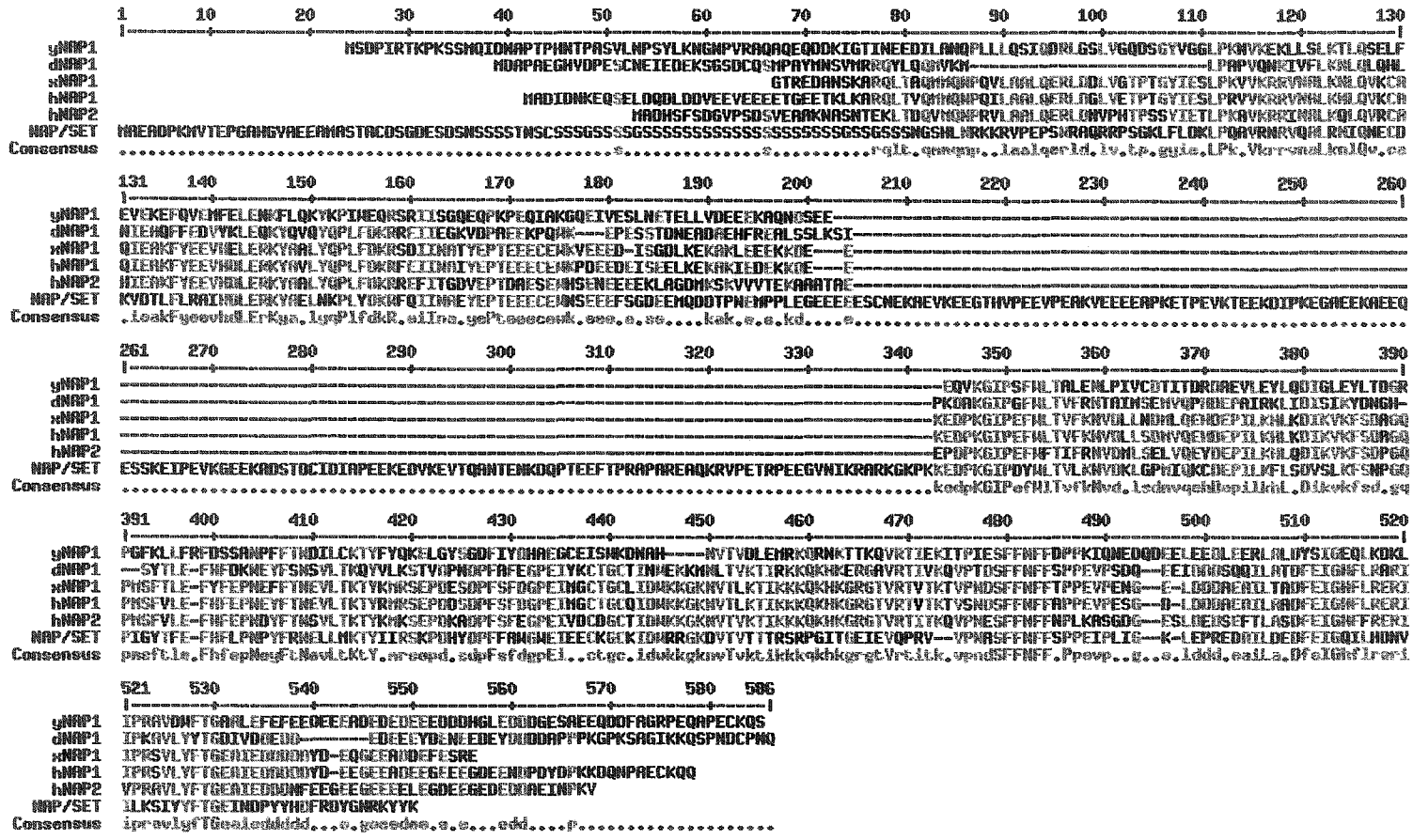

Figure 1. Multiple sequence alignment of nucleosome assembly protein (NAP) family proteins. yNAP1, DNAP1, XNAP1, and hNAP1(hNAP1) represent (y)*yeast, (d) Drosophila, (x) Xenopus laevis,* and *(h) Homo sapiens* nucleosome assembly protein 1. Red color indicates highly conserved amino acid residues or from all of the NAP family proteins.

highly conserved regions among all NAP proteins: 1) KGIPFWLT situated at positions 183-191, 2) ESFFNFFDP situated at positions 310-318 and 3) positions 276-305. The conserved nature of these regions from yeast to mammals suggests that they may play important roles in NAP-1 function. In addition, two of four cysteine residues present in yNAP-1 are also present in the other NAP homologues, suggesting conservation of the disulfide bridge interaction [Ishimi and Kikuchi, 1991].

There are two or three highly acidic domains in NAP proteins. It was thought that NAP-1 may require the long acidic regions to interact with basic N-terminal tails of histones, and it was hypothesized that NAP-1 may interact with H2A-H2B dimer or H3-H4 tetramer using two or three large acidic tracts [Fujii Nakata et al., 1992; Ishimi et al., 1987]. However, the exact roles of the acidic regions in nucleosome assembly proteins have not been defined yet. N-terminal tails of histones are thought to be important. In *Drosophila*, NAP-1 is a part of the multifactorial chromatin-assembly machinery that mediates the ATP-facilitated assembly of regularly spaced nucleosomal arrays [Ito et al., 1996a; Ito et al., 1996b]. Although biochemical studies of chromatin assembly provide a lot of information, many structural questions remain to be answered.

1.6 A NAP-1 functions

While biochemical approaches clearly suggest that NAP-1 has a role in chromatin assembly, genetic studies reveal other functions for this protein. In

addition to the histone-binding activity, NAP-1 protein of yeast has been shown to interact specifically with B type cyclins (clb2), a protein belonging to the cyclin B family. This suggests that NAP-1 participates in the control of mitotic events [Kellogg and Murray, 1995]. In mouse, knocking out the neuron-specific *NAP-1/2* gene resulted in embryonic lethality at the mid-gestation stage [Rodriguez et al., 1997]. This is accompanied by an overproduction of neural precursor cells, arguing for a role of NAP-1 in the regulation of neuronal cell proliferation. Taken together, these data argue for a role of NAP proteins in cell cycle control.

Some of the reports extended the possible role of NAP-1 to regulating gene expression. NAP-1 and nucleoplasmin were also shown to co-operate with the ATPase SWI/SNF complexes in chromatin remodeling, allowing transcription factor binding to nucleosomal DNA *in vitro* [Cote et al., 1994]. On nucleosomal templates, these histone chaperones were required to bind and sequester histone proteins during nucleosome disassembly and core histone octamer displacement from DNA by the SWI/SNF complex. In mouse, a new member of the NAP/SET gene family was isolated from brain. NAP/SET plays a unique role in modulating nucleosome structure and gene expression during brain development [Shen et al., 2001]. Additionally, in studying mechanisms by which transcription factors approach nucleosomal DNA, Walter [Walter et al., 1995] and Chen [Chen et al., 1994] indicated that yNAP-1 or nucleoplasmin stimulated transcription factor binding to nucleosomal DNA and induced core histone displacement. This suggested a model in which nucleoplasmin or NAP-1 carry out the first step in transcription factor-induced nucleosome disassembly by

removing the H2A-H2B dimer. Unwrapping of nucleosomal DNA may be an important mechanism for increasing access of regulatory protein to their target DNA sequence; as an example, RNA polymerase II preferentially associates with nucleosome deficient in one or both H2A-H2B dimers [Baer and Rhodes, 1983]. The H2A-H2B dimer organizes 30 base pairs towards either end of the DNA. The penultimate 10 base pairs of nucleosomal DNA are organized by a region of H3 that does not form an integral part of the $(H3\text{-}H4)_2$ tetramer, and is most likely not able to bind DNA in the absence of H2A-H2B dimers [Luger et al., 1997a]. Thus, dissociation of H2A-H2B dimers frees about 40 bases pairs of DNA from either end of the nucleosome core particle. These data indicate that octamer or histone displacement may be caused by nucleoplasmin or NAP-1.

1.6.B. The role of NAP-1 in the DNA replication coupled (RC) and replication independent (RI) chromatin assembly

The interesting features of NAP-1 are its distribution within the cell. NAPs were shown to interact with newly synthesized histones and might be involved in their transport to the nucleus [Chang et al., 1997]. Microscopic analyses also showed that while NAP-1 is located in the nucleus in S phase, it is found in the cytoplasm during the G2 phase of the cell cycle. A cytoplasmic localization is observed in various species [Marheineke and Krude, 1998], suggesting that NAP-1 could shuttle histones between the cytoplasm and the nucleus. This hypothesis is further supported by the finding that NAP-1 interacted with

Kap114p, a member of the karyopherin (importin) family of proteins, responsible for the nuclear import of H2A and H2B. Although Kap114p is a specific importin protein for NAP-1, other importin poteins, Kap114p, Kap121p, and Kap95, also can interact with H2A-H2B NLSs. It was proposed that NAP-1 serves as a Kap specificity determinant by inhibiting the association of the H2A-H2B dimer with Kaps, other than Kap114p [Mosammaparast et al., 2002]. Recently, Nagata and co-workers also reported that a region of NAP involved in histone binding is important for nuclear import of NAP-1, and nuclear export of NAP is dependent on a nuclear export signal (NES)–like sequence [Miyaji-Yamaguchi et al., 2003].

NAP-1 could be involved in not only de novo assembly of canonical histone H2A-H2B dimer but also replication-independent replacing histone variant assembly, although we do not know an exact function of NAP-1 in the replication independent chromatin assembly. A variety of NAP-1-interacting proteins have been identified, and their intracellular functions are closely related to the regulation of the cell cycle [Altman and Kellogg, 1997; Kellogg and Murray, 1995; Shimizu et al., 2000] and transcription progression [Chen et al., 1994; Ito et al., 2000; Kawase et al., 1996; Shikama et al., 2000]. It is possible that some of the interacting proteins may determine the specific target histone of NAP-1. Indeed, as an example, the complex of NAP-1 with histone variant H2A.Z-H2B dimer is identified from SWRI complex as having a role in histone-variant H2AZ specific incorporation. Mizuguchi and co-workers report that Swr1, a member of the Swi2/Snf2 family of chromatin-remodeling ATPases, catalyzes H2A.Z-specific histone exchange [Mizuguchi et al., 2004]. They identified 12 proteins in the Swr1

complex. Interestingly, a significant proportion of Nucleosome Assembly Protein 1 associated H2A.Z (Htz1) was found to associate with the SWR1 complex. Remarkably, two other groups discovered identical results [Kobor et al., 2004; Korber and Horz, 2004; Krogan et al., 2003]. However, the direct role of NAP-1 in histone-variant H2A.Z-H2B dimer exchange and replication-independent chromatin (RI) formation has yet been examined.

1.6 C The post-translational modifications of NAP: Phosphorylation

NAP proteins have a large number of potential phosphorylation sites by casein kinase II. In Drosophila, casein kinase II binds and phosphorylates NAP-1 [Li et al., 1999] and there is a conserved serine site among mammalian NAPs [Rodriguez et al., 1997]. Although phosphorylation by casein kinase II is not yet detected in yeast NAP-1, the presence of two predicted casein kinase II phosphorylation sites, S/TXXD/E (X represents any amino acid), is significant. In the case of nucleoplasmin, phosphorylated protein binds to sperm basic proteins and decondenses chromatin more effectively [Banuelos et al., 2003; Schmidt-Zachmann et al., 1987]. Therefore, it was thought that its phosphorylation modification may regulate the activity of histone chaperon. According to recent results, both NAP-1 and NAP-2 can be phosphorylated by casein kinase II (CKII) [Li et al., 1999; Rodriguez et al., 2000]. NAP-2 undergoes cell-cycle-dependent changes in the phosphorylation state. In G0/G1 as well as in G2/M phase, the protein is phosphorylated, but it is dephosphorylated in S phase. Phosphorylated

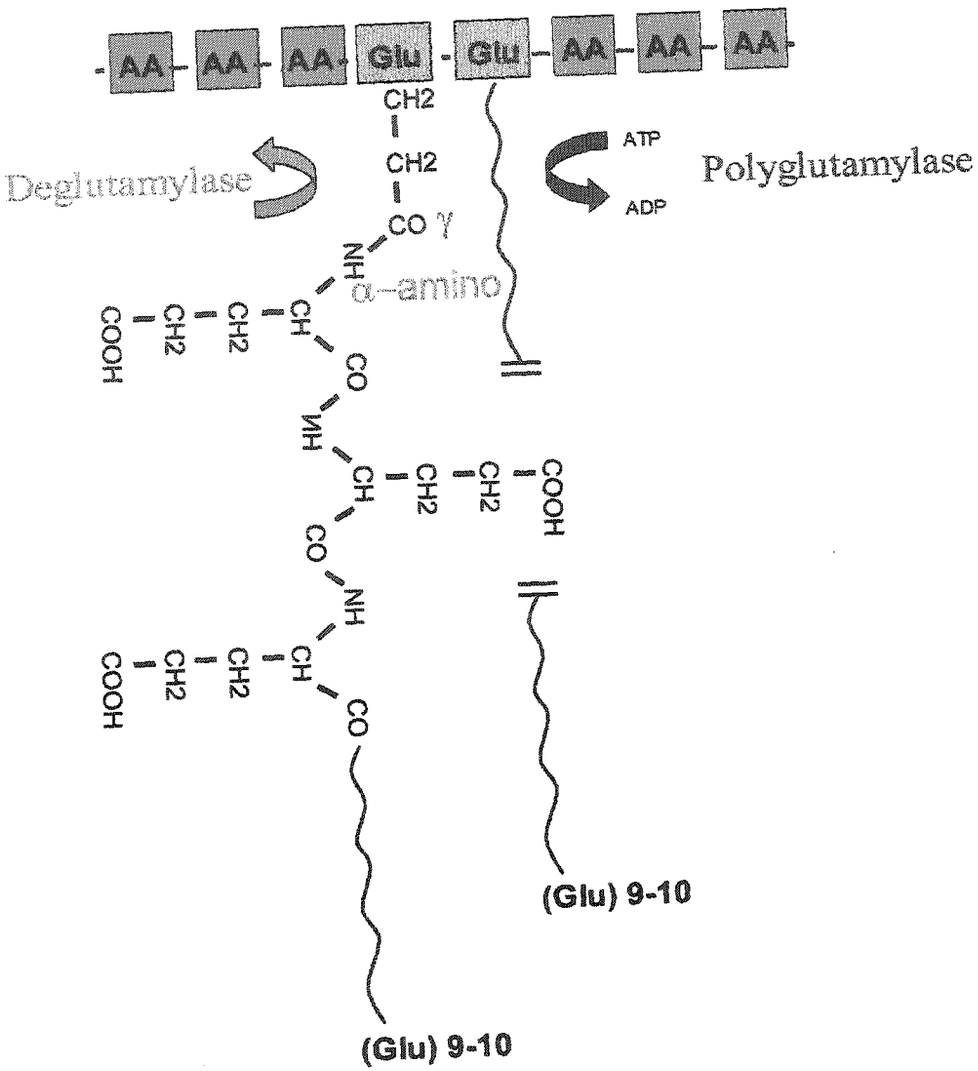

Figure 2 Schematic representation of the polyglutamylation [Regnard et al., 2000]

NAP2 is complexed with histones and remains in the cytoplasm, whereas dephosphorylated NAP2 is translocated into the nucleus in S phase. These results support the hypothesis that histone chaperones may be regulated by CKII-mediated phosphorylation [Rodriguez et al., 2000].

1.6 D The post-translational modifications of NAP: Polyglutamylation

The C-terminus of NAP exhibits a high degree of polymorphism due to covalent post-translational modifications. Two putative glutamylation sites were identified from the C-terminal of NAP-1 and NAP-2. This posttranslational modification occurs by ATP-dependent enzymatic glutamylation. Polyglutamylation is a very unusual posttranslational modification [Regnard et al., 2000]. The α-amino group of the first glutamate is linked by an isopeptide bond with the γ-carboxylic group of a glutamate residue of the main polypeptide chain. Additional glutamates are linked together by normal peptide bond, thus leading to the formation of a second or third C terminus that extends from the main polypeptide chain (Fig. 1). Nine or ten glutamyl units were observed from the C-terminal domain of NAP-1 or NAP-2 [Regnard et al., 2000]. It is thus possible that the total negative charge of the C-terminal acidic domain can be easily changed in a reversible manner. The presence of glutamylated NAPs is not restricted to HeLa cells but is also observed in different tissues and in different organisms. Interestingly, this modification seems to be conserved in other histone chaperones too. Bernard et al. (2002) mention as "data not shown" that nucleoplasmin, one of the histone-chaperone proteins, also can be polyglutamylated, suggesting that polyglutamylation may act as a regulation

method of histone-chaperone activity. They also proposed that proliferative cell-specific polyglutamylase (type I) is only active on NAP substrates [Regnard et al., 2003]. These results demonstrate that posttranslational modifications may be a new perspect for studying NAP function.

1.7 Specific aims of thesis and general dissertation layout

The current hypothesis is that structural changes occur in the histone octamer due to corporation of histone variants or the action of chromatin-remodeling factors, resulting in altered transcription. Even less is known about the mechanisms of histones variant deposition. One role of histone chaperone protein may be histone-variant exchange. NAP-1 appears to be involved in the conformational changes of the nucleosome core particle, too. We test these hypotheses by first testing the stability of nucleosome-containing histone variant, H2A.Z, followed by the investigation of the role of histone chaperone NAP-1 in histone-variant exchange. We then determined the structure of the yeast NAP-1.

The stability of nucleosomes containing histone variant, H2A.Z, was investigated. The results of this study are presented in chapter 2 and were published in *The Journal of Biological Chemistry*. I have examined the role of yeast NAP-1 in the histone variant-containing H2A-H2B dimer exchange mechanism. This study revealed the dynamic structure mode of nucleosomes in the presence of yeast NAP-1. The results of this study are presented in chapter 3, and a manuscript describing this study was accepted in *The Journal of*

Biological Chemistry. Chapters 4 and 5 include the studies involving the atomic structure of NAP-1. This structural information provided by these studies will allow to better understand the biological role of histone chaperones.

Chapter 2

A new FRET approach demonstrates that the histone variant H2AZ stabilizes the histone octamer within the nucleosome

This chapter was published in *The Journal of Biological Chemistry*. The text of this manuscript and the figures are presented as they appeared in this journal. The author list for this submission is as follows: Young-Jun Park, Pamela N. Dyer, David J. Tremethick, and Karolin Luger. Pamela N. Dyer gave support and technical advice.

2.1 Abstract

Nucleosomes are highly dynamic macromolecular complexes that are assembled and disassembled in a modular fashion. One important way in which this dynamic process can be modulated is by the replacement of major histones with their variants, thereby affecting nucleosome structure and function. Here we use fluorescence resonance energy transfer between fluorophores attached to various defined locations within the nucleosome to dissect and compare the structural transitions of a H2A.Z-containing and a canonical nucleosome in response to increasing ionic strength. We show that the peripheral regions of the DNA dissociate from the surface of the histone octamer at relatively low ionic strength, under conditions where the dimer – tetramer interaction remains unaffected. At around 550 mM NaCl, the (H2A-H2B) dimer dissociates from the $(H3\text{-}H4)_2$ tetramer – DNA complex. Significantly, this latter transition is stabilized in nucleosomes that have been reconstituted with the essential histone variant H2A.Z. Our studies firmly establish FRET as a valid method to study nucleosome stability, and shed new light on the biological function of H2A.Z.

2.2 Introduction

Chromatin is built from nucleosomes, the universally repeating protein-DNA complexes in all eukaryotic cells. The crystal structure of the nucleosome core particle (NCP) [Luger et al., 1997a] reveals an octameric histone core around which 147 base pairs of DNA are wrapped in 1.65 tight superhelical turns. The histone octamer itself is a modular assembly of two copies each of the four histone proteins H2A, H2B, H3, and H4. Two histone pairs, composed of either of H2A and H2B, or H3 and H4, form stable heterodimers. In solution, two H3-H4 dimers form a tetramer in the shape of a flat, twisted horse-shoe that binds the central 60 base pairs of the nucleosomal DNA around its outside [Luger et al., 1997a], [Van Holde, 1988]. One (H2A-H2B) dimer is tethered to each face of the $(H3\text{-}H4)_2$ tetramer – DNA complex, to complete a 'helical ramp' for continued DNA binding (reviewed in [Akey and Luger, 2003]).

The interaction between the two histone sub-complexes occurs via two spatially distinct interaction interfaces of quite different character (Fig. 1). A four-helix bundle structure (formed by H2B and H4) is characterized mainly by hydrophobic interactions, and buries 1000 $Å^2$ [Luger et al., 1997a]. The second, larger interface (1600 $Å^2$) is characterized mostly by direct and solvent-mediated hydrogen bonds between the 'docking domain' of H2A, and the histone fold extensions of H3 and H4 [Suto et al., 2000]. In addition, a small interface is formed between the L1 loops of the two H2A molecules, which may contribute to holding together the two gyres of the DNA superhelix at the back of the

nucleosome (Fig. 1) [White et al., 2001]. Under physiological conditions, the (H2A-H2B) dimer associates stably with the $(H3\text{-}H4)_2$ tetramer only in the presence of DNA [Eickbush and Moudrianakis, 1978]. Each (H2A-H2B) dimer organizes 30 base pairs towards either end of the DNA. The penultimate 10 base pairs of nucleosomal DNA on either side are organized by a region of H3 that does not form an integral part of the $(H3\text{-}H4)_2$ tetramer, and that is most likely not positioned to bind DNA in the absence of the (H2A-H2B) dimer [Luger and Richmond, 1998a]. The interactions between protein and DNA in this region are weaker than anywhere else in the NCP [Luger and Richmond, 1998a].

Several lines of evidence indicate that the association of the (H2A-H2B) dimer with the $(H3\text{-}H4)_2$ tetramer – DNA complex is highly dynamic, and that this may be important for the *in vivo* assembly and biological function of the nucleosome. First, *in vivo* and *in vitro* exchange of (H2A-H2B) dimers occurs at a considerable rate in non-replicating chromatin [Louters and Chalkley, 1984]-[Kimura and Cook, 2001]. Second, it has been shown that transcriptionally active chromatin is depleted in (H2A-H2B) dimers [Baer and Rhodes, 1983] and this has later been confirmed for RNA polymerase II *in vitro* [Kireeva et al., 2002]. Third, recent results indicate that chromatin remodeling at the promoter of the Pho5 gene involves the complete transient loss of histones [Reinke and Horz, 2003].

The *in vivo* nucleosome assembly pathway begins with the deposition of the $(H3\text{-}H4)_2$ tetramer onto the DNA, followed by the addition of two (H2A-H2B) dimers to complete the nucleosome. The ordered assembly of histone complexes onto cellular DNA is orchestrated by histone chaperones and

assembly factors *in vivo* (see [Ito et al., 1996b], [Akey and Luger, 2003], for review). In the absence of assembly factors, the sequential *in vitro* deposition of histone sub-complexes is simulated by combining $(H3\text{-}H4)_2$ tetramers, (H2A-H2B) dimers, and DNA at high salt concentrations, followed by a gradual reduction of the ionic strength by either dialysis or dilution. The $(H3\text{-}H4)_2$ tetramer associates with the DNA first, at around 1.1 M NaCl. (H2A-H2B) dimers associate with a preformed $(H3\text{-}H4)_2$ tetramer - DNA complex upon further decreasing the ionic strength [Burton et al., 1978]. This *in vitro* assembly pathway is fully reversible. Although little is known about the mechanism by which nucleosomes are transiently or permanently disassembled *in vivo*, it seems obvious that disassembly *in vivo* occurs in a reversal of the assembly pathway, with the possible involvement of histone chaperones and chromatin assembly factors.

Nucleosomes and chromatin regulate all processes that utilize DNA as a template. One way to regulate these processes, in addition to posttranslational histone modifications and ATP-dependent chromatin remodeling, is to change interactions within the nucleosome, or between nucleosomes, by the incorporation of histone variants [Malik and Henikoff, 2003]. Interestingly, most variants belong to the H2A class that probably reflects the unique role H2A plays in the nucleosome. H2A, more than any other histone, makes significant contributions to the surface and stability of the nucleosome by forming an acidic patch on the surface of the histone octamer, and by generating a large interaction interface with the $(H3\text{-}H4)_2$ tetramer (the H2A docking domain) [Luger

and Richmond, 1998b]. In addition, the L1 loop of H2A is the only area of contact between the two (H2A-H2B) dimers within the NCP, and it is the only histone variant with a flexible N- and C-terminal tail [Ausio and Abbott, 2002].

Of all histone variants, H2A.Z is probably the one which is best characterized biophysically and biologically [Clarkson et al., 1999]. The structure of an NCP in which major H2A has been replaced by H2A.Z (H2A.Z-NCP) has been determined previously [Suto et al., 2000]. The structure suggests that subtle localized changes in the interaction of H2A.Z with H3 (compared to the interaction between major H2A and H3 [Luger et al., 1997a]) may result in a decreased overall stability of the NCP, due to destabilization of the interface between the (H2A-H2B) dimer and the $(H3\text{-}H4)_2$ tetramer. However, the small interface between two H2A.Z subunits within H2A.Z-NCP (formed by the L1 loops, Fig. 1) actually appeared to be stabilized compared to major-NCP. Due to the highly complex network of the numerous diverse molecular interactions between the histone subunits and between histones and DNA, it is virtually impossible to accurately predict the relative stability of the two nucleosomes from structural data. For example, as pointed out previously, the strength of a hydrogen bond depends strongly on angle and distance, and the entropic penalty of immobilizing water molecules in solvent-mediated interactions is difficult to quantify [Davey et al., 2002].

Recently, we found that H2A.Z was enriched at constitutive heterochromatin in early mouse embryos [Rangasamy et al., 2003] and that the loss of H2A.Z protein by RNAi-produced chromosome segregation defects in mammalian cell

lines (manuscript submitted). To gain insights into this function of H2A.Z, and the *in vivo* function of histone variants in general, it is important to compare not only the overall stability of variant and 'major-type' nucleosomes, but to investigate which of the many inter-subunit interactions are affected by the sequence changes. Due to the complicated architecture of the nucleosome, data derived from previously used methods such as fluorescence [Eshaghpour et al., 1980]-27) and CD spectroscopy [Burton et al., 1978], [Lee et al., 1982], analytical ultracentrifugation [Wilhelm and Wilhelm, 1980], hydroxy-radical cleavage [Puhl and Behe, 1993] and gel shift assays [Gottesfeld and Luger, 2001], cannot be directly linked to individual molecular events of nucleosome disassembly and assembly. With a growing awareness for the dynamic nature of chromatin, and with the realization that histone variants and posttranslational modifications may exert part of their function by modulating nucleosome structure and stability, the need for a precise analysis of nucleosome stability *in vitro* has become obvious.

We have devised a fluorescence-based assay to dissect the step-wise disassembly of nucleosomes, and to test the hypothesis that the incorporation of histone variants alters nucleosome stability *in vitro*. Here, we describe a comprehensive analysis of the salt-induced dissociation of two types of nucleosome core particles, either containing 'major' (replication-dependent) H2A (major-NCP), or the essential histone variant H2A.Z (H2A.Z-NCP), using fluorescence resonance energy transfer (FRET) [Fairclough and Cantor, 1978]. By attaching fluorescence donor – acceptor pairs to i) either end of the DNA, ii) to H4 and to the DNA, and iii) to H4 and H2B within the NCP, we can monitor

distinct events in nucleosome dissociation. Earlier fluorescence-resonance-energy transfer experiments were limited by available attachment sites for fluorophores [Eshaghpour et al., 1980], [Chung and Lewis, 1986], and by the highly buried nature of the only available cysteine group in the middle of the H3-H3' four-helix bundle structure (Fig. 1). We have overcome this limitation by developing a system to prepare highly defined 'recombinant nucleosomes' [Muthurajan et al., 2003]. This allows us to use histone mutants in which selected residues have been mutated to cysteines, which are readily reacted with commercially available maleimide derivatives of most fluorophores. The presence of the fluorophores does not affect the overall stability of the modified nucleosomes.

We demonstrate that FRET is a versatile method to dissect the multi-state dissociation of nucleosomes. We show that the peripheral regions of the DNA dissociate from the histone octamer in a fast equilibrium at relatively low ionic strength (~320 mM NaCl). At this ionic strength, the dimer – tetramer interaction remains unaffected. At a midpoint of 530-570 mM NaCl, the (H2A-H2B) dimer dissociates from the $(H3\text{-}H4)_2$ tetramer – DNA complex, followed by the dissociation of the DNA from the tetramer at even higher salt concentrations. Only one of these transitions, the dissociation of the (H2A-H2B) dimer from the $(H3\text{-}H4)_2$ tetramer, is subtly stabilized in H2A.Z-NCP compared to major-NCP. This stabilization could potentially attenuate the transcription process by impeding the displacement of a dimer, and is consistent with the emerging role of H2A.Z in silenced heterochromatin.

2.3 Experimental Procedures

Purification of 5S 146-bp DNA—24 repeats of a 146bp 5S rRNA gene have been cloned into a pUC18 – derivative [Richmond et al., 1988]. The plasmid was propagated in *E. coli* HB101 cells. Plasmids and inserts were purified from 6 L DNA preparations as described [Muthurajan et al., 2003].

Separation of 5S 146mer double strand DNA into its single strands – Complementary single strands were separated on a DEAE-5PW-HR column in an alkaline (10mM NaOH) salt gradient (10mM NaCl to 0.5M NaCl). 5S DNA was incubated with the appropriate amounts of NaOH/NaCl at room temperature for 15 minutes. The DNA was loaded onto the DEAE-5PW-HR column equilibrated with 10mM NaOH, and eluted with increasing NaCl concentrations in the presence of 10 mM NaOH, resulting in two clearly separated peaks. The pH of the DNA fractions was neutralized by adding 3 M sodium acetate (pH 5.2). Each single strand of DNA was precipitated with 2.5 volumes of ethanol.

Modification of 5' ends of the 146bp DNA (synthesis of the 5'-cystamine adduct) – Each DNA strand was resuspended in TE (10 mM Tris/HCl, pH 8.0, 0.1 mM EDTA). Both DNA strands require modification with a thiol group (in this case, a cystamine) at the 5'phosphate end to react with the maleimide group of the chromophore. The 5'-cystamine-P-146bp oligonucleotide was prepared in a one-step synthesis in the presence of carbodiimide, 1-methylimidazole and cystamine. A reaction mix containing freshly prepared 3mg/ml 1-ethyl-3,3-

dimethylaminopropylcarbo-diimide (EDC), 0.1M 1-methylimidazole, single stranded DNA, and 0.5M cystaminedihydrochloride was incubated at 50°C for 5hrs [Rasmussen et al., 1991]. The reaction was cooled slowly to room temperature, and diluted ten-fold by the addition of TE (10, 0.1; pH 8) before purifying on a DEAE 5PW HR column (Rohm/Haas). Both modified single strands were ethanol precipitated, and analyzed by PAGE on a 10% TBE gel in 7M-urea to ensure presence of cystamine.

Labeling of the DNA with fluorescent dyes — The disulfide group of cystamine at the 5' end of the 5S 146mer ssDNA was reduced in 0.4 mM TCEP (Tris (2-carboxyethyl) phosphine hydrochloride in TE 10, 0.1; pH 7.0). The corresponding fluorescent dye dissolved in solvent (DMF = N,N-dimethylformamide or DMSO = dimethylsulfoxide) was immediately added in a 30-fold molar excess. The dyes used in this study were 7-diethylamino-3-(4'-maleimidylphenyl) -4-methylcoumarin (CPM) and fluorescein-5-maleimide (FM). This pair has a Förster distance of 52 Å [Wu and Brand, 1994]. The W and C strands were labeled with CPM and FM, respectively. ssDNA was then separated from unreacted dyes by a sephadex G25 spin column. Removal of unreacted dye was monitored by PAGE (10%, 0.5 x TBE) and observed under UV trans-illumination at 365 nm. The labeled DNA was concentrated (Vivaspin 20, Vivascience, USA) in preparation for re-annealing. Labeling efficiency was routinely ~ 90 – 95 %, as determined by absorption spectroscopy. The separated and labeled single strands are shown on supplementary Fig. 1B. To verify that fluorophore-maleimides do not react with DNA nonspecifically, single-

stranded DNA was dephosphorylated and subjected to the same labeling procedures as described above. No cystamine adduct is obtained, nor are the DNA samples fluorescently labeled.

Reannealing of double-stranded DNA — Labeled complementary single strands of DNA were reannealed, yielding a double-stranded DNA fragment labeled with an FM group and a CPM group on opposite ends. Single strands were mixed at equimolar amounts in 200 mM NaCl, 2 mM $MgCl_2$, 10 mM Tris/HCl at pH 7.0, heated to 90°C for 3 minutes, followed by cooling on ice for 5 minutes, then re-heated at 75°C for 15 minutes. The DNA was allowed to cool down to room temperature slowly for ~2.5 hours. The double-labeled double stranded DNA was checked on a 10% TBE gel (supplementary Fig. 1B, lane 5)

Preparation of fluorescently labeled histone octamer – Recombinant *Xenopus laevis* full-length histone proteins [Luger et al., 1997b] were produced in bacteria and purified as we described before [Dyer et al., 2004]. Site-directed mutagenesis was used to prepare expression clones for H2B T112C and H4 T71C mutants. H3 C110A was used to avoid any unwanted cysteine/dye reaction. The purified histones were unfolded in 6 M guanidinium HCl (20 mM Tris/HCl, pH 7.5, 0.4 mM TCEP), and their concentration was checked spectrophotometrically [Dyer et al., 2004]. After unfolding, the sulfhydryl groups were labeled using the same method used for DNA 5' end labeling (see above). CPM (or FM) was added in a final molar ratio of 30:1 fluorescence dye to protein in the presence of 6 M guanidine HCl. The labeling reaction was carried out for 4 hours at room temperature, in the dark. Free fluorescent dye was removed by a

sephadex G25 spin column, using 6 M guanidine HCl as the elution buffer. Mass spectroscopy verified that only one labeling site exists within histone proteins as we expected. Labeling efficiencies for proteins were routinely ~ 70%, as determined by absorption spectroscopy. Recombinant *Xenopus laevis* histone proteins, and recombinant mouse H2A.Z histone variant [Suto et al., 2000] were refolded to histone octamers using a previously described protocol [Dyer et al., 2004]. No difference was found upon refolding histone octamer from fluorescently labeled histones, as evident in identical gel filtration elution profiles and refolding efficiencies of histone octamers from modified histones

Reconstitution of labeled NCP – Nucleosome reconstitution was performed by dialysis against decreasing salt concentration as previously described [Dyer et al., 2004]. Reconstituted nucleosomes were heat-shifted for 60 minutes at 37°C to obtain a unique species of nucleosomes. To purify the completely shifted nucleosomes from excess DNA and other aggregated species, samples were purified by preparative gel electrophoresis using a Prep Cell (Bio-Rad Laboratories, Richmond, CA, U.S.A.). All FRET studies were performed with purified labeled NCPs.

Tyrosine fluorescence quenching – All fluorescence measurements were done using an AVIV AT105 spectrofluorometer (AVIV Instruments, Lakewood, NJ, USA) with temperature control. The temperature was fixed at 20 °C. To verify that fluorescently labeled histones and DNA indeed form stable and functional NCPs, the global stability of fluorescently labeled and non-modified NCPs was measured by quenching of intrinsic tyrosine fluorescence by nearby

DNA bases. In all of the tyrosine quenching experiments, 0.28 μM NCP in 20 mM Tris pH 7.5, 1mM EDTA, and 1mM DTT were brought to the indicated salt concentration with 5 M NaCl and equilibrated at 25°C. Tyrosine fluorescence was measured at an emission of 306nm and excitation of 275nm, and was plotted against the salt concentration.

Fluorescence anisotropy – Steady-state fluorescence anisotropy measurements were performed in 20 mM Tris, pH 7.5, 25°C, at 0.25 μM sample concentration at an excitation wavelength of 385nm and an emission wavelength of 480nm. The anisotropy $r = (I_{VV} - G I_{VH}) / (I_{VV} + 2 G I_{VH})$ was calculated from the parallel I_{VV} and perpendicular I_{VH} polarized fluorescence intensities. Two subscripts of I_{VH} represent the relative fluorescence intensity at vertical (V) and horizontal (H) position of the excitation and emission polarizer. G is the ratio of the intensity of the perpendicular to the parallel components of the fluorescence emission measured for the sample. G was used to correct for the differential sensitivity of the instrument to vertically and horizontally polarized light.

Steady state fluorescence experiments – All samples were subjected to constant stirring during readout. Bandpass slits for excitation and emission were maintained at 2 nm. The excitation wavelength used in all FRET experiments was 385 nm and CPM intensities were measured at the emission maximum wavelength. All samples contained a final concentration of 0.23 μM for NCP in Tris buffer (20 mM Tris/HCl, pH 7.5, 100 mM NaCl, 1 mM EDTA, 1 mM dithiothreitol). The buffer was scanned in the same range used in all experiments for background contributions to the readings and was corrected for in each

spectrum. In all experiments, samples were incubated for 5 minutes at each salt concentration prior to readout. Scans of samples incubated for greater than 5 min (up to 30 min) showed no change in CPM emission intensity, indicating that an apparent equilibrium had been reached within 5 min. Control samples with donor (CPM)-only labeled NCP, and acceptor (FM)-only labeled NCP were analyzed like wise to discount salt effects on fluorescence.

Experimental data were normalized using the upper and the lower plateau values as baselines, obtained by least squares fit. We used at least five data points to calculate the baselines. To calculate the fraction of the dissociation of the (H2A-H2B) dimer (or the dissociation of DNA ends), we adopted the simple two-state dissociation model to compare the stability of NCPs. The curves are divided into three regions; the pre-transition (lower base line), the transition, and the post-transition region (upper baseline) [Thomson et al., 1989]. The fraction of 'unfolded' was calculated using the equation $F_u = (y_f - y_{obs})/(y_f - y_u)$. y_{obs} is the observed variable parameter (intensity of fluorescence), and y_f and y_u are obtained by extrapolation of the linear portions of the pre- and post-transition regions of the unfolding curve. From normalized data (five data sets for labeling combination I, three data sets for combination II, and three data sets for combination III) , we calculated the mean values (average), standard deviation(σ), and standard error (error on the mean = (σ)/(square roots of N). N is the total number of the data points).

2.4 Results

2.4.A The presence of fluorophores on histones and DNA does not compromise nucleosome structure

Fluorescence resonance energy transfer (FRET) requires the presence of a donor and an acceptor fluorophore within the critical distance of transfer (Förster distance, or R_0). A prerequisite for energy transfer is an overlap of the emission spectrum of the fluorescence donor with the excitation spectrum of the fluorescence acceptor. In this study, we used fluorescein-5-maleimide (FM) as an acceptor, and 7-diethylamino-3-(4'-maleimidylphenyl)-4-methylcoumarin (CPM) as a donor. This pair has an R_0 of 52 Å [Wu and Brand, 1994], a value that is well suited for the overall dimensions of the NCP (110 Å x 55 Å; Fig. 1, Table 1). Attachment sites for the fluorophores were chosen with the requirement in mind that both of the fluorophores should have considerable rotational freedom to enable efficient energy transfer, and that fluorescence donor and acceptor are within a distance of the order of R_0 for the CPM - FM pair. Amino acid residues to be changed to cysteines were selected after careful inspection of the structure, and we are confident that both sites in either histone H4 or H2B fulfill these criteria.

To allow a direct correlation of our results with the protein – protein interactions reported in the previously determined crystal structures [Luger et al., 1997a], [Suto et al., 2000], we used recombinant *Xenopus laevis* histones in combination with recombinant mouse H2A.Z. Since we were particularly

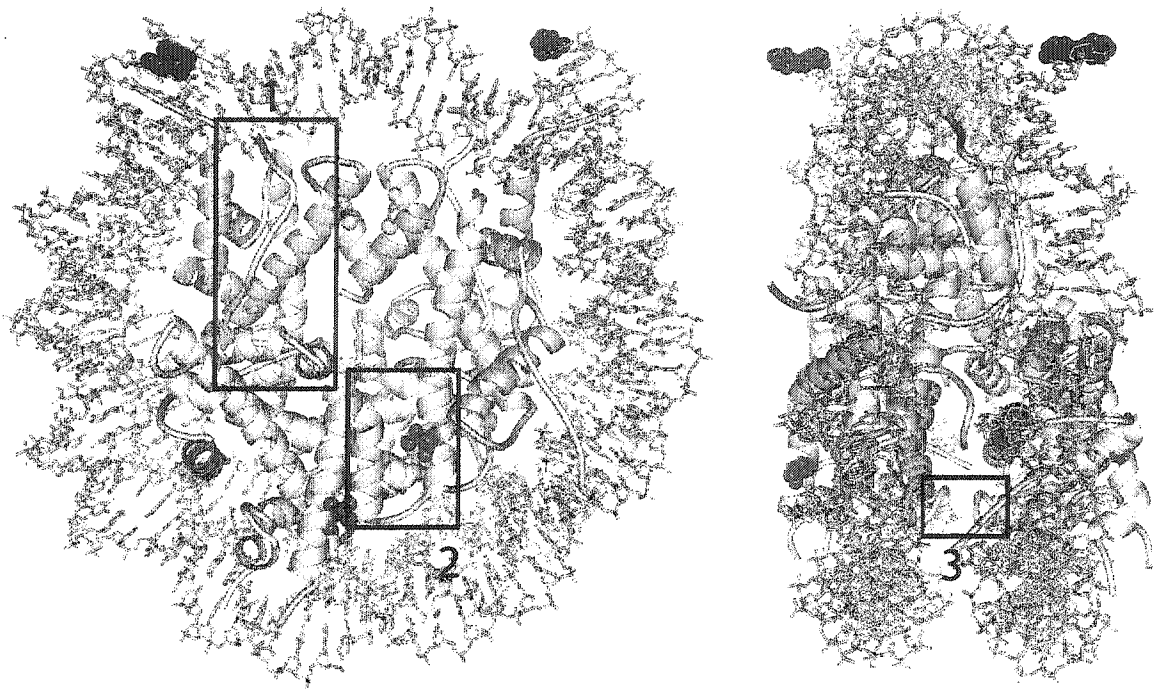

Figure 1: Location of fluorescence probes in the nucleosome structure. The NCP is shown in two orientations, with H3, H4, H2A, and H2B shown in blue, green, yellow, and red, respectively. The location of the fluorescent probes (black, red, and blue, respectively for fluorophores attached to the DNA, to H2B, and to H4, respectively) is indicated. H3 C110, which has been previously used for fluorescence labeling, is shown in yellow. Note its buried character which is obvious in the side view. The H2A docking domain (1), the H4/H2B four-helix bundle (2), and the H2A L1-L1 interface are boxed (3).

Table 1: Förster distances for the three chromophore combination groups within a folded nucleosome. Distances were obtained by measuring the distances between the Cβ atom of the mutated amino acid residues in the available crystal structure (pdb access code 1AOI), and do not take into account the presence of the flexible linker.

Chromophore combination	Donor: CPM Ex/Em: 384/469 nm	Acceptor: FM Ex/Em: 492/515 nm	Distance	Distance to 2nd fluorophore
I	DNA W-strand	DNA C-strand	65 Å	NA
II	H4 T71C	DNA C-strand	76 Å	84 Å
III	H2B T112C	H4 T71C	20 Å	42 Å

interested in comparing the strength of the interaction interface between the $(H3\text{-}H4)_2$ tetramer and either the (H2A-H2B) or the (H2A.Z-H2B) dimer within the nucleosome, we designed experiments that would allow us to monitor (I) changes in distance between the ends of the DNA; (II) changes in distance between both ends of the DNA and the $(H3\text{-}H4)_2$ tetramer; and (III) changes in distance between the $(H3\text{-}H4)_2$ tetramer and the (H2A-H2B) dimer. Fig. 1 shows the location of fluorophores on the nucleosome, and the corresponding distances are shown in Table 1. Because of the inherent symmetry of the NCP, two copies of each fluorophore are present in combinations II and III. Site-directed mutagenesis was performed to introduce cysteine residues into H2B and H4 (H2B-T112C, and H4 T71C). Both mutated residues are surface exposed and are not engaged in any intramolecular interactions. To avoid difficulties in the interpretation of results, we also mutated the only native cysteine present in any of the four histones, H3 C110, to alanine (H3 C110A). This cysteine is buried within the four-helix bundle that forms the H3-H3' interface, and has no discernable structural function. It is an alanine in yeast, and the structure of the yeast NCP in this particular region is virtually identical [White et al., 2001].

Maleimide derivatives of each fluorophore were reacted with the unfolded histone proteins, and unbound fluorophore was removed by gel filtration. Mass spectrometry confirmed the covalent linkage of only one fluorophore per cysteine residue (not shown). Histones were refolded to histone octamers using previously described protocols [Dyer et al., 2004]. A comparison of the elution profiles of refolded histone octamers from a size exclusion column, and analysis

of refolded histone octamers by SDS PAGE, before and after staining with coomassie blue, clearly demonstrates the correct folding and stoichiometry of the histone octamers, a high efficiency of labeling of H4 and H2B, and the absence of fluorescence label on histones H3 and H2A (compare upper and lower panel in supplemental Fig. 1A).

Because of the necessity to attach donors and acceptors to the Watson and Crick strand of a 146 bp DNA fragment respectively (chromophore combination group I, Table 1), we used an asymmetric 146 bp DNA fragment derived from the 5S-rRNA gene in all experiments [Richmond et al., 1988]. Strands were separated by ion exchange chromatography under highly basic conditions (supplemental Fig. 1B), and 5' DNA phosphates were modified with a cystamine group. For chromophore combination groups II and III, the double stranded DNA was labeled without strand separation. The reactive SH groups were reacted with the maleimide forms of fluorescence donor and acceptor, as indicated in Table 1, and fluorescence of the individual strands was demonstrated by PAGE (supplemental Fig. 1B).

NCPs with three different combinations of donor and acceptor fluorophores (as listed in Table 1) were prepared by salt gradient dialysis. The quality of the assemblies was analyzed by native gel electrophoresis, which is a very sensitive measure for the structural integrity of nucleosomes [Luger et al., 1999] (Fig. 2A-C). None of the fluorophores compromised reconstitution efficiency or the ability of the histone octamer to reposition in a temperature-dependent manner on the DNA (a process referred to as heat shifting [Luger et al., 1999]; for example Fig.

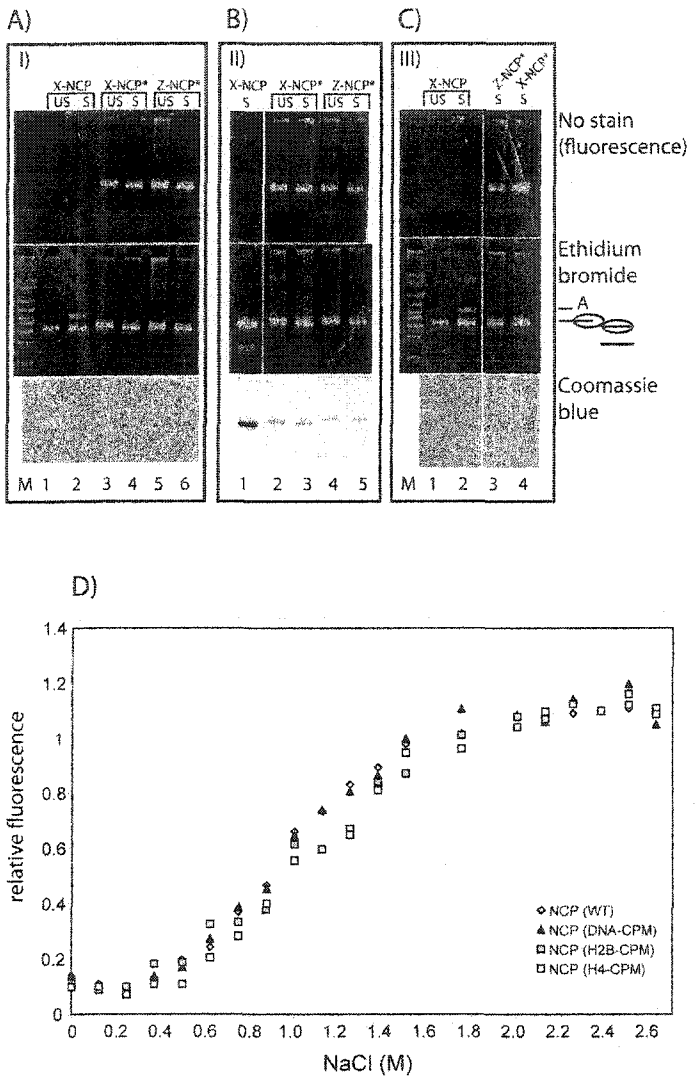

Figure 2: Nucleosomes can be modified with fluorescent probes without effects on structure or dynamic behavior. NCPs reconstituted with either recombinant *Xenopus laevis* histones (major-NCP, or *Xla*-NCP) or with recombinant *Xenopus laevis* H3, H4, H2B, and recombinant H2A.Z (Z-NCP) were analyzed by native PAGE (5% polyacrylamide, 0.25x TBE). Fluorescently labeled nucleosome samples are indicated by a star. Samples were analyzed prior to heat shifting (indicated with US, for unshifted), and after heat shifting (S). DNA markers (M) are 100; 200; 300; 400; 500; 700; 10,000; 15,000; and 20,000 bp. Gels were first viewed on a transilluminator without staining (upper panel), followed by staining with ethidium bromide (middle panel) and coomassie brilliant blue (lower panel), as indicated. **(A)** major-NCPs (lanes 3 and 4) and H2A.Z-NCPs (lanes 5 and 6) labeled with CPM and FM at the 5' ends of the DNA (fluorophore combination I, Table 1). Unlabeled nucleosomes (lanes 1 and 2) are shown as controls. **(B)** major-NCPs (lanes 2 and 3) and H2A.Z-NCPs (lanes 3 and 4) labeled with CPM on histone H4, and with FM on the 5' end of the DNA (combination II, Table 1). Unlabeled NCP is shown as control (lane 1). A DNA size marker is also shown (M, see above). **(C)** major NCP (lane 4) and H2A.Z-NCP (lane 3), labeled with CPM and FM on H2B and H4, respectively (combination III, Table 1). *Xla*-NCP is shown as a control (lanes 1 and 2). Symbols denoting unshifted and shifted nucleosome species, and an aggregate species (A) that is sometimes observed in older nucleosome preparations, are given on the right. **(D)** Salt-induced nucleosome dissociation profiles for fluorescently labeled NCPs and wild type NCP. Fluorescence intensity of tyrosine was measured at an emission of 306nm and excitation of 275nm, and was plotted against the salt concentration. White diamonds: unmodified wild type NCP (n=5), Black triangles: DNA-CPM NCP (n=3), Gray squares: H2B-CPM NCP (n=2), white squares: H4-CPM NCP (n=1). n denotes the number of measurements. Error bars are omitted for clarity.

2A, compare lanes 1 and 2 with lanes 3-6). The new band that appears for the unlabeled X-NCP control is aggregate that we usually observe with older nucleosome preparations, and is not apparent in the species that were used for the actual FRET experiments. Note that the samples contain no traces of free DNA (Fig. 2, middle panel). This is important since residual free DNA could serve as a sink for the (H2A-H2B) dimer during dissociation, and could thus shift the equilibrium of dissociation towards lower salt concentration. Control NCPs labeled only with fluorescence donor at the relevant sites were prepared and analyzed similarly (data not shown).

We wanted to test whether the overall stability of the NCP towards salt-induced dissociation was in any way altered by the presence of the fluorophores. In a folded nucleosome, histone tyrosine fluorescence is quenched by the presence of the nearby DNA bases, and the loss of quenching is concomitant with nucleosome dissociation (27, 51). We monitored tyrosine fluorescence in response to increased ionic strength for unlabeled NCPs, and for NCPs in which DNA, H2B, or H4 has been labeled with CPM. The results are shown in Fig. 2D. No changes within experimental error in the dissociation profile is seen between unlabeled NCP and the differently labeled NCPs, providing additional proof that the fluorescently labeled nucleosomes are indeed stably folded and, to all practical purposes, indistinguishable from their unlabeled counterpart.

To verify the rotational freedom of the attached fluorophores, fluorescence anisotropy measurements were performed with NCPs and histone complexes labeled with various labeling combintations. The results are listed in Table 2. In

Table 2: Fluorescence anisotropy. Steady-state fluorescence anisotropy measurements were performed in 20mM Tris, pH 7.5, 25°C, 0.25 μM sample concentration at an excitation wavelength of 385nm and an emission wavelength of 480nm. The anisotropy $r = (I_{VV} - G I_{VH}) / (I_{VV} + 2 G I_{VH})$ was calculated from parallel I_{VV} and perpendicular I_{VH} polarized fluorescence intensities.

Labeling	Anisotropy
NCP-H2B-CPM	0.186
NCP-H4-CPM	0.190
NCP-DNA-CPM	0.144
DNA-CPM	0.071
(H2A-H2B) dimer-CPM	0.071
CPM alone	0.049

all cases, the measured anisotropy was below 0.2, indicative of significant rotational freedom of all fluorophores, especially in light of the overall size of the NCP (210 kDA). In addition, the comparison between anisotropy values obtained for NCP labeled at the DNA ends and NCPs labeled on the histone proteins (Table 2) strongly suggests that the fluorophores are not buried in hydrophobic regions of the histones. A two-carbon linker was used for the former, whereas the fluorophore is linked directly to the cysteine side chain in the latter. Nevertheless, anisotropy was very similar for these two particles tested (Table 2).

Based on these results, we conclude that fluorophores attached to histone proteins and to DNA are likely to be rotationally flexible and solvent accessible, and thus will be suitable for FRET. Importantly, the presence of fluorophores does not affect the formation of functional nucleosomes, as shown by analysis by gel electrophoresis and tyrosine fluorescence quenching.

2.4.B FRET can be used monitor nucleosome dissociation

The fluorescence properties of each NCP preparation were first analyzed by fluorescence emission scans. Fig. 3 shows a typical example for nucleosomes with chromophore combination I upon excitation of donor emission at 385 nm. In the folded state, acceptor fluorescence as a result of FRET is clearly evident by the appearance of an emission peak for the acceptor at 520 nm. This peak is absent if labeled free DNA is assayed, since the distance spanned by the 5' ends of a linear 146 bp DNA fragment is far beyond the critical distance for FRET for

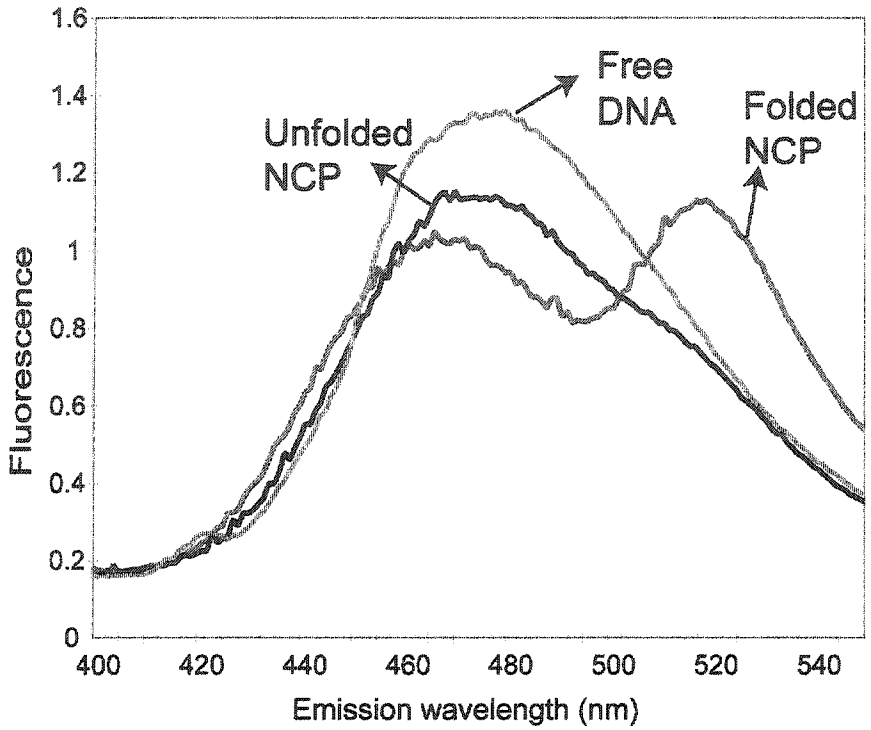

Figure 3: FRET is an indicator for completely folded nucleosomes. Both ends of nucleosomal DNA have been labeled with CPM and FM, respectively (fluorophore combination I, Table 1). The excitation wavelength was set at 385 nm to monitor donor emission. Acceptor emission for folded NCP is observed at 520 nm. Free DNA, labeled identically (gray trace), and NCP in 1.5 M NaCl (black trace) are shown as controls. Note the absence of fluorescence acceptor emission at 520 nm in the two control samples.

this pair (~ 100 Å). In 1 M NaCl, the ends of the DNA are completely unraveled from the surface of the histone octamer, extending the distance between the fluorophores attached to both ends of the DNA significantly past the critical transfer distance. Its emission spectrum thus resembles that of free DNA. The slight shift in the emission maximum for the donor chromophore upon nucleosome unfolding is an indication for different interactions of the chromophore with its environment. Very similar results were obtained with the other two fluorophore combinations (not shown). Note that whereas only one donor and one acceptor is present in chromophore combination group I, two donor-acceptor pairs exist for the other two combinations, due to the inherent two-fold symmetry of the nucleosome core particle. Since none of the distances are significantly above R_0, each donor can excite each acceptor (Fig. 1, Table 1). We verified that true FRET was observed by measuring the same spectra in the absence of acceptor, with donor-only labeled DNA and nucleosomes (see below). In addition, we measured spectra of donor –only and donor-acceptor labeled DNA at different salt concentrations, and observed no shoulder at 520 nm upon donor excitation (not shown).

2.4.C Different steps in the dissociation of NCPs are observed with different donor-acceptor pairs

Having established loss of FRET as a signal for nucleosome dissociation, we monitored changes in donor emission quenching in response to increasing ionic strength. As the salt concentration is increased gradually, the nucleosome

dissociates into its components, as is evident by an increase in donor emission intensity (or loss of FRET, see Fig. 3). Equilibrium dissociation curves are obtained by plotting the increase in donor emission against the salt concentration. Fig. 4A shows representative normalized curves for NCPs reconstituted with the three chromophore combinations listed in Table 1.

We find that the release of the DNA ends (monitored by loss of FRET between fluorophores attached to the two ends of nucleosomal DNA) takes place over a relatively wide salt rage (Fig. 4, triangles), and occurs via an intermediate state. No significant dissociation is observed below 200 mM NaCl. Between 200 and 400 mM NaCl, the peripheral regions of the DNA exhibit increased 'breathing'. This transition is fully reversible even under the dilute conditions (0.12 μM NCP) of the experiment, since FRET re-appeared immediately after dilution to lower salt concentrations (not shown). The second transition is interpreted as the loss of one or both (H2A-H2B) dimers from the nucleosome. Under the dilute conditions of the experiments, this transition is only partially reversible (not shown). This interpretation is consistent with the observation that the loss of FRET between the $(H3\text{-}H4)_2$ tetramer and the DNA end also occurs in two transitions (Fig. 4A). The midpoint for the first transition is identical with that observed for nucleosomes labeled with combination I, and signifies 'breathing' of the DNA ends away from the histone octamer. Dissociation of one or both (H2A-H2B) dimers from the DNA (and $(H3\text{-}H4)_2$ tetramer) then allows the DNA to unravel further, resulting in complete loss of FRET between the ends of the DNA and histone H4. Similar biphasic behavior is observed if FRET between the

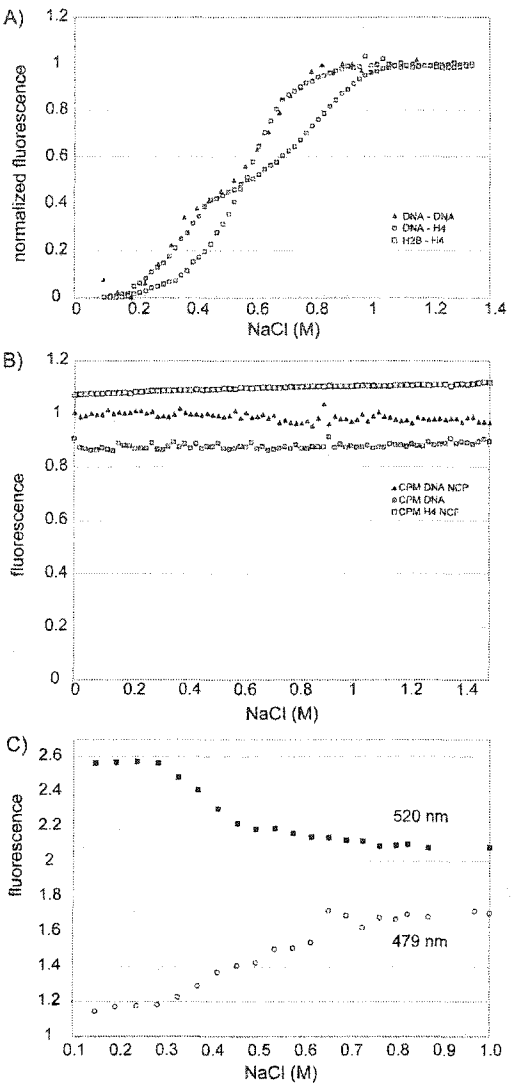

Figure 4: The salt-induced dissociation of NCPs can be monitored by FRET using all three fluorophore combinations. **(A)** Normalized equilibrium dissociation curves (obtained by monitoring changes fluorescence donor emission upon donor excitation at 385 nm) are shown for major-NCP. Curves are shown for the three fluorophore combination groups listed in Table 1 (indicated by black triangles, gray and white squares respectively for group I, II, and III). **(B)** Nucleosomes and DNA labeled with fluorescence donor only were analyzed over the same salt range. Black triangles: NCPs labeled with CPM on the 5' ends of the DNA; gray squares: DNA labeled with CPM on its 5' ends; white squares: NCPs with CPM on histone H4. **(C)** Donor and acceptor emission for a nucleosome core particle from fluorophore combination I was monitored simultaneously in response to increased ionic strength. Excitation wavelength was set at 385 nm, and donor emission (white circles) was monitored at 479 nm, whereas acceptor emission (black squares) was monitored at 520 nm.

(H2A-H2B) dimer and the DNA end is observed (not shown). Consistent with the above interpretation, the dissociation of the (H2A-H2B) dimer from the $(H3\text{-}H4)_2$ tetramer – DNA complex clearly occurs in a single transition, with a midpoint at 580 mM NaCl.

Several controls were performed to verify that the observed signal is not an artifact of changes in fluorophore environment as a result of increased ionic strength. First, we performed salt titration experiments for donor-only labeled NCP preparations (Fig 4B, triangles and white squares). This experiment showed that donor fluorescence emission in the absence of acceptor was unaffected by increased ionic strength. Second, we monitored salt-dependent dissociation of an NCP (labeling combination I) by simultaneously monitoring acceptor and donor emission, and observe that acceptor emission decreases as donor emission increases (Fig. 4C). Finally, to exclude the possibility that FRET was due to intermolecular interactions between two nucleosomes in solution, we incubated different ratios of nucleosomes either labeled only with fluorescence donor, or only with fluorescence acceptor. No FRET was observed at any of the tested ratios (not shown). Equimolar amounts of these two nucleosomes were then incubated with increasing salt concentrations. Again, no FRET was apparent under these conditions (not shown). We can therefore exclude FRET due to intermolecular reactions or due to exchange of subunits at elevated salt concentrations. In addition, salt-induced effects on the observed signal are negligible.

2.4.D Differences in subunit interactions within major and variant NCP can be observed by FRET

Having established a system with which we can monitor the dissociation of individual components within a nucleosome, we compared the properties of H2A.Z-NCPs with those of major-NCPs, to test the hypothesis that the observed changes in the dimer – tetramer interface may result in the altered stability of the variant nucleosomes. The same labeled DNA and histone preparations were used for assembly of major-NCP and H2A.Z-NCP. Fig. 5A shows a typical experiment for chromophore combination I. Again, the multiphasic nature of the equilibrium dissociation curve is apparent. The separation is not clear enough for the two parts of the curve to be treated individually. Nevertheless, it is clear that H2A.Z-NCP is stabilized against salt-induced dissociation compared to major-NCP. This is apparent in the inset for Fig. 5A, showing a linear fit for parts of the data. The midpoint for the overall transition observed with this chromophore combination is 440 mM (±15 mM) NaCl for major-NCP, and 506 mM (± 10 mM) NaCl for H2A.Z-NCP, respectively. The two curves exhibit the same slope, indicating that the same types of protein – DNA interactions (e.g. hydrogen bonds) are disrupted in the two types of nucleosomes.

When the salt-dependence of FRET between the ends of the DNA and histone H4 is monitored (Fig. 5B), the first transition is completely super-imposable for the two nucleosomes, whereas the second transition clearly occurs over a wider salt range in H2A.Z-NCPs. This can be interpreted by a stronger interaction between the (H2A.Z-H2B) dimer and the $(H3\text{-}H4)_2$ tetramer – DNA

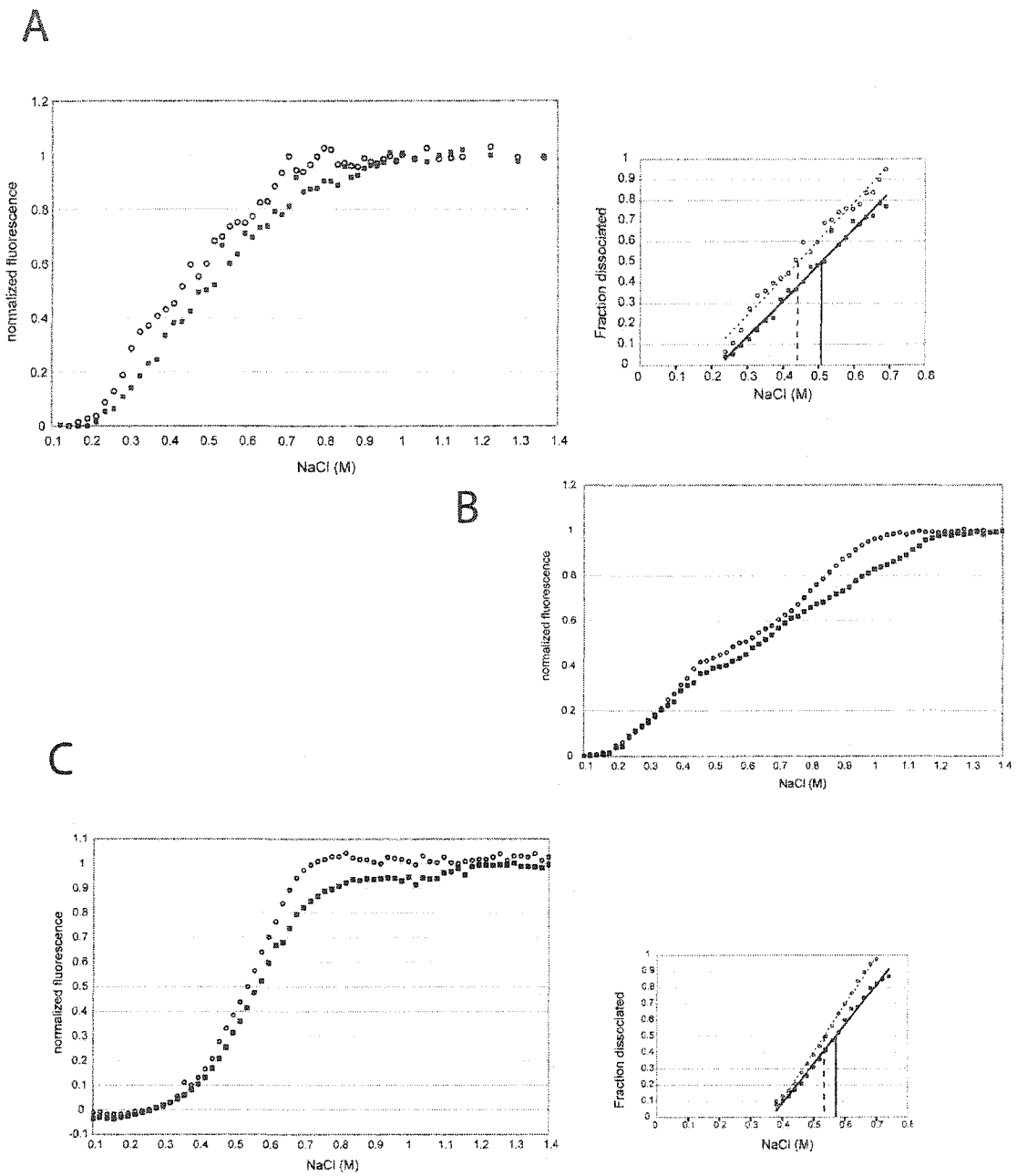

Figure 5: H2A.Z-NCP is stabilized against salt-induced dissociation. (A) comparison of dissociation of major-NCP (white circles) and H2A.Z-NCP (black squares), by monitoring loss of FRET between the ends of the DNA (fluorophore combination I, Table 1). The lower panel shows a least-square fit through the central part of the dissociation curve. **(B)** as (A), but here the loss of FRET between H4 and the DNA ends were monitored (combination II). **(C)** as (A), but obtained by monitoring the loss of FRET between H4 and H2B upon increasing ionic strength.

complex, compared to the (H2A-H2B) dimer – $(H3\text{-}H4)_2$ tetramer interaction. The differences in the slopes of the second dissociation curves between the two types of nucleosomes may either indicate a lesser degree of cooperativity in dimer dissociation, or may reflect differences in the nature of the affected molecular interactions. In fact, we reproducibly observe a third transition (centering around 900 mM NaCl) in the dissociation curves obtained with H2A.Z-NCP, which is absent in major-NCPs. Again, there is indication of a second minor transition at high salt for H2A.Z-NCP which is absent in major-NCP.

Our interpretation that the (H2A.Z-H2B) dimer – $(H3\text{-}H4)_2$ tetramer interaction may be stabilized in H2A.Z-NCPs is confirmed by monitoring the loss of FRET between the (H2A-H2B) (or (H2A.Z-H2B) dimer and the $(H3\text{-}H4)_2$ tetramer within the NCP, using fluorophore combination III (Fig. 5C). In this system, dissociation clearly occurs in a single transition which is shifted towards higher salt concentrations for H2A.Z-NCP. The midpoints for the loss of FRET between the (H2A-H2B) dimer and the $(H3\text{-}H4)_2$ tetramer are 533 mM (±9 mM) NaCl for major-NCP and 569 mM (± 10 mM) NaCl for H2A.Z-NCP. Again, the different slopes of the dissociation curves for the (H2A-H2B) dimer and $(H3\text{-}H4)_2$ tetramer between H2A.Z-NCP and major-NCP indicate that the dissociation of the major and variant dimer may be affected differently at different salt concentrations. This is entirely possible, since the protein – protein interface between the (H2A-H2B) dimer and $(H3\text{-}H4)_2$ tetramer is a composite of hydrophobic interactions, hydrogen bonds, salt links, and van-der Waals interactions.

2.5 Discussion

Nucleosomes within the context of higher-order chromatin structures are highly complex modular assemblies that respond dynamically to ATP-dependent chromatin remodeling factors, histone tail modifications, the incorporation of histone variants, the binding of architectural chromatin-associated proteins and transcription factors, and to advancing DNA and RNA and DNA polymerases [Jackson, 1990], [Kimura and Cook, 2001]. The 'breathing' of DNA ends, and the dynamic exchange of histone subunits are likely to be key aspects in the biological function of nucleosomes [Polach and Widom, 1996]. For example, the ends of the bound nucleosomal DNA are thought to dissociate and re-associate with the histone core in a rapid equilibrium, to allow access of factors to nucleosomal DNA [Polach and Widom, 1995]. The (H2A-H2B) dimer can exchange dynamically in interphase nuclei, independent of replication-dependent chromatin assembly pathways [Louters and Chalkley, 1985], [Kimura and Cook, 2001]. The replacement of histone H2A with histone variants would be a simple and efficient way to alter the thermodynamic properties of the nucleosome, and thus change the local and global structure of chromatin (for example, [Fan et al., 2002a]). The strength of the interactions between i) the DNA and the histone octamer, and ii) between the (H2A-H2B) dimer and the $(H3\text{-}H4)_2$ tetramer within the nucleosome will determine the stability of higher-order conformations as well as the ease by which chromatinized DNA is made accessible to the cellular machinery *in vivo*. In order to investigate the effect of histone variants and

mutants on these processes, it is important to study the relative strength of these interactions independently of others.

We have shown that the complex dissociation behavior of the nucleosome in response to salt can be dissected by FRET. Using fully recombinant nucleosomes [Dyer et al., 2004], [Luger et al., 1999], fluorophores can be attached virtually anywhere on the histones, and on the 5' ends of the DNA, while maintaining significant rotational freedom. The structure and stability of fluorescently labeled nucleosomes remains unaffected, as judged by native gel electrophoresis and tyrosine fluorescence experiments. Using this system, we observed that the ends of nucleosomal DNA dissociate in a reversible manner at relatively low salt concentrations, followed by dissociation of the (H2A-H2B) dimer at more elevated salt concentrations. This is apparent in the appearance of an intermediate state in the dissociation curve when loss of FRET between the ends of the DNA, and between the DNA ends and the $(H3\text{-}H4)_2$ is observed. The latter transition is also observed by monitoring FRET between the (H2A-H2B) dimer and $(H3\text{-}H4)_2$ tetramer, which obeys two-state behavior. We applied this experimental system to compare nucleosomes containing the histone variant H2A.Z with canonical nucleosomes containing replication-dependent 'major' histones, and found that the dissociation of the (H2A.Z-H2B) dimer from the nucleosome occurs at higher salt concentrations, and over a broader salt range compared to the (H2A-H2B) dimer.

The transient exposure of DNA sites as a result of sequential dissociation of the ends of the DNA from the surface of the histone core has been postulated

and proven indirectly in an elegant series of experiments by Widom and colleagues ([Anderson and Widom, 2000], and references therein). By monitoring salt-dependent changes in FRET between the ends of the DNA, we show that significant partial dissociation of DNA takes place with the (H2A-H2B) dimer and the $(H3\text{-}H4)_2$ tetramer still firmly in place. Although partial dissociation of the DNA ends from the surface of the histone octamer has been suggested as an important mechanism in nucleosome dissociation, it has never been demonstrated directly. In a related study, we used this technique to demonstrate that transcription factor binding near the nucleosomal dyad results in transient dissociation of the DNA ends (White, C.L. and K. L., manuscript submitted). The observed dissociation of the (H2A-H2B) dimer at relatively low ionic strength is consistent with *in vivo* observations [Louters and Chalkley, 1985], [Kimura and Cook, 2001], [Jackson, 1990].

Several studies have addressed the structural changes in nucleosomes in response to increased ionic strength, using a variety of methods, and arriving at different conclusions (see [Yager et al., 1989], and references therein). Most studies agree that all four core histones are bound to the DNA up to ~600 mM NaCl, and that dissociation of the (H2A-H2B) dimer from the DNA occurs before that of the $(H3\text{-}H4)_2$ tetramer (e.g. [Burton et al., 1978], [Wilhelm and Wilhelm, 1980], [Oohara and Wada, 1987a]). Up to ~ 700 mM NaCl, the nucleosomal DNA appears to maintain its rotational positioning [Puhl and Behe, 1993]. Since ends of nucleosomal DNA are notoriously difficult to map with DNase

footprinting, our results are consistent with previous observations that the structure of the DNA in the nucleosome remains unaffected up to 800 mM NaCl.

In contrast with our own findings, Eshaghpour and coworkers demonstrated by FRET that the DNA - H3 C110 distance remains constant up to 600 mM NaCl, and in the presence of moderate amounts of urea; the effect of higher salt concentrations has not been investigated [Eshaghpour et al., 1980]. However, analysis of the nucleosome structure (which was not available at the time these studies were performed) shows that the deeply buried H3 C110 is unlikely to sustain modification without significant structural disruption of the $(H3\text{-}H4)_2$ tetramer. The same authors also analyzed FRET between the DNA ends and a fluorophore attached to residue 73 of H4, with basically the same results. Chung and coworkers identified a minor, undefined transition centered around 0.2 M NaCl, indicative of changes in the conformation of the $(H3\text{-}H4)_2$ tetramer, by monitoring FRET between the two H4 molecules [Chung and Lewis, 1986], however, this has not been observed with other methods.

Oohara and Wada monitored CD and quenching of tyrosine fluorescence by nearby DNA bases as a measure for the degree of nucleosome folding, and identified three transitions in the salt-dependent dissociation: an unidentified structural change near 0.55 M NaCl, dissociation of the (H2A-H2B) dimer near 0.95 M NaCl, and dissociation of the $(H3\text{-}H4)_2$ tetramer near 1.45 M NaCl [Oohara and Wada, 1987b]. These transitions are at significantly higher ionic strength than those identified here. The reason for this probably lies in the tendency of basic histone complexes to associate with DNA in a random manner

once they are released from the nucleosome [Samso and Daban, 1993], which would still result in significant fluorescence quenching. The strength of the experimental system described here lies in the rigorous quality control of labeled nucleosomes, and in the defined location of fluorophores, allowing us to independently study the dynamic behavior of histone sub-complexes.

We applied this experimental approach to a comparison between canonical nucleosomes and nucleosomes in which H2A has been replaced by the essential histone variant H2A.Z [Clarkson et al., 1999]. We find that nucleosomes reconstituted with H2A.Z are somewhat stabilized towards salt-induced dissociation, as a result of the increased stability in the interaction between the (H2A.Z-H2B) dimer and $(H3\text{-}H4)_2$ tetramer. A previous comparison of the crystal structures of H2A.Z-NCP with major-NCP was inconclusive: a slight destabilization of the (H2A.Z-H2B) dimer – $(H3\text{-}H4)_2$ tetramer interface as a result of loss of two interactions between the H2A.Z docking domain and H3 is apparently counterbalanced by an increase in the number of interactions between the L1 loops of H2A.Z [Suto et al., 2000]. Our results that the dimer – tetramer interaction is overall stabilized towards salt-induced dissociation demonstrate the importance of this interface in maintaining nucleosome stability. Our results are also in accordance with an earlier observation that the (H2A.Z-H2B) dimer elutes at higher salt concentrations from hydroxyl-apatite bound chromatin than the (H2A-H2B) dimer (D. J. T., unpublished results). This finding can also explain our previous observation that incorporation of H2A.Z into a nucleosomal array *in vitro* restricts nucleosome translational positioning [Fan et

al., 2002a]. The increase in the stability of the (H2A.Z-H2B) dimer – $(H3\text{-}H4)_2$ tetramer interaction suggests that replacement of a H2A-H2B dimer with a dimer containing H2A.Z may impede elongation of transcription by RNA polymerase II, and is consistent with our proposal that H2A.Z plays an important role in establishing an architecturally distinct higher-order chromatin structure at constitutive heterochromatin [Rangasamy et al., 2003]. They are however in disagreement with earlier studies in which structural transitions in H2A.Z NCPs were studied using analytical ultracentrifugation. These authors showed that the ionic strength dependence of the sedimentation coefficient of these particles exhibits a destabilization, and attribute this destabilization to the less stable binding of the (H2A.Z-H2B) dimer with the remainder of the nucleosome. We attribute these discrepancies to differences in the way nucleosomes were prepared, resulting in potentially mis-folded nucleosomes.

The methodology introduced here should be useful for the analysis of nucleosomes containing other histone variants and histone mutants. Furthermore, it can easily be adapted for kinetic measurements, or to monitor the fate of the nucleosome during transcription and remodeling events under physiological conditions. Such studies will provide long-overdue information on the structural transitions imparted onto chromatin during these biologically highly relevant processes.

2.6 Acknowledgements

We thank Devin W. Close and Robert K. Suto for assistance in the initial stages in this project. This research has been supported by a joint grant from the Human Frontiers Science Program (RG00059) to K.L and D. J. T., and by an NIH grant (GM61909) to K. L.

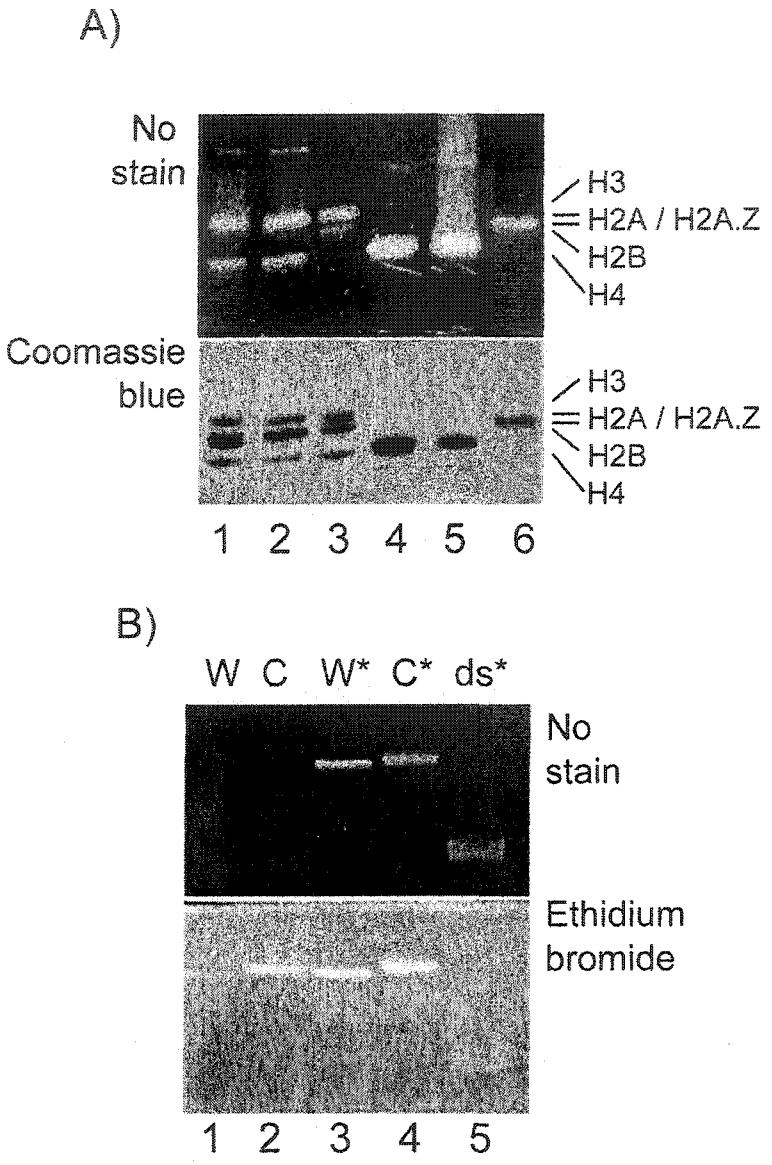

Supplementary Figure 1: Fluorescence labeling of nucleosomal components. **(A)** Purified fluorescently labeled histone octamer, separated on an 18% SDS gel. Lane 1: H2A.Z-octamer (consisting of H3, H2A.Z, H2B, and H4), where H2B and H4 has been labeled with CPM and FM, respectively. Lane 2: as 1, but for major-octamer (H3, H2A, H2B, and H4). Lane 3: major-octamer with CPM-labeled H2B. Lane 4: FM-labeled H4. Lane 5: CPM-labeled H4. Lane 6: FM-labeled H2B. The upper panel shows histone fluorescence in the absence of staining, the lower- panel shows the same gel stained with coomassie brilliant blue. **(B)** Purified single DNA strands, either before (lanes 1 and 2) or after (lanes 3 and 4) fluorescence labeling. Lane 5 shows the annealed double strand that is used for nucleosome assembly. The upper and lower panels show the gel before and after staining with ethidium bromide, respectively.

Chapter 3

Nucleosome assembly protein 1 exchanges histone H2A-H2B dimers and assists nucleosome sliding

This chapter was published in *The Journal of Biological Chemistry*. The text of this manuscript and the figures are presented as they appeared in this journal. The author list for this submission is as follows: Young-Jun Park, Jayanth V. Chodaparambil, Yunhe Bao, Steven J. McBryant, and Karolin Luger. "yNAP-1 mediated nucleosome sliding on a 196bp DNA fragment (Fig. 5)" and the control experiments for nucleosome sliding nucleosome positioning were performed by Jayanth V. Chodaparambil. Y.B. and S.M. gave support and technical advice.

3.1 Abstract

Eukaryotic chromatin is highly dynamic and turns over rapidly even in the absence of DNA replication. Here we show that the acidic histone chaperone NAP-1 from yeast reversibly removes and replaces H2A-H2B or histone variant dimers from assembled nucleosomes, resulting in active histone exchange. Transient removal of H2A-H2B dimers facilitates nucleosome sliding along the DNA to a thermodynamically favorable position. Histone exchange as well as nucleosome sliding is independent of ATP and relies on the presence of the C-terminal acidic domain of yeast NAP-1, even though this region is not required for histone binding and chromatin assembly. Our results suggest a novel role for NAP-1 (and perhaps other acidic histone chaperones) in mediating chromatin fluidity by incorporating histone variants and assisting nucleosome sliding. NAP-1 may function either untargeted (if acting alone) or may be targeted to specific regions within the genome through interactions with additional factors.

3.2 Introduction

The organization of DNA into chromatin has profound consequences for all processes that involve the DNA template, and the biochemical makeup of the nucleosome has important regulatory functions. The nucleosome consists of an octamer of two copies each of the four histone proteins H2A, H2B, H3 and H4, around which 147 bp of DNA are wrapped in 1.65 superhelical turns [Luger et al., 1997a]. A $(H3\text{-}H4)_2$ tetramer organizes the central ~ 70 bp of DNA, and is flanked on either side by one H2A-H2B dimer that each organizes about 40 bp of DNA. Structural and functional variability is introduced by highly regulated reversible posttranslational modifications of individual histones and by the introduction of histone variants, in particular H2A and H3 variants, at specific regions in the genome (reviewed in [Khorasanizadeh, 2004]; [Malik and Henikoff, 2003]). Despite the high degree of DNA compaction, chromatin is surprisingly dynamic and fluidic, and its histone components are exchanged at a high rate in the absence of transcription and replication. Histone H2A-H2B dimers (and, to a certain extent, also $(H3\text{-}H4)_2$ tetramers), appear to be in rapid exchange in most regions of compacted chromatin [Jackson, 1990]; [Kimura and Cook, 2001], and histone variants are incorporated in replication-independent assembly pathways (e.g. [Ahmad and Henikoff, 2002]). ATP-dependent chromatin remodeling factors, in collaboration with histone modifying activities, further enhance chromatin fluidity [Flaus and Owen-Hughes, 2001]; [Becker and Horz, 2002];

[Geiman and Robertson, 2002], with pronounced effects on gene expression patterns.

The transient removal of one or both H2A-H2B dimers from a nucleosome is involved in many vital cellular processes. For example, it has been known for over 20 years that transcriptionally active chromatin is depleted in H2A and H2B [Baer and Rhodes, 1983]. The FACT complex is likely to be at least in part responsible [Belotserkovskaya et al., 2003], but, a possible role for the histone chaperone NAP-1 has also been described recently [Levchenko and Jackson, 2004]. RNA polymerase II alone is also able to displace H2A-H2B dimers during elongation *in vitro* [Kireeva et al., 2002]. H2A-H2B destabilization occurs as a consequence of nucleosome sliding catalyzed by several chromatin remodeling complexes [Bruno et al., 2003]. Finally, it was recently found that a specific ATP-dependent chromatin remodeling factor, Swr1, is responsible for the replication-independent incorporation of the histone variant H2A.Z into yeast chromatin (reviewed in [Korber and Horz, 2004]).

Histones are highly basic, and are usually found in complex with histone chaperones when not bound to DNA (reviewed in [Loyola and Almouzni, 2004]). These acidic proteins (several non-related families exist) are quite abundant in most eukaryotic cells, but their role in nucleosome turnover has not been thoroughly investigated (reviewed in [Tyler, 2002]; [Akey and Luger, 2003]). A renewal of interest has come with the recent discovery in yeast that the acidic histone chaperone NAP-1 is found in association with an H2A.Z-H2B dimer *in vivo*. This NAP-Z complex is thought to supply H2A.Z-H2B dimers to the Swr1

complex [Krogan et al., 2003]; [Mizuguchi et al., 2004]; [Kobor et al., 2004] to promote assembly of H2A.Z-containing chromatin.

NAP-1 is an average size (~ 400 amino acids) acidic protein of unknown structure with a molecular mass of ~ 47,000 Da and a pI of 4.25. Approximately 21% of all amino acids are either aspartic or glutamic acid, clustered in several acidic stretches. The exact amino acid sequence of NAP-1 is only moderately conserved between different organisms [Ito et al., 1996a]; however, their character is maintained throughout most of its length. Although its roles in histone transport and nucleosome assembly are best characterized, NAP-1 appears to have pleiotropic roles *in vivo*. In *Drosophila*, NAP-1 is a part of the multi-factorial chromatin assembly machinery that mediates the ATP-facilitated assembly of regularly spaced nucleosomal arrays [Ito et al., 1996b]; [Ito et al., 1996a]. NAP-1 and other acidic histone chaperones were also shown to co-operate with SWI/SNF complexes in chromatin remodeling, and to facilitate transcription factor binding to nucleosomal DNA *in vitro* [Chen et al., 1994]; [Cote et al., 1994]; [Walter et al., 1995]. Furthermore, direct functional and physical interactions between transcriptional activators and human NAP-1 were reported [Asahara et al., 2002]; [Shikama et al., 2000]; [Rehtanz et al., 2004]. Systematic deletion of the *NAP-1* gene in yeast had no pronounced effect on yeast cells [Tong et al., 2004], suggesting redundancy in its function. However, genome-wide expression analysis of *NAP-1* deletions in yeast has shown that the transcription level of ~10 % of all yeast open reading frames changed by at least

two-fold [Ohkuni et al., 2003]. Deletion of the *NAP-1* gene in flies is lethal [Lankenau et al., 2003].

Analytical ultracentrifugation has shown that yeast NAP-1 (yNAP-1) exists as an obligate dimer in solution [McBryant and Peersen, 2004a]. Functional analysis of NAP-1 *in vitro* is based primarily on its ability to introduce negative supercoils into relaxed circular DNA in the presence of core histones [Fujii Nakata et al., 1992], and to generate regularly spaced nucleosomes on salt-assembled chromatin [McQuibban et al., 1998] a quality which has been employed for *in vitro* nucleosome assembly reactions [Fyodorov and Kadonaga, 2003]. Using deletion analysis, it was also shown that residues 65 to 365 of yNAP-1 were necessary and sufficient for histone binding and *in vitro* assembly reaction, and that a long negatively charged stretch at the C-terminus was dispensable for its assembly activity *in vitro* [Fujii Nakata et al., 1992]; [McBryant et al., 2003].

The functions described above can be ascribed to the well-characterized ability of NAP-1 to specifically bind and sequester histone complexes ([McBryant et al., 2003], and references therein). However, only a few studies address the interactions of NAP-1 or any other chaperone with nucleosomes and chromatin, or its effect on chromatin structure and dynamics [Walter et al., 1995]; [Ito et al., 2000]; [Bruno et al., 2004] [Levchenko and Jackson, 2004]. Here we study yNAP-1 as a model system to investigate if and how histone chaperones contribute to dynamic histone exchange, a property that is emerging as an essential feature of eukaryotic chromatin. Using fluorescently labeled histones and nucleosomes we find that yNAP-1 (in the absence of ATP or other protein

factors) is capable of removing H2A-H2B dimers from folded nucleosomes, and actively exchanges histone dimers containing an H2A variant into completely assembled nucleosomes. We characterize the ability of yNAP-1 to assist nucleosome sliding on DNA, and show conclusively that this activity requires the yNAP-1 – dependent transient dissociation of H2A-H2B dimers from folded NCPs.

3.3 Experimental Procedures

Preparation of DNA, histones, yNAP-1, and nucleosomes – a 146bp DNA fragment derived from a 5S rRNA gene [Simpson and Stafford, 1983] was prepared as described [Dyer et al., 2004]. Both ends of the DNA were labeled with 7-diethylamino-3-(4'-maleimidylphenyl)-4-methylcoumarin (CPM), respectively [Park et al., 2004b]. To prepare the fluorescently labeled histones, H2B T112C and H4 T71C mutants were used [Park et al., 2004b]. Recombinant histones and histone H2A variants (H2A.Z, macroH2A histone domain, and H2A Bbd) were refolded to histone dimer or octamers. Nucleosomes were reconstituted by dialysis against decreasing salt concentration as previously described [Dyer et al., 2004], and analyzed by native PAGE on 5% polyacrylamide gels (acrylamide : bis-acrylamide 59 : 1) in 0.2 X TBE. Full-length yNAP-1, GST-yNAP-1, and truncated versions (yNAP-1ΔN and yNAP-1ΔNC) were expressed and purified as described [McBryant et al., 2003]. The C-terminal domain (CTD, aa 302-417) of yNAP-1 was purified over a nickel affinity

resin. The his-tag was cleaved off with thrombin, followed by purification over a mono-Q column.

Detection of H2A-H2B dimer dissociation from the nucleosome – Nucleosomes containing fluorescently labeled histones or DNA were prepared as described above. 3.5 μM CPM-labeled NCP was incubated with increasing molar ratios of yNAP-1 at 4° C for 10 hours in buffer A (20 mM Tris/Cl, pH 7.5, 100 mM NaCl, 1 mM DTT). H2A-H2B dimer dissociation was analyzed by native PAGE as described above. Nucleosomal bands (N1, S1, S2, and S3) were electro-eluted from gel slices into 0.05 x TBE, and were analyzed by 15 % SDS-PAGE. As controls, fluorescently labeled NCP (as indicated) was incubated with a 4- to 24-fold molar excess of albumin (obtained from Sigma) under the same conditions.

Histone dimer exchange – 3.5 μM unlabeled NCP was incubated with pre-incubated yNAP-1– histone dimer mixtures (3.5 μM H2A-H2B CPM dimer, and 3.5 μM yNAP-1 dimer) at 4 °C for 10 hours in buffer A. Nucleosomes containing fluorescently labeled (H2A-H2BT112C) dimer were prepared as a control. The exchange of fluorescently labeled H2A-H2B dimer or (H2A.Z-H2B) dimer was analyzed by native PAGE as described above. Exchange was quantified by ImageQuant v5.1 (Amersham Biosciences). Gels were first photographed without staining to view fluorescence at 365nm, followed by staining with ethidium bromide and / or coomassie blue as indicated. Control experiments using fluorescently labeled $(H3\text{-}H4)_2$ tetramer were performed analogously.

Nucleosome sliding assay –Nucleosomes were assembled on a previously characterized 196-bp DNA fragment derived from the 5S rRNA gene [Simpson and Stafford, 1983]; [Dong et al., 1990]. Nucleosomes located at the center (N1) or edge (N2) of the 196bp 5S DNA fragment were fractionated by preparative gel electrophoresis using Prep Cell (Bio-Rad Laboratories, Richmond, CA, U.S.A.), using methods previously described for 146-bp NCP [Dyer et al., 2004]. Incubation in the presence or absence of yNAP-1 was performed at 4°C for 10 hours in buffer A. 3.5 μM NCP was incubated with the indicated amounts of yNAP-1. Samples were analyzed by native PAGE. Identical amounts of N1 and N2 nucleosomes (~ 6μg of DNA) were digested with 3.0 units of MNase (Worthington) at 37°C [Bao et al., 2004]. To analyze histone content, nucleosomes were first fractionated on a 5% native gel in 0.2 X TBE, and the nucleosome species were electro-eluted into 0.05 X TBE for 45 minutes at 150 W and 4° C. The eluate was concentrated and analyzed by 18% SDS-PAGE. MvaI (MBI Fermentas), ScaI and AatII (New England Bio Labs) were used to for restriction-enzyme protection assays. ~ 50 μM of NCP was digested with 10 units of enzyme for 4 hours at 37°C, using prescribed buffers. Samples were treated with proteinase K (Sigma-Aldrich) at a concentration of 50 μg/ml (50° C, 3 hours). The digested DNA products were analyzed on a 10% acrylamide gel and were viewed by staining with ethidium bromide.

3.4 Results

3.4.A yNAP-1 removes H2A-H2B dimers from the nucleosome core particle

To investigate the structural changes in NCP structure resulting from yNAP-1 action, we used native gel electrophoresis, a highly sensitive assay for nucleosome structure [Dyer et al., 2004], in conjunction with fluorescence labeling [Park et al., 2004b]. We verified that yNAP-1 binding was not compromised (at least qualitatively) by addition of the label to H2B (supplemental Fig. 1B), and that a yNAP-1 – H2A-H2B dimer complex was formed in solution (supplemental Fig. 1C). CPM-labeled H2B T112C was utilized in all subsequent experiments in which fluorescently labeled H2A-H2B or (H2A.Z-H2B) dimers were used. The stoichiometry of the yNAP-1 – H2A-H2B dimer complex has been shown to be one yNAP-1 dimer per histone fold dimer [McBryant et al., 2003]. Molar ratios given throughout this manuscript take into account the dimeric nature of yNAP-1 [McBryant and Peersen, 2004a].

Upon incubation of purified NCP reconstituted with fluorescently labeled H2B with increasing amounts of yNAP-1, two new bands were detected by native PAGE, and one additional band that is also present in the control significantly increased in intensity. Only two of these bands were visible without staining (Fig. 1A, upper panel, denoted with S1 and S2), demonstrating that only they contained H2B. One additional band, apparent at higher yNAP-1 to NCP ratios, is visible only after staining with ethidium bromide (not shown) and commassie brilliant blue (Fig. 1A, lower panel, S3). Even at the largest excess of yNAP-1

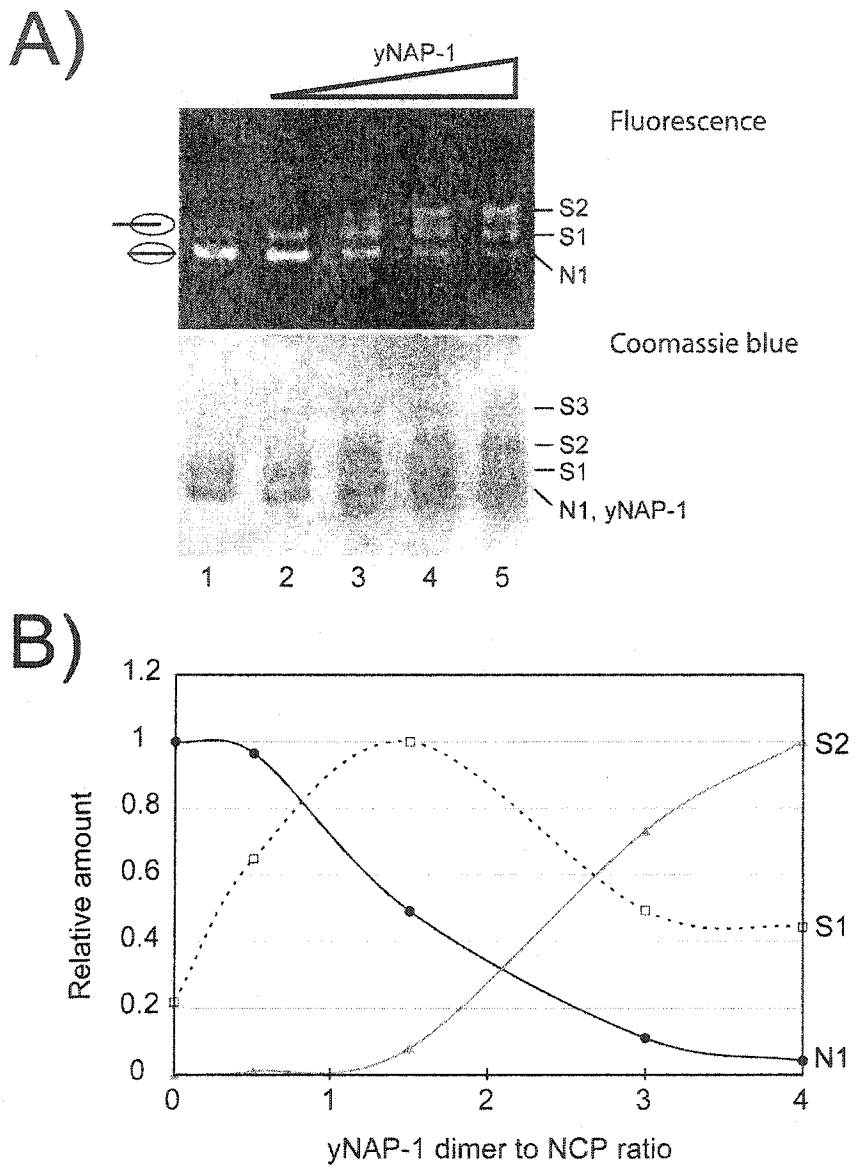

Figure 1. yNAP-1 – induced H2A-H2B dimer dissociation from the NCP. (A) 3.5 μM NCP, reconstituted with CPM-labeled H2A-H2B dimer was incubated with increasing molar ratios of yNAP-1 (lane 1: no yNAP-1, lanes 2-5: 0.5, 1.5, 3, 4, fold molar excess of yNAP-1 dimer over NCP). Samples were incubated at 4° C for 10 hours and analyzed by native PAGE. The gel was first photographed without staining to view fluorescence (upper panel), then stained with coomassie blue (lower panel). The nucleosome and novel species are indicated with N1, S1, S2, and S3, respectively. **(B)** Quantitation of the gel shown in (A). The lanes were scanned, and the intensity of the lanes was analyzed by ImageQuant v5.1 (Amersham Biosciences). Numbers were normalized in terms of ratio of N1, S1, or S2 species.

dimer over NCP (four-fold, lane 5), only very small amounts (< 2 %) of free DNA are released. The unstained gel was digitized under fluorescent light and the relative amounts of the nucleosomal bands (N1, S1 and S2) were plotted against the ratio of yNAP-1 to NCP (Fig. 1B). This plot reveals that S1 is present in maximum amounts at a yNAP-1 dimer to NCP ratio of ~1.5, and that S2 appearsat the expense of N1 upon increasing yNAP-1 / NCP ratios. S3 was too faint to be quantified.

To further investigate the composition of each band, we expanded the previous experiment and prepared NCPs in which either H2B, H4, or the DNA was fluorescently labeled as described earlier [Park et al., 2004b]. The purified NCPs were incubated with a two-fold molar excess of yNAP-1 dimer over nucleosomes (refer to lane 3 in Fig. 1A), and the products were analyzed by native PAGE (Fig. 2A). The gels were analyzed without staining to visualize only fluorescent species. Importantly, we do not observe any detectable $(H3\text{-}H4)_2$ tetramer – yNAP-1 complexes under moderate conditions (Fig. 2A, lanes 4 and 5); however, at higher temperature (37° C for 12 hours) and a large (12-fold) excess of yNAP-1 over NCP, some dissociation of the $(H3\text{-}H4)_2$ tetramer from the DNA is observed (not shown). We show conclusively that N1 and S1 contain DNA, $(H3\text{-}H4)_2$ tetramer, and H2A-H2B dimers, since both of these bands light up if nucleosomes reconstituted with fluorescently labeled DNA (lane 3), H4 (lane 5), and H2B (lane 7) are used. S1 co-migrates with the off-centered NCP species that we routinely observe after salt-gradient reconstitution onto this particular DNA fragment, and is thus identified as a NCP with an altered

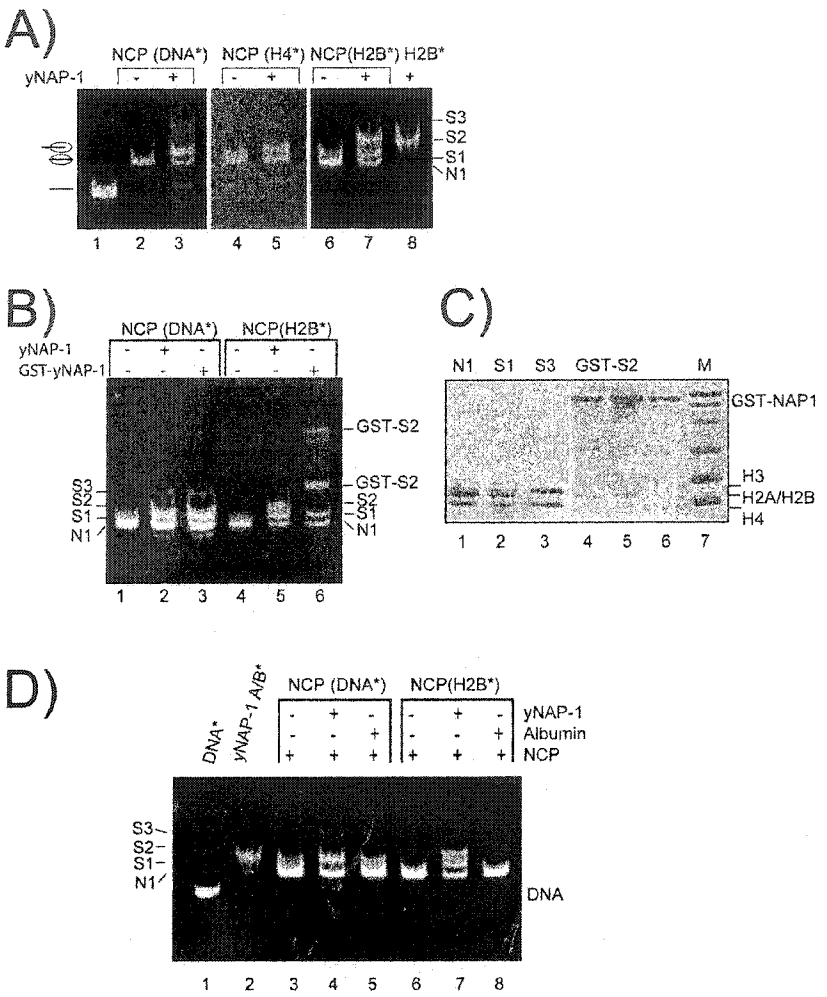

Figure 2. Analysis of novel nucleosomal species. (A) Native PAGE: NCPs were reconstituted from DNA that had been labeled with CPM at the 5'-phosphate groups (DNA*), at H4 T71C (H4*), or at H2B T112C (H2B*) [Park et al., 2004b]. Nucleosomes (3.5 µM) were incubated in the presence (+) or absence (-) of a 2-fold molar excess of yNAP-1. Incubation and gel electrophoresis was done as in Fig. 1A. Lane 1: CPM-labeled DNA, lanes 2 and 3: DNA-labeled NCP in the absence and presence of yNAP-1, lanes 4 and 5: H4-labeled NCP in the absence and presence of yNAP-1, lanes 6 and 7: H2B-labeled NCP in the absence and presence of yNAP-1; lane 8: CPM-labeled H2A-H2B dimer with yNAP-1. **(B)** Analysis of yNAP-1 – H2A-H2B complex (S2) was carried out by electromobility shift assay. Fluorescently labeled NCPs were incubated without yNAP-1 (lane 1 and 4), with yNAP-1(lane 2 and 5), or with GST-yNAP-1 (lane 3 and 6). GST-yNAP-1 – H2A-H2B dimer complex (GST-S2) is indicated. **(C)** Analysis of the protein composition of yNAP-1 – generated nucleosome species by 15% SDS PAGE. Lane 1-5: N1, S1, S3, GST-S2 (lower band) and 2GST-S2 (upper band). Nucleosome species were electro-eluted from 5% native gel slices (as seein in B). Lane 6: GST-NAP-1. Lane 7: protein marker (M) 14.5, 21.5, 31, 45, 66.2, and 94.4 kDa. **(D)** The observed effect is specific for yNAP-1. NCP (3.5µM) containing fluorescently labeled H2A-H2B dimer or fluorescently labeled DNA was incubated with a 2-fold molar excess of yNAP-1 or a 4-fold molar excess of albumin at 4°C for 10 hours. Lane 1: fluorescently labeled DNA; lane 2: fluorescently labeled (H2A-H2B) dimer with yNAP-1 complex; lane 3 and 6: fluorescently labeled NCP without yNAP-1 or albumin; lane 4-5 and 7-8: fluorescently labeled NCP was incubated with yNAP-1 or albumin as indicated.

translational position of the DNA with respect to the histone octamer [Flaus et al., 1996]; [Muthurajan et al., 2003]. S3 only contains $(H3\text{-}H4)_2$ tetramer and DNA, but no H2A-H2B dimer (lanes 3 and 5), and is thus identified as a 'tetrasome' (a $(H3\text{-}H4)_2$ tetramer – DNA complex). S2 contains fluorescently labeled H2A-H2B dimer (lane 7), but no DNA or $(H3\text{-}H4)_2$ tetramer, and co-migrates with a H2A-H2B dimer – yNAP-1 complex (lane 8).

To confirm that S2 contains yNAP-1, we performed a similar experiment with GST-tagged yNAP-1 and visualized its electrophoretic migration by fluorescence. GST-yNAP-1 is just as efficient in converting N1 to S1 and S3, but only S2 is supershifted (Fig. 2B, lane 6). Consistent with the propensity of GST to dimerize, we observe an additional higher band on our native gels (denoted with 2GST-S2). Our experiments show no evidence of a stable yNAP-1 – NCP complex, since the electrophoretic migration of N1 and S1 remains unchanged (Fig. 2B).

We next excised N1, S1, and S3 from a native gel and analyzed the protein content of these bands by SDS-PAGE (Fig. 2C). Consistent with our interpretation of the results shown above, we found that N1 and S1 contain stoichiometric amounts of the four histones. S3 contained only histone H3 and H4, confirming that at higher yNAP-1 / NCP ratios, yNAP-1 removes both H2A-H2B dimers from a folded NCP. Identical results were obtained using a GST fusion of yNAP-1 (not shown). Using GST-yNAP-1, we could also verify that S2 contained only H2A, H2B, and GST-yNAP-1 (Fig. 2C).

Since yNAP-1 is highly acidic, it is formally possible that the observed

removal of H2A-H2B dimers from the NCP is a 'salt effect' due to competition between yNAP-1 and DNA and for the histones. To evaluate the specificity of yNAP-1 in H2A-H2B dimer dissociation, we compared the ability of yNAP-1 and albumin to structurally alter the NCP, using gel shift assays. Albumin is a protein of similar size and acidic pI. Unlike yNAP-1, a four-fold molar excess of albumin had no effect on the nucleosomal band (Fig. 2D, compare lane 4 with 5, and 7 with 8). No H2A-H2B dimer dissociation or disruption of the NCP was observed upon addition of an up to 24-fold molar excess of albumin (data not shown).

3.4.B The C-terminal acidic domain of yNAP-1 is necessary for the dissociation of the H2A-H2B dimer from the NCP, although it is not required for histone binding

We and others have shown previously that the N-terminal domain (NTD, amino acids 1-73) and the C-terminal acidic domain (CTD, amino acids 366-417) of yNAP-1 are not required for histone binding and nucleosome assembly [McBryant et al., 2003]; [Fujii Nakata et al., 1992]. In order to test whether these regions of yNAP-1 are required for the interactions with the nucleosome, we analyzed the ability of truncated yNAP-1 constructs [lacking 73 amino acids from the N-terminus (yNAP-1ΔN), or the 73 N-terminal and 52 C-terminal amino acids (NAP-1ΔNC)] to remove H2A-H2B dimers from the folded NCP (Fig. 3). NAP-1ΔN retained the ability to dissociate H2A-H2B dimers from the NCP. In striking contrast, NAP-1-ΔNC has completely lost the ability to structurally alter the NCP.

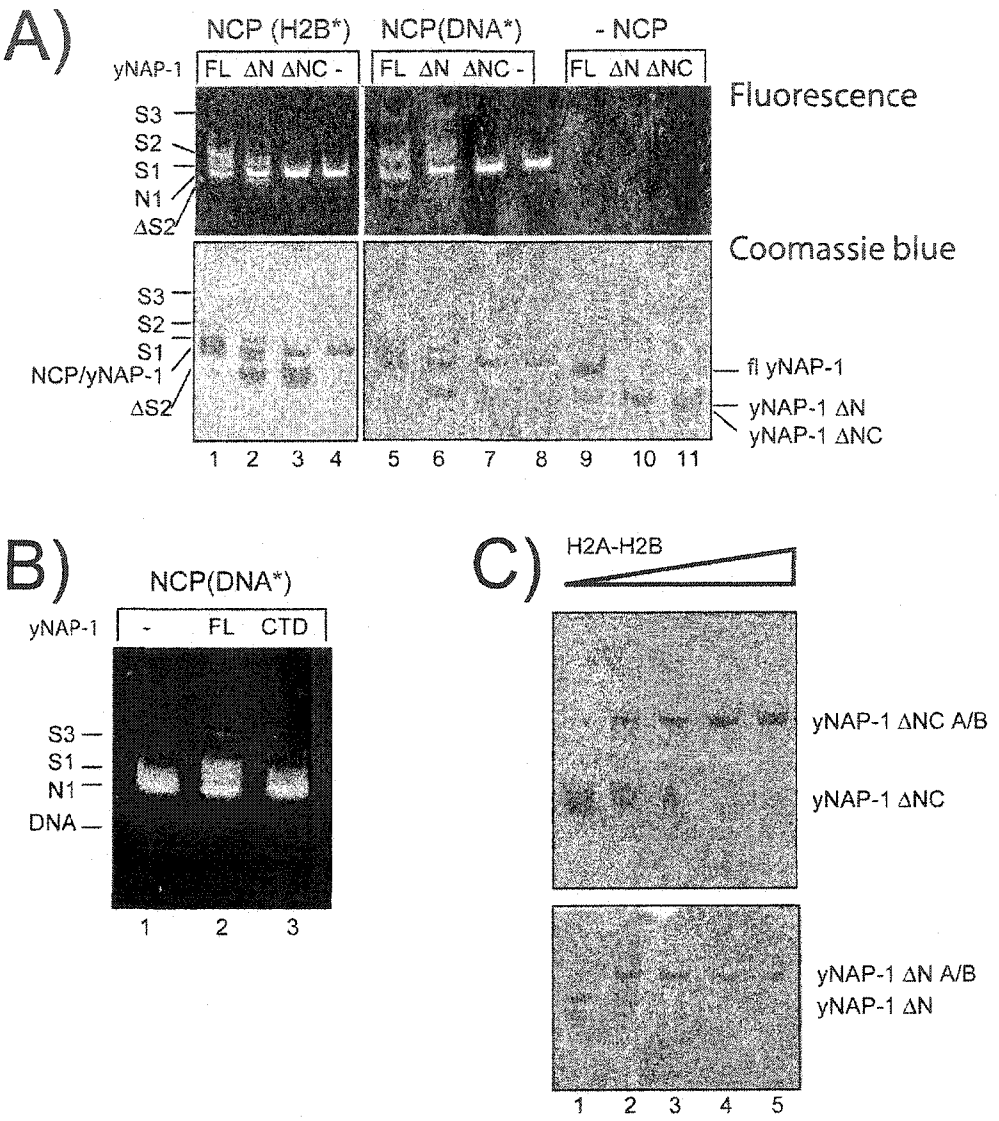

Figure 3. The C-terminal acidic domain (CTD) of yNAP-1 is required for the dissociation of the H2A-H2B dimer. (A) NCP (3.5μM) containing fluorescently labeled H2A-H2B dimer (lanes 1-4) or fluorescently labeled DNA (lanes 5-8) was incubated with a 2-fold molar excess of full length yNAP-1 (lanes 1, 5, and 9), NAP-1ΔN (lanes 2, 6, and 10), or NAP-1ΔNC (lanes 3, 7, and 11). Full length, NAP-1ΔN, and NAP-1ΔNC in the absence of NCP are shown in lanes 9-11. The gels were first photographed without staining to view fluorescence (upper panel), followed by staining with coomassie blue to visualize protein complexes (lower panel). The location of N1, S1-3, and the yNAP-1ΔN – H2A-H2B dimer complex (ΔS2) is indicated. **(B)** NCP containing fluorescently labeled DNA (lane 1) incubated with full length yNAP-1 (lane 2) and the CTD of yNAP-1(lane 3). **(C)** Truncated versions of yNAP-1 still form complexes with the H2A-H2B dimer. 10 μM of NAP-1ΔN (74-417) or NAP-1ΔNC was incubated with H2A-H2B dimer (lanes 1-5: 1, 4, 6, 8, 10 μM, respectively) at 4° C for 10 hours, and analyzed by native PAGE. yNAP-1 – H2A-H2B dimer complexes are indicated.

This was shown conclusively using native PAGE of two different fluorescently labeled NCPs (Fig 3A, lanes 1-4 and 5-8). Importantly, the CTD alone (yNAP-1 amino acids 302–417; pI 3.66) has no effect on the NCP (Fig. 3B), just as has been observed for albumin (Fig. 2D). It is however formally possible that the N-terminus can sustain activity in the absence of the C-terminal domain, and thispossibility remains to be tested.

Full length yNAP-1, yNAP-1ΔN, and yNAP-1ΔNC are all capable of forming a complex with the H2A-H2B dimer (supplemental Fig. 1A, and Fig. 3B), confirming earlier data with GST-constructs of yNAP-1 [McBryant et al., 2003]. Thus, the core domain of yNAP-1 is sufficient to bind the H2A-H2B dimer in solution, as well as to assemble chromatin from DNA and histone components. However, this core domain is not sufficient to remove H2A-H2B dimers once they are assembled into a functional NCP, but additionally requires the acidic C-terminal domain.

3.4.C H2A-H2B dimers are exchanged in and out of nucleosomes by yNAP-1

Having established that yNAP-1 is capable of removing H2A-H2B dimers from a folded NCP, we wanted to investigate whether yNAP-1 is capable of replacing one H2A-H2B dimer with another. To distinguish between the newly exchanged species and un-altered NCP, and to overcome the complication that yNAP-1 co-migrates with the NCP in our gel system, we again exploited our

library of fluorescently labeled histone subunits. A saturating amount of fluorescently labeled H2A-H2B dimer was pre-incubated with yNAP-1 to allow complex formation under previously established conditions (see supplemental Fig. 1). Complexes (which do not contain free yNAP-1) were incubated with previously assembled, unlabeled NCP preparations. The products were analyzed by native PAGE, and fluorescent species were visualized without staining (Fig. 4, upper panel). Exchange by yNAP-1 in about 17 - 22 % of the nucleosome population (in four independent experiments) was observed, as evident in the appearance of a fluorescent NCP band (N1) when incubated with a preformed fluorescently labeled H2A-H2B dimer – yNAP-1 complex, but not with dimer or yNAP-1 alone (Fig. 4, upper panel, compare lanes 1-3). A strong fluorescent band corresponding to the yNAP-1 – H2A-H2B dimer complex (S2) is also observed in lanes 1 and 2. No significant amounts of free DNA are released in this process, as is shown in the ethidium bromide-stained gel (Fig. 4, lower panel). When nucleosomes were incubated with fluorescently labeled $(H3\text{-}H4)_2$ tetramer – yNAP-1 complex under identical conditions, no incorporation of fluorescently labeled $(H3\text{-}H4)_2$ tetramer into nucleosomes was observed (data not shown). When a H2A-H2B dimer – yNAP-1 complex was incubated with free DNA, no H2A-H2B – DNA complex or ternary DNA-H2A-H2B-yNAP-1 ternary complex was detected (data not shown; also see [Nakagawa et al., 2001]). Together, these results demonstrate that yNAP-1 - mediated H2A-H2B dimer exchange does not occur by complete dissociation of the NCP, and that the exchange reaction is limited to the histone H2A-H2B dimer, despite the proven

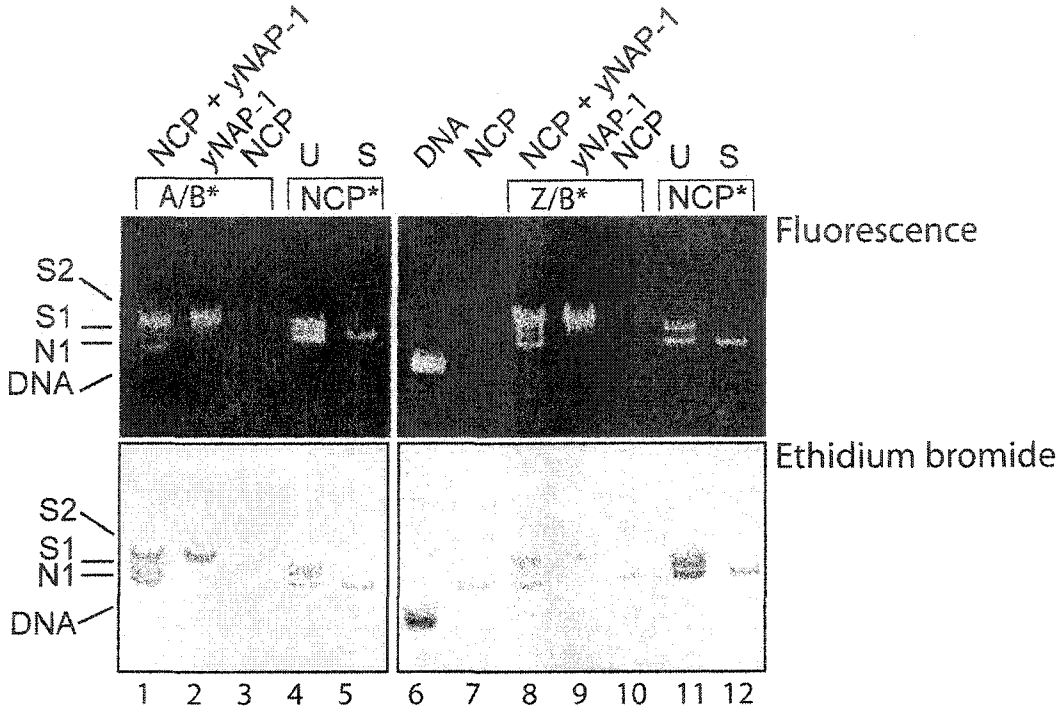

Figure 4. yNAP-1 mediated exchange of canonical H2A-H2B dimer or histone variant (H2A.Z-H2B) dimer into nucleosomes. Unlabeled NCP was incubated with pre-formed yNAP-1 – H2A-H2B dimer (or H2A.Z-H2B) dimer mixtures as indicated. The gel was first photographed without staining to view fluorescence (upper panel), followed by staining with ethidium bromide (lower panel). 3.5 μM NCP, 3.5 μM yNAP-1 with H2A-H2B or (H2A.Z-H2B) dimer complex were used. Lane 1: unlabeled NCP, yNAP-1 and CPM-labeled H2A-H2B dimer. Lane 2: yNAP-1 and CPM-labeled H2A-H2B dimer. Lane 3: unlabeled NCP, CPM-labeled H2A-H2B dimer. Lane 4 and 5: NCP containing CPM-labeled H2A-H2B dimers, unshifted (U) and shifted (S). Lane 6: CPM-labeled DNA. Lane 7: unlabeled NCP. Lane 8: unlabeled NCP, yNAP-1 and CPM-labeled (H2A.Z-H2B) dimer. Lane 9: yNAP-1 and CPM-labeled (H2A.Z-H2B) dimer. Lane 10: unlabeled NCP, CPM-labeled (H2A.Z-H2B) dimer. Lane 11 and 12: as lanes 4 and 5.

ability of yNAP-1 to bind the $(H3\text{-}H4)_2$ tetramer in solution with equal or higher affinity [McBryant et al., 2003].

We next examined whether yNAP-1 is capable of replacing major-type H2A-H2B dimer with a dimer containing an H2A variant. yNAP-1 does not display a markedly different ability to bind the major-type compared to several histonevariant complexes (supplemental Fig. 1A). Upon incubation of unlabeled NCP with fluorescently labeled (H2A.Z-H2B) dimer, a fluorescent NCP species was observed (Fig. 4, lane 8). These experiments show conclusively that yNAP-1 mediates exchange of histone H2A-H2B dimers into folded nucleosomes. Our finding that histone variants are stably bound by yNAP-1 (supplemental Fig. 1A) and are readily utilized in this exchange reaction leads us to predict that not only H2A.Z, but other H2A histone variants in complex with H2B may be exchanged into assembled NCPs under physiological conditions.

3.4.D yNAP-1 facilitates nucleosome sliding

Upon incubation of yNAP-1 with nucleosomes reconstituted on a 146-bp DNA fragment at 4° C, we reproducibly observe a second species (S1 in Fig. 1A and Fig. 4), which contains a full complement of histone proteins and DNA (Fig. 2C) and co-migrates with a well-characterized species that is routinely observed after salt-gradient reconstitution on this particular DNA fragment. This species represents an NCP in which the histone octamer is positioned asymmetrically on the DNA; it is stable over weeks at 4 °C, but can be converted into a

thermodynamically more favorable species in which the DNA is placed symmetrically around the histone octamer by incubation at elevated temperatures (for example, Fig. 4, compare lanes 4 and 5). It appears that the significant energy barrier that exists towards repositioning of the histone octamer along the DNA is relieved by the transient yNAP-1 – mediated removal of the H2A-H2B dimer.

To further investigate the possibility that yNAP-1 facilitates nucleosome sliding, we reconstituted NCPs on a 196-bp DNA fragment derived from the 5S rRNA gene [Simpson and Stafford, 1983]. Upon salt-gradient reconstitution, two major nucleosome species (N1 and N2) are routinely obtained (Fig. 5A, lane 1). These have been described earlier as nucleosomes with different translational positions [Dong et al., 1990]. The two species were separated from each other by preparative gel electrophoresis (Fig. 5A, lanes 2-3). SDS-PAGE revealed that N1 and N2 contained an identical and stoichiometric composition of histones (Fig. 5B, compare lanes 1 and 3 with lane 5). Micrococcal nuclease treatment of the isolated species demonstrated that both protected ~ 146 bp of DNA (not shown).

Purified N1 and N2 were incubated independently with yNAP-1. Intriguingly, N1 was transformed completely into N2 in the presence of equimolar amounts of yNAP-1 dimer and NCP (Fig. 5A, lane 7). The same phenomenon was observed at yNAP-1 to NCP ratios as low as 0.15 : 1 (not shown), indicating that yNAP-1 acts catalytically. In contrast, yNAP-1 had no effect on the electrophoretic mobility of N2 (lane 6). Incubation in the absence of yNAP-1 at elevated

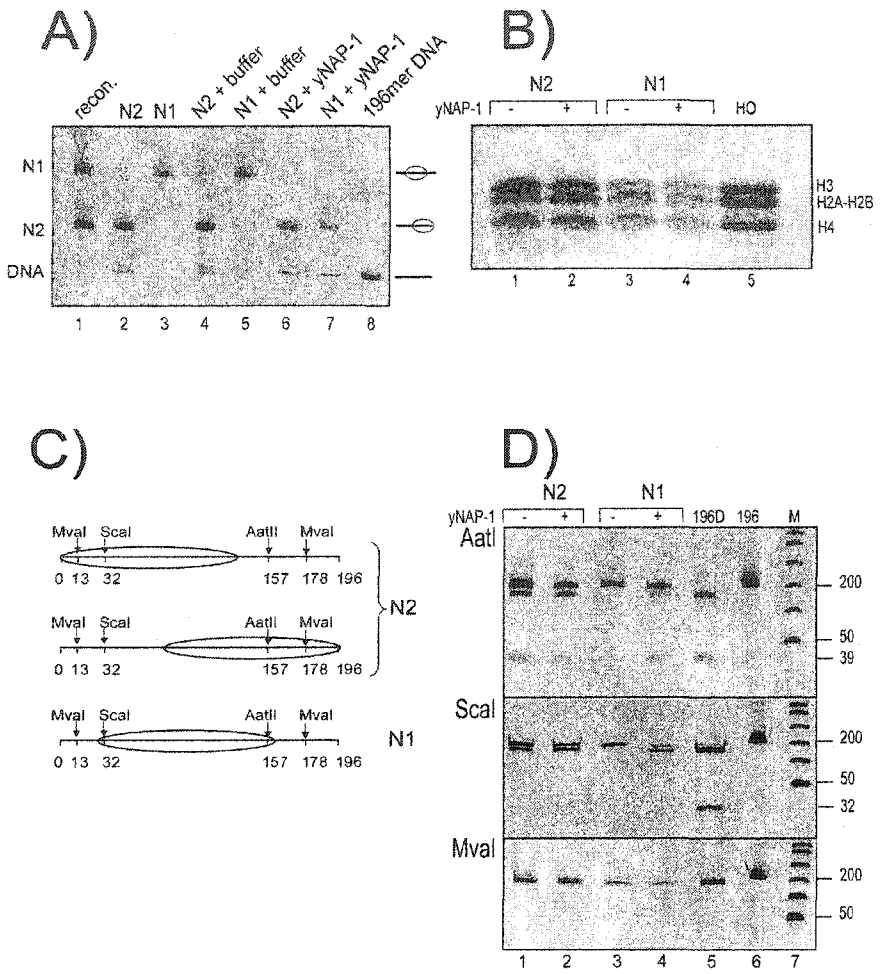

Figure 5. yNAP-1 mediated nucleosome sliding on a 196bp DNA fragment. **(A)** Effect of yNAP-1 two nucleosomal species. Lane 1: nucleosomes after reconstitution; lanes 2 and 3: purified N2 and N1 bands; lanes 4 and 6: N2 in absence and presence of yNAP-1; lanes 5 and 7: N1 in absence and presence of yNAP-1. Lane 8: 196 bp DNA. N1 and N2 were incubated with NAP-1 for 10 hours at 4° C. **(B)** Histone composition of N1 (lanes 3 and 4) and N2 (lanes 1 and 2) in the absence and presence of yNAP-1, as indicated. Lane 5 shows purified histone octamer (HO). **(C)** Overview of nucleosome positions and restriction endonuclease sites used for nucleosome mapping **(D)** Restriction endonuclease protection assays of N1 and N2 before and after yNAP-1 treatment, using AatII, ScaI, and MvaI. N1 (lanes 3 and 4) and N2 (lanes 1 and 2) were analyzed in the absence and presence of yNAP-1, as indicated. Lane 5 shows digestion of the free 196 bp DNA fragment, lane 6 is undigested DNA, and lane 7 a DNA ladder. Molecular weights of restriction products are indicated. 10 % polycrylamide gels were stained with ethidium bromide, colors were reversed for clarity.

temperatures (37 and 45 °C) had no effect on the electrophoretic mobility of either N1 or N2. Importantly, the histone composition of both nucleosomal species (Fig. 5B) and the amount of DNA that is protected against digestion with micrococcal nuclease (not shown) remains unchanged upon yNAP-1 incubation.

To investigate whether treatment of N1 with yNAP-1 results in true nucleosome sliding, it was necessary to characterize the position of the histone octamer with respect to the DNA in N1 and N2 before and after yNAP-1 addition, using restriction enzyme protection assays in conjunction with micrococcal nuclease digestion. Sites for restriction enzymes MvaI, ScaI, and AatII in the 196 bp DNA fragment are depicted in Fig. 5C. In the absence of yNAP-1, N2 is digested to about 30 - 50% with ScaI and AatII, and an apparent 100 % with MvaI (Fig. 5D). In this latter experiment, the two expected fragments of 178 and 183 base pairs in length cannot be distinguished, nevertheless this result strongly suggests that the regions of the DNA not occupied by nucleosomes is free of non-specificially bound histones. Together with the finding that 146 bp are protected from digestion with MNase (not shown), this is consistent with positions for N2 at either end of the nucleosomal DNA (Fig. 5C). N1 is cut to 100 % with MvaI, but is completely protected from digestion with AatII and ScaI. This places N1 between bp 32 and 157, which corresponds to the previously identified positioning sequence on this particular DNA fragment [Simpson et al., 1985].

Incubation with yNAP-1 does not change the behavior of N2 in Mnase (not shown) and restriction enzyme protection assays (Fig. 5D), consistent with the observation that yNAP-1 has no effect on the electrophoretic behavior of N2. In

contrast, N1 behaves like N2 after yNAP-1 treatment in MNase and restriction endonuclease protection assays (Fig. 5D, compare lane 2 and 4), and contains a full complement of all four histones (Fig. 5B), confirming our interpretation that yNAP-1 causes true nucleosome sliding.

We next investigated whether the ability of yNAP-1 to exchange histone H2A-H2B dimers is required to facilitate nucleosome sliding. To this end, we exploited our earlier observation that a truncated version of yNAP-1 (NAP-1ΔNC) was incapable of dissociating histone dimers from nucleosomes, although this yNAP-1 mutant was perfectly capable of assembling chromatin and binding histone complexes. NAP-1ΔN and full-length yNAP-1 were used as controls. Purified N1 was incubated with a 2-fold molar excess of different yNAP-1 truncations under the same conditions as above, and examined by native PAGE. As shown in Fig. 6 (upper panel), wild type yNAP-1 and yNAP-1ΔN were able to induce the redistribution of N1 nucleosomes to N2 (Fig. 6, lanes 3-5), concomitant with the formation of a H2A-H2B dimer – yNAP-1 (or yNAP-1ΔN) complex (Fig. 6, lower panel, lanes 4 and 5). In striking contrast, no effect was observed in the presence of yNAP-1ΔNC (Fig. 6, lane 6), and no H2A-H2B dimer – yNAP-1ΔNC complex was observed. This finding demonstrates that transient H2A-H2B dimer dissociation from the NCP facilitates nucleosome sliding in the presence of yNAP-1. Under these conditions, only minimal amounts of free DNA are released and $(H3\text{-}H4)_2$ tetramer is not exchanged, indicating that nucleosome sliding occurs without complete nucleosome dissociation. As was the case with nucleosome core particles reconstituted on 146-bp DNA fragments, bands that

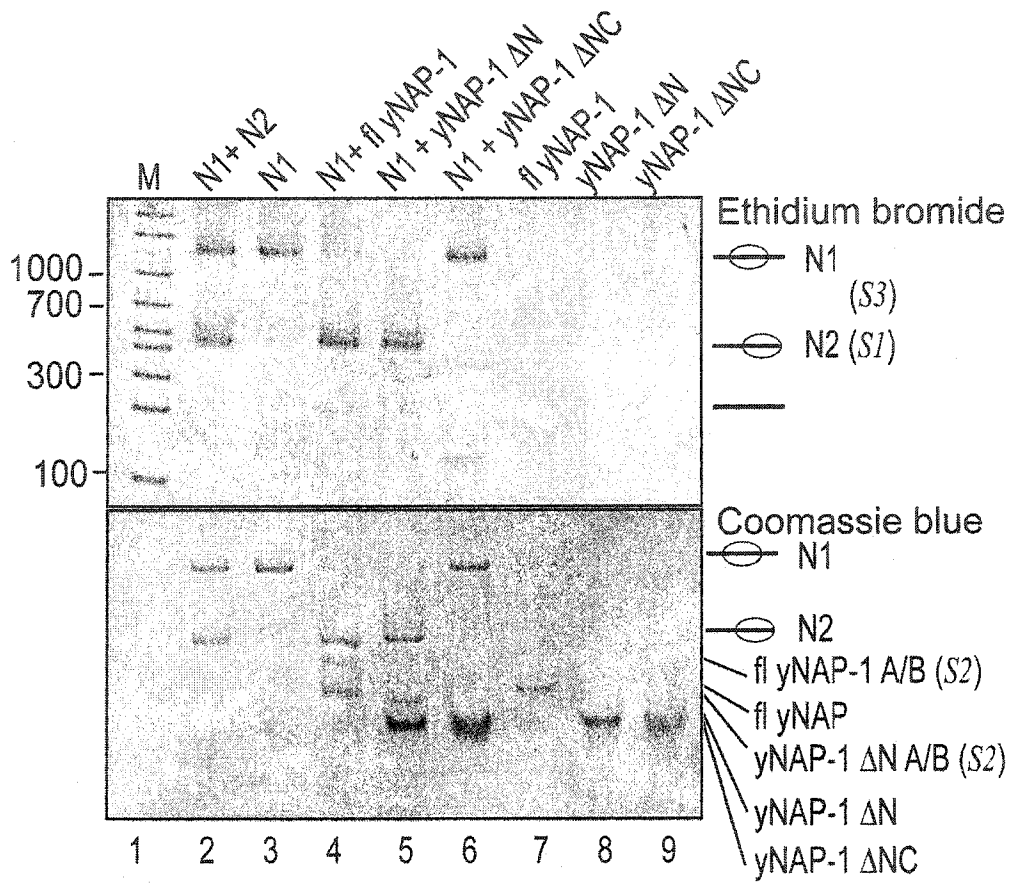

Figure 6. The C-terminal acidic domain of yNAP-1 is required for nucleosome sliding. 3.5 μM NCP was incubated with a 2-fold molar excess of full length yNAP-1 (1-417), yNAP-1ΔN (74-417), or yNAP-1ΔNC (74-365) for 10 hours at 4° C. Samples were analyzed by native PAGE, and visualized by ethidium bromide (top panel) and coomassie blue staining (bottom panel). Lane 1: DNA marker (M), lane 2: N1 and N2 nucleosomes; lane 3: purified N1, lane 4: N1 with full length yNAP-1, lane 5: N1 with yNAP-1ΔN; lane 6: N1 nucleosome with yNAP-1ΔNC; lanes 7-9: full length yNAP-1, yNAP-1ΔN, and yNAP-1ΔNC as a control. The weak S3 band (lane 5) is indicated with an asterisk.

were equivalent to S3 were observed in all cases (indicated by asterisks in Fig. 6).

3.5 Discussion

yNAP-1 is an abundant, phylogenetically conserved acidic histone chaperone that has been shown to be involved primarily in histone transport and chromatin assembly. Here we have demonstrated that yNAP-1 is also capable of transiently removing H2A-H2B dimers from a folded nucleosome. This results in the active exchange of H2A-H2B or histone variant dimers into nucleosomes in an ATP- and DNA replication independent fashion, but also facilitates sliding of the nucleosome along the DNA to help it attain a thermodynamically more favorable position. These roles for yNAP-1 are likely to be of biological significance, and may be a general characteristic of acidic histone chaperones.

yNAP-1 facilitates the removal of one or both H2A-H2B dimers from a folded nucleosome at yNAP-1 dimer to nucleosome stoichiometries of approximately 1:1, whereas the $(H3\text{-}H4)_2$ tetramer is removed only at much higher molar ratios. This is consistent with previous results [Ito et al., 2000] and with the observed rapid exchange of H2A-H2B dimers *in vivo* [Jackson, 1990]; [Kimura and Cook, 2001], and is expected if one considers the central position of the $(H3\text{-}H4)_2$ tetramer on the DNA [Luger et al., 1997a]. The removal of H2A-H2B dimers is likely to facilitate transcription [Levchenko and Jackson, 2004]; [Ito et al., 2000]. This mechanism has also been recently attributed to the FACT complex

[Belotserkovskaya et al., 2003]; also see [Rhoades et al., 2004]. Easier access of transcription factors to nucleosomal DNA in the presence of nucleoplasmin (an acidic histone chaperone with a different quarternary structure and no sequence homology to yNAP-1) and yNAP-1 has also been attributed to their ability to deplete mono-nucleosomes of H2A-H2B dimers [Chen et al., 1994]; [Walter et al., 1995]. Complete nucleosome dissociation and reassembly has emerged as an important regulator of the Pho5 promoter [Reinke and Horz, 2003]; [Boeger et al., 2004]. The recent finding that the H3-H4 histone chaperone Asf1p mediates nucleosome disassembly from the PHO5 promoter *in vivo* [Adkins et al., 2004] suggests that histone chaperones in general may have a more prominent role than previously assumed in promoting nucleosome dissociation during transcription.

Here we have shown that the ability of yNAP-1 to remove a H2A-H2B dimer from a nucleosome depends on the C-terminal acidic region of yNAP-1, which is dispensable for histone binding and nucleosome assembly ([McBryant et al., 2003]; and references therein). Therefore, histone removal from a folded nucleosome is not a simple reversal of the mechanism involved in histone deposition during nucleosome assembly. The extreme acidic character of the residues contained in the C-terminal domain (30 residues out of a total of 52 in the CTD are acidic, comprising one third of all acidic residues in the entire protein) may simply be required to compete with the DNA for the histone dimer, or it may contribute to histone removal via a more complex mechanism that remains to be elucidated. Interestingly, the acidic C-terminal region of the FACT

subunit Spt16 is required for interaction with the nucleosome. However, unlike in case of yNAP-1, it appears to be required also for histone deposition onto DNA [Belotserkovskaya et al., 2003].

The removal of one or both H2A-H2B dimers from a mono-nucleosome is reversible, and can lead to an exchange reaction with histone dimers containing variants of histone H2A, such as H2A.Z (this study), and H2A.Bbd (Y. Bao and Y-J. Park, unpublished). We have also observed the reverse reaction in which a histone-variant containing nucleosome is converted into a canonical nucleosome (data not shown), demonstrating the lack of discrimination that yNAP-1 has for various H2A-H2B dimers, both free in solution and when bound to a nucleosome. Importantly, yNAP-1 – mediated histone exchange is independent of replication, does not require ATP, and does not result in the release of a significant amount of DNA or exchange of $(H3\text{-}H4)_2$ tetramer. This indicates that complete nucleosome disassembly and reassembly is not required.

yNAP-1 alone is unlikely to target histone variants to specific regions within chromatin. However, it is possible that yNAP-1 and other assembly proteins contribute to the incorporation of histone variants at specific regions within chromatin upon association with histone variant – specific chromatin assembly factors, such as the Swr1 complex that functions in conjunction with a yNAP-1 – H2A.Z-H2B dimer complex (the 'Nap-Z complex'; [Krogan et al., 2003]; [Kobor et al., 2004]; [Mizuguchi et al., 2004]). The Swr1 complex catalyzes the exchange of an H2A-H2B dimer for an H2A.Z-H2B dimer in yeast in an ATP-dependent manner in both nucleosomal arrays and in mono-nucleosomes. Despite the

presence of the Nap-Z complex, these authors see very little exchange in the absence of ATP, in contrast to the 20% efficiency of yNAP-1 – dependent exchange of ~ 20% reported here.

Finally, we have shown conclusively that the ability of yNAP-1 to transiently remove one or both H2A-H2B dimers from a nucleosome facilitates nucleosome sliding from a positioning sequence to an energetically more favorable end position. Our data indicate that yNAP-1 functions in a catalytic manner, independent of ATP. A truncated version of yNAP-1 lacking the acidic C-terminal domain, which is capable of binding histones and assembling chromatin, but has lost its ability to extract a H2A-H2B dimer from the NCP, is incapable of promoting this sliding reaction. Repositioning is directional in that no yNAP-1 – mediated nucleosome movement from the end-position to the central position is observed. In this, yNAP-1 functions like the ATP-dependent remodeling factor dMi-2 and its recombinant ATPase subunit ISWI, which also moves centrally positioned nucleosomes to an end-position, but is unable to facilitate movement from the end to the center of the DNA [Langst and Becker, 2001]. Intriguingly, it has been found earlier that yNAP-1 and nucleoplasmin increase the stimulation of Gal4 binding to mono-nucleosome brought upon by the SWI/SNF complex, indicating that histone chaperones and remodeling factors may act synergistically [Cote et al., 1994].

While the net effect of yNAP-1 and ATPases such as ISWI is similar, the mechanism by which these factors act is likely to be distinct. First, yNAP-1 dependent nucleosome-sliding depends completely on its ability to remove and

subsequently replace one or both H2A-H2B dimers. In contrast, in the presence of ATP-dependent remodelers, dimer exchange occurs subsequent to the movement of nucleosomes away from their initial locations coincident with and subsequent to the arrival of nucleosomes at positions at and beyond DNA ends, suggesting that H2A-H2B destabilization is not an obligate step in nucleosome movement [Bruno et al., 2003]. Second, yNAP-1 does not require energy from ATP hydrolysis to dissociate the histone dimer or to slide the nucleosome. Third, although apparently catalytic, yNAP-1 is not a motor and therefore does not actively move nucleosomes along the DNA, but rather appears to lower the energy barrier that normally prohibits spontaneous nucleosome sliding to energetically favorable positions.

Since members of the class of acidic histone chaperones (of which yNAP-1 is just one representative) are very abundant in the cell, their *in vivo* role may well be significant. For example, histone chaperones may play a role in introducing H2A variants into chromatin in a replication-independent manner, and in aiding nucleosome (re)-positioning along the DNA by lowering the significant energy barrier that must exist for nucleosome sliding. NAP-1 may also contribute to the disassembly and reassembly of nucleosomes during transcription initiation and elongation, as discussed above (Fig. 7).

The role of NAP-1 (and presumably that of other acidic histone chaperones) is clearly evolving, from being viewed as a mere histone escort that manages histone transport into the nucleus before handing its precious cargo over to chromatin assembly and remodeling factors, to a much more glamorous role in

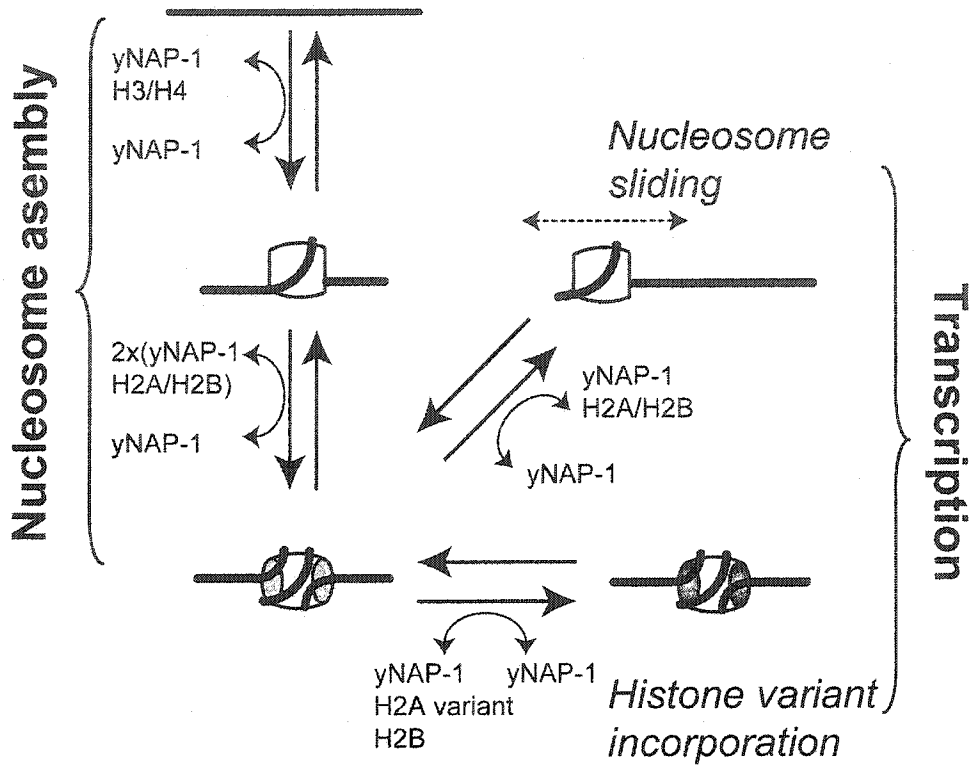

Figure 7. The multiple faces of yNAP-1. yNAP-1 is capable of stepwise assembly of nucleosomes *in vitro,* and appears to be involved in this process *in vivo.* A $(H3\text{-}H4)_2$ tetramer (white cylinder) is deposited on the DNA, followed by addition of two H2A-H2B dimers (grey ovals) to form a folded nucleosome. The reactions are reversible, resulting in transient H2A-H2B dimer removal leading to H2A/H2B exchange (and possibly the incorporation of histone variant dimers, dark grey ovals) and / or nucleosome sliding.

maintaining chromatin and nucleosome fluidity and dynamics. Similarly, chromatin, once assembled, has once been viewed as an 'immovable object' that only an advancing replication fork (and possibly an advancing RNA polymerase) can displace [Kornberg and Lorch, 1991], to a highly dynamic and malleable assembly that is capable of extensive cross-talk with the cellular machinery. Much remains to be learned on how this is achieved mechanistically, and doubtlessly many activities that are involved in this important aspect of chromatin metabolism remain yet to be discovered.

3.6 Acknowledgements

Supported by grants from the National Institutes of Health (GM561909 and GM067777)

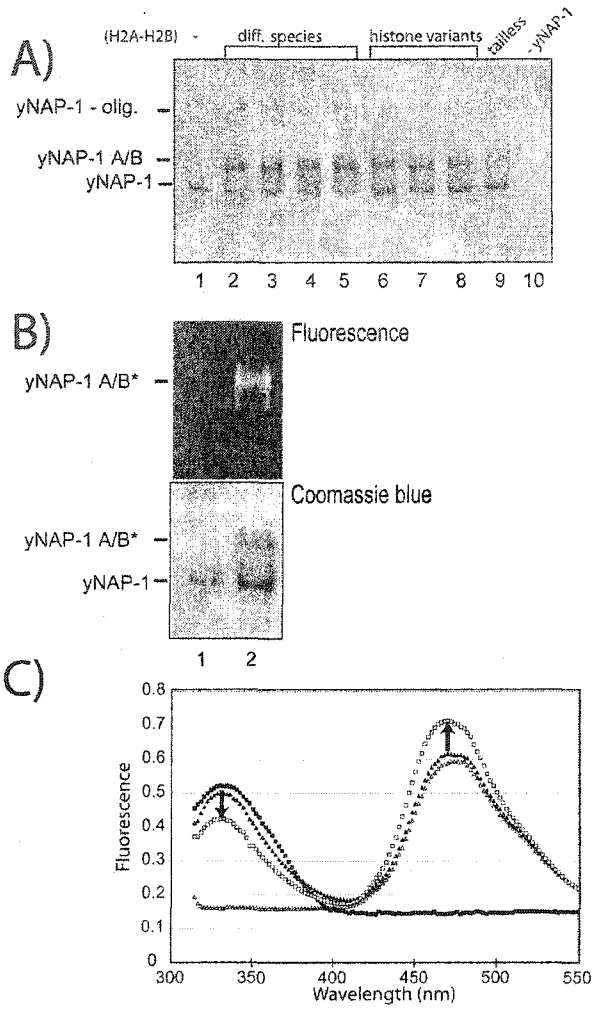

Supplementary Figure 1. Interaction of yNAP-1 with histone (H2A-H2B) dimer. (A) 10 µM yNAP-1 was incubated in the absence of (H2A-H2B) dimer (lane 1) or presence of 5 µM (H2A-H2B) dimer derived from yeast (lane 2), *Xenopus laevis* (lane 3), mouse (lane 4) and drosophila (lane 5). Lanes 6-9 shows binding of yNAP-1 to 5 µM dimers composed of human H2A Bbd and mouse H2B (lane 6), mouse H2A.Z and *Xenopus laevis* H2B (lane 7), human macroH2A histone domain and *Xenopus laevis* H2B (lane 8), and *Xenopus laevis* H2A and H2B in which the tails had been deleted (lane 9). Lane 10 shows *Xenopus laevis* (H2A-H2B) dimer in the absence of yNAP-1. Samples were incubated at 4 °C for 10 hours, and complex formation was analyzed by native PAGE. The position of yNAP-1 – (H2A-H2B) dimer complex (yNAP-1 A/B) and yNAP-1 are indicated, as is the an oligomeric form of yNAP-1 that we sometimes observe **(B)** (H2A-H2B) dimer from *Xenopus laevis* was labeled with CPM at H2B T112C. 10 µM yNAP-1 was incubated in the absence or presence of fluorescently labeled (H2A-H2B) dimer (A/B*; lane 1-2: 0 and 5µM). Incubation and gel electrophoresis was done as in (A). The gel was photographed without staining to view fluorescence (upper panel), then stained with coomassie blue (lower panel). **(C)** A complex of yNAP-1 with fluorescently labeled (H2A-H2B) dimer was prepared at a molar ratio of 1:1. Under these conditions, no free yNAP-1 is present. Tryptophan was excited at 300nm, and fluorescence of the complex was monitored (□). The same complex was analyzed at 1.25 M NaCl (▲). The emission spectrum of free (CPM labeled H2A-H2B) dimer (Δ) and yNAP-1 (■) is shown as a control.

Chapter 4

X-ray Crystallography studies on the structure of Nucleosome Assembly Protein 1 (NAP-1)

Young-Jun Park performed all of the experiments. Brant Eutzy and Derek J. Williams identified the initial crystallization condition of full length NAP-1 and NC-truncated NAP-1.

4.1 Abstract

Nucleosome assembly protein 1 (NAP-1) is a key cellular component for chromatin assembly. Here we describe the crystal structure of yeast NAP-1. The structure shows that the entire molecule has 2-fold rotational symmetry composed of a dimerization domain and concave β-strands. The arrangement of structural elements within NAP-1 results in a new protein fold with unique features.

Although the current structure of NAP-1 from yeast displays a previously unknown fold, there are nevertheless some structural similarities with other histone chaperone proteins. A substructure, four anti-parallel β-strands, is shared by all of the histone chaperones (NAP-1, Nucleoplasmin, ASF-1, CAF-1, and HirA), and may represent their common mode of binding to histones. This comparison shows that although there are overall structural differences, related structural elements may be employed for similar tasks. The different stages of oligomerization provide a good structural basis for the various approaches to the chromatin assembly reaction. This observation might be interesting in terms of structural evolution of proteins involved in histone binding or nucleosome assembly.

4.2 Introduction

Chromatin contains the genetic information in all eukaryotic cells. The basic structural unit of chromatin is the nucleosome in which 146 base pair of DNA are wrapped around the histone octamer that consists of two molecules each of the histones H2A-H2B and H3-H4 [Luger et al., 1997a].

Nucleosome assembly occurs through the stepwise deposition of the H3-H4 tetramer followed by H2A-H2B onto replicating DNA. The chromatin assembly factor 1 (CAF1) binds histones H3 and H4, and targets these histones to the DNA replication fork (reviewed in [Krude and Keller, 2001]). The nucleosome-assembly protein 1 (NAP1) directly binds to core histones H2A-H2B and transfers them onto naked DNA (reviewed in [Ishimi and Kikuchi, 1991; Krude and Keller, 2001]).

NAP1 was first identified in mammalian cell extracts by its intrinsic ability to facilitate nucleosome assembly *in vitro* [Ishimi et al., 1984; Ishimi et al., 1987]. Subsequent studies have demonstrated that NAP-1 is conserved in all eukaryotes from yeast to human [Ishimi and Kikuchi, 1991; Ishimi et al., 1983; Ito et al., 1996a; Steer et al., 2003]. In addition to its nucleosome assembly activity, recent studies suggest that NAP-1 is involved in transcriptional regulation [Chen et al., 1994; Ito et al., 2000; Kawase et al., 1996; Shikama et al., 2000]. It may also function in the regulation of cell cycle. NAP-1 has been shown to interact with CLB2, kinase Gin4, and NAP-1 binding protein [Altman and Kellogg, 1997; Kellogg and Murray, 1995; Shimizu et al., 2000]. The role of NAP-1 in regulation

of the nucleosome dynamics was also investigated (Chapter 3 or [Park et al., 2004a]). Park and co-workers found that NAP-1 has the ability to remove and replace H2A-H2B dimers from nucleosomes, and nucleosome sliding occurs as a consequence of H2A-H2B dimers destabilization. The C-terminal acidic region (365-417) of the NAP-1 is required for the dissociation of histone H2A-H2B dimer.

Fujii-Nagata and co-workers used a deletion mutations to analyze the function and structure of NAP-1 [Fujii-Nakata et al., 1992]. McBryant and co-worker also have used a similar approach to show that core domain (74-365) is the minimum domain for the stability of structure and the function of nucleosome assembly [McBryant et al., 2003]. Sedimentation equilibrium experiments revealed that stable yNAP1 dimers and self-associated oligomers exist in a solution state [McBryant et al., 2003].

To investigate the atomic structure of NAP-1, we used X-ray crystallography. Here we report the crystal structure of NAP-1. Full-length NAP-1 and truncated proteins were crystallized. Phases were determined by Multiwavelength Anomalous Dispersion (MAD). Experimental density maps were calculated, and the partial backbone structure of NAP-1 was built. This study reveals that NAP-1 exhibits a novel fold containing a long α-helix and the concave β-strands that bear some similarity with other known histone chaperon proteins. The results of this study represent the first step toward mapping the interactions with histone and provide important information about the structural relationship between

histone chaperones in the different functions.

4.3 Experimental Procedures

Preparation of yeast NAP-1 protein - An expression plasmid for yeast NAP-1 (yNAP-1) was introduced into *E. coli* (BL21-DE3) cells [Fujii-Nakata et al., 1992]. To prepare the selenomethionine (SeMet) derivative protein, we modified previously used protocols to purify yNAP-1 protein [McBryant et al., 2003]. We used the same E. coli host strain as that used in the previous culture grown in regular growth medium, together with the same plasmid construct. The expression host does not have to be a methionine auxotroph. The first cells were cultured in Luria-Bertani (LB) broth `medium (1% tryptone, 0.5% yeast extract, and 10% NaCl). The cells from overnight culture in LB medium were spun down and resuspended in M9 medium (6.8g anhydrous Na2HPO4, 3g KH_2PO_4, 0.5g NaCl, 1g NH_4Cl, 0.4% glucose, 2mL of 1M $MgSO_4$, 0.1mL of 1M $CaCl_2$, 100 µl of 0.5% thiamine per liter), and then added to 1liter of the same, pre-warmed medium. The final fermentation culture in M9 minimal medium contained glucose (0.4% w/v). The cells were cultured until the OD600 reached 0.8. At this point, the selenomethionine amino acid cocktail (60mg selenomethionine, 100mg lysine hydrochloride, 100mg threonine, 100mg phenylalanine, 50mg leucine 50mg isoleucine, 50mg valine per liter) was added. Fifteen minutes later, yNAP-1 was induced by the addition of isopropyl β–D-thiogalactopyranoside (IPTG) for 4 hours. The cells were lysed, and the protein was precipitated by ammonium sulfate (from 35 to 65%). The protein was further purified using a Q-sepharose

column and Mono-Q column. Employing these optimized approaches, we were able to obtain 5mg of yeast NAP-1 per liter of cell culture. The incorporation of all four selenomethioniones was verified by mass spectrometry. Mass spectra of SeMet-labeled protein showed that ~ 90% of the protein had the methionine derivative incorporatedh.

Crystallization and data collection - Recombinant yeast NAP-1 was crystallized at 4°C by the hanging drop vapor diffusion method from the protein sample (15 mg/ml, in 20 mM Tris-HCl pH 7.5, 1 mM dithiothreitol) combined in a 1:1 ratio with reservoir solution. The crystals were transferred to stock solutions containing the stepwise increased glycerol (0, 5, 10, 15, 20 and 25 %) with stabilization solution, and were flash frozen in liquid nitrogen. The structure was determined by multiwavelength anomalous dispersion (MAD) method, mainly using selenomethionine derivative crystals and platinum-derivative crystals. The heavy atom derivative was obtained by soaking the crystal in the heavy atom stock solution. Diffraction data were collected at beamline ALS 5.0.2. Data were processed with Denzo, and reduced with SCALEPACK [Otwinowski and Minor, 1997]. The positions of the heavy atoms were determined using SOLVE [Terwilliger, 2004]. The structure model was refined against the native dataset using CNS [Brunger et al., 1998]. Graphical presentations were prepared using PYMOL [DeLano, 2002]. Structure-superimpositions were carried out using LSQMAN. The accessible surface area for each of the individual proteins and the surface of the complex were calculated using CCP4 program "AREAIMOL" [Lee and Richards, 1971]. The area of interaction per monomer (buried surface area)

was calculated by ((Area of monomer + Area of monomer) - Area of dimer) / 2.

4.4 Results

4.4.A Crystallization and data collection of NAP-1 - After surveying approximately 500 crystallization conditions, we obtained diffracting yNAP-1 crystals. All screens were created in the same fashion using the hanging drop technique. To find optimal crystallization conditions, the screen consisting of varying concentrations of salt, varying concentrations of yNAP-1 and varying temperature was set up. Crystals were obtained from a solution of 250mM ammonium phosphate, 4° C and the pH of the crystallization solution was close to the theoretical isoelectric point of yNAP-1. Large crystals with dimension of approximately 0.5mm x 0.5mm x 0.3mm were formed after 3 weeks. yNAP-1 protein in crystals was characterized by electrophoresis (Fig. 1).

We tested initial diffraction at room temperature using conventional capillary mounting. To improve the results, we proceeded to screen for conditions that allow us to collect data under cryogenic temperature. The effects of cryo-protectant and stabilization conditions on diffraction quality were tested using our own rotating anode x-ray generator. Some crystals diffract strongly up to 3Å on the Rigaku rotation anode X-ray generator with mirror optics at 50KV and 90mA.

Recombinant protein substituted with selenomethionine (SeMet) was crystallized by cross-seeding with native crystals. The crystal diffraction was

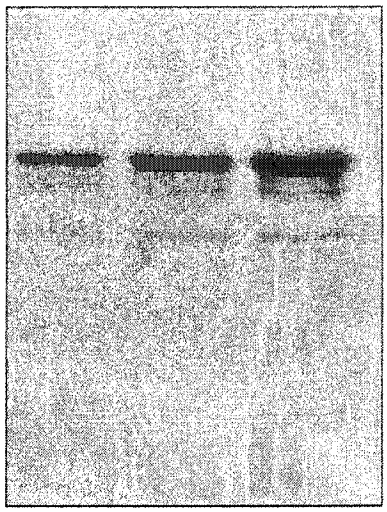

Figure 1. An analysis of the yNAP-1 protein in crystals. 15% SDS denaturation gel electrophoresis was used to analysis the protein in crystals; lane 1, full-length yNAP-1 protein control; lane 2, mother liquor; lane 3, crystals.

highly anisotropic, with a resolution of about 2.8 Å in the best direction and about 3.5 Å in the other two directions, as observed for native crystals of similar size. The space group ($P4_32_12$ or $P4_12_12$) and cell dimensions were maintained compared to unmodified protein crystals.

4.4.B The heavy atom derivative protein crystals - Incorporation of selenium atom in protein via selenomethionine is a preferred method for protein crystallography [Hendrickson et al., 1990]. However, in hindsight, SeMet MAD was not the best method because only two out of the four selenomethionines within 417 amino acids are sufficiently ordered in the crystal structure. A rough rule of thumb is that 1 selenomethionine per 100 amino acids is sufficient for a SeMet MAD experiment [Garman and Murray, 2003]. As an alternative method, we used heavy atom derivatives. To prepare a heavy atom soaked protein crystal, 75 different heavy atoms were tested. We tested 5 different conditions (variation of concentration and soaking time) for each heavy atom. Diffraction quality was tested using an in-house rotating anode x-ray generator. Hg or Au heavy atom derivative crystals did not diffract. W and Pt were the only heavy atoms that we could use for this study. Using MIR (multiple isomorphous replacement) phasing method, we tried to find the heavy atom positions. All of the derivative data were scaled against the scaled native data. After scaling, the data for the derivatives were combined with the native data to generate the isomorphous difference Patterson map. A crystal with a heavy atom should have corresponding peaks in the difference Patterson map, which is located at a

crystallographic symmetry -related position. These heavy atoms produce peaks in a Harker section corresponding to this crystallographic symmetry. The search for these self-vector peaks started from the Harker section. Two heavy atom sites were found in two different platinum derivatives.

As an alternative approach, we used intrinsic anomalous scattering from the 8 sulfur atoms in the full-length NAP-1 native crystals [Yang et al., 2003]. Although a few of the new structures have been solved from sulfur anomalous scattering data collected on a rotating anode source rather than at a synchrotron [Debreczeni et al., 2003; Schuermann and Tanner, 2003], the main problem of this approach is the small anomalous signal obtained from sulfur with conventional copper anode targets. To overcome this problem, we used a chromium anode [Olsen et al., 2004]. Data were collected using a rotating chromium anode with a helium x-ray path. Unfortunately, we could not obtain a solution because of weak phasing power. As examples, peptide structure with 17 sulfurs /207 amino acids, 14 sulfurs /245 amino acids and 8 sulfurs /219 amino acids s were determined by sulfur anomalous scattering method [Phillips et al., 2004; Yang et al., 2003]. In contrast, in NAP-1, only five-ordered sulfur atoms exist in a 417-amino acid protein.

4.4.C MAD (Multiple wavelength anomalous dispersion) - The primary difficulty in macromolecular X-ray crystallography is the phase problem. This is a problem of determining the phase angle to be associated with each structure factor, so that an electron density map may be calculated from a Fourier series with the structure factors as coefficients. Currently, there are several available

methods for overcoming this fundamental problem: Molecular Replacement (MR), Multiple Isomorphous Replacement (MIR), Multiple Wavelength Anomalous Dispersion (MAD), Single Isomorphous Replacement (SIR) and Direct Methods (Fig. 2). For yeast NAP-1 structure, we mainly applied the MAD method using heavy atom derivatives. One of the heavy atoms that we used is selenium. It is useful both for phase determination by MAD and for the location of methionine residues as an aid to polypeptide chain tracing. Because MAD data are observed from a single frozen crystal, non-isomorphism is usually negligible. Furthermore we used the inverse-beam method, known as the "Friedel flip method", to minimize errors in collecting anomalous data. The anomalous signal is much lower than that of isomorphous replasement experiments. To maximize the anomalous scattering signal, we collected data at different wavelengths. The absorption edge wavelengths were identified by X-ray fluorescence scan (Fig. 3). A scan of X ray-induced fluorescence showed selenium, platinum and tungsten absorption peaks at 0.97949Å, 1.072Å and 1.2147Å, respectively. We collected two or three complete data sets from a single crystal containing full-length heavy atom-soaked crystals (Table 1). Data were processed with Denzo and reduced with SCALEPACK [Otwinowski and Minor, 1997]. Indexing of diffraction patterns was successful, assuming tetragonal symmetry. Because the intensities along the (00L) direction showed significant values only for L = 4n, the presence of a screw operation (4_3 or 4_1) was indicated. Data collection statistics are shown in Table 1. The coordinates for two of the four possible Se atom positions were determined by SOLVE from a multiwavelength anomalous

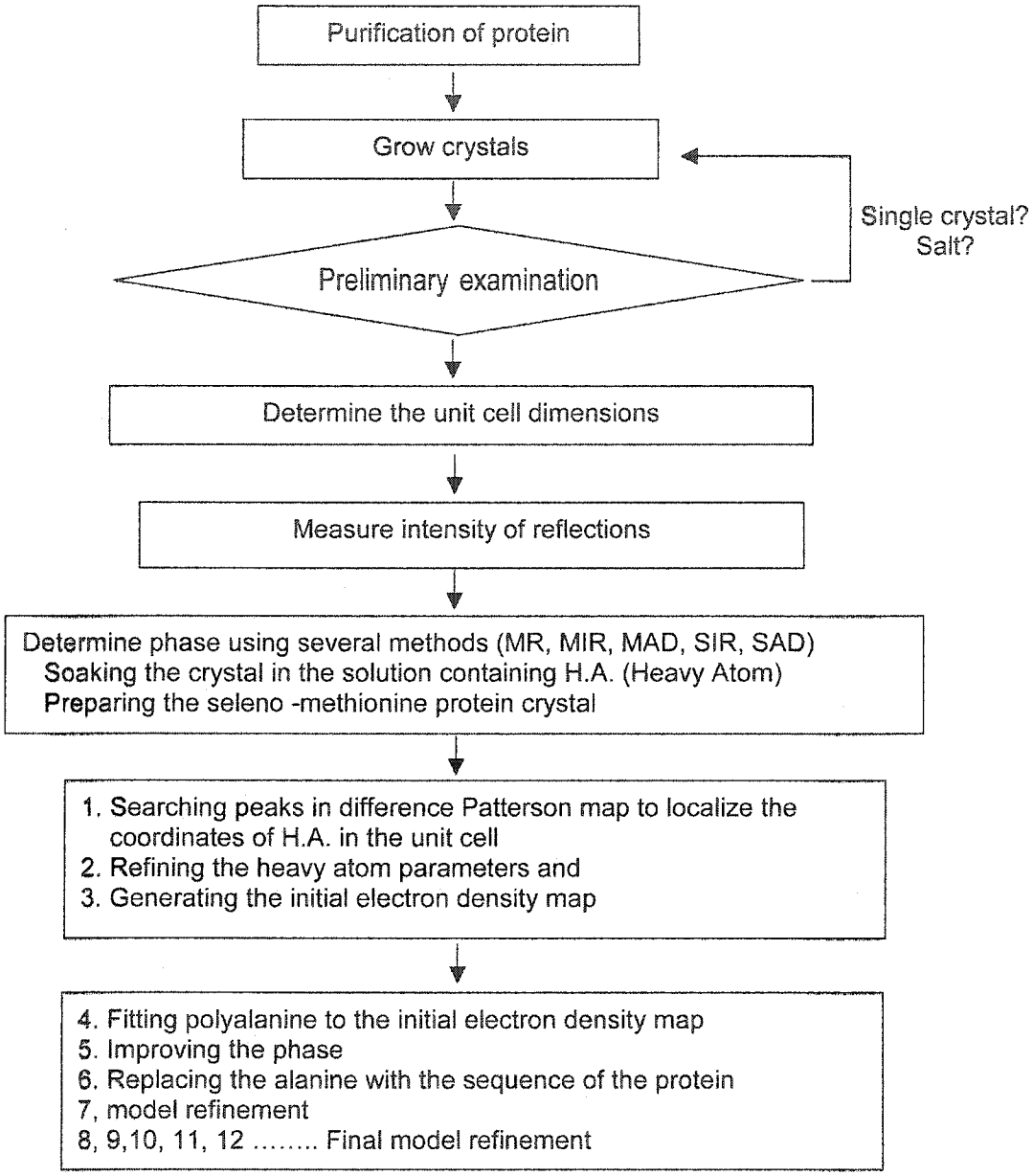

Figure 2. Schematic of the determining the protein structure

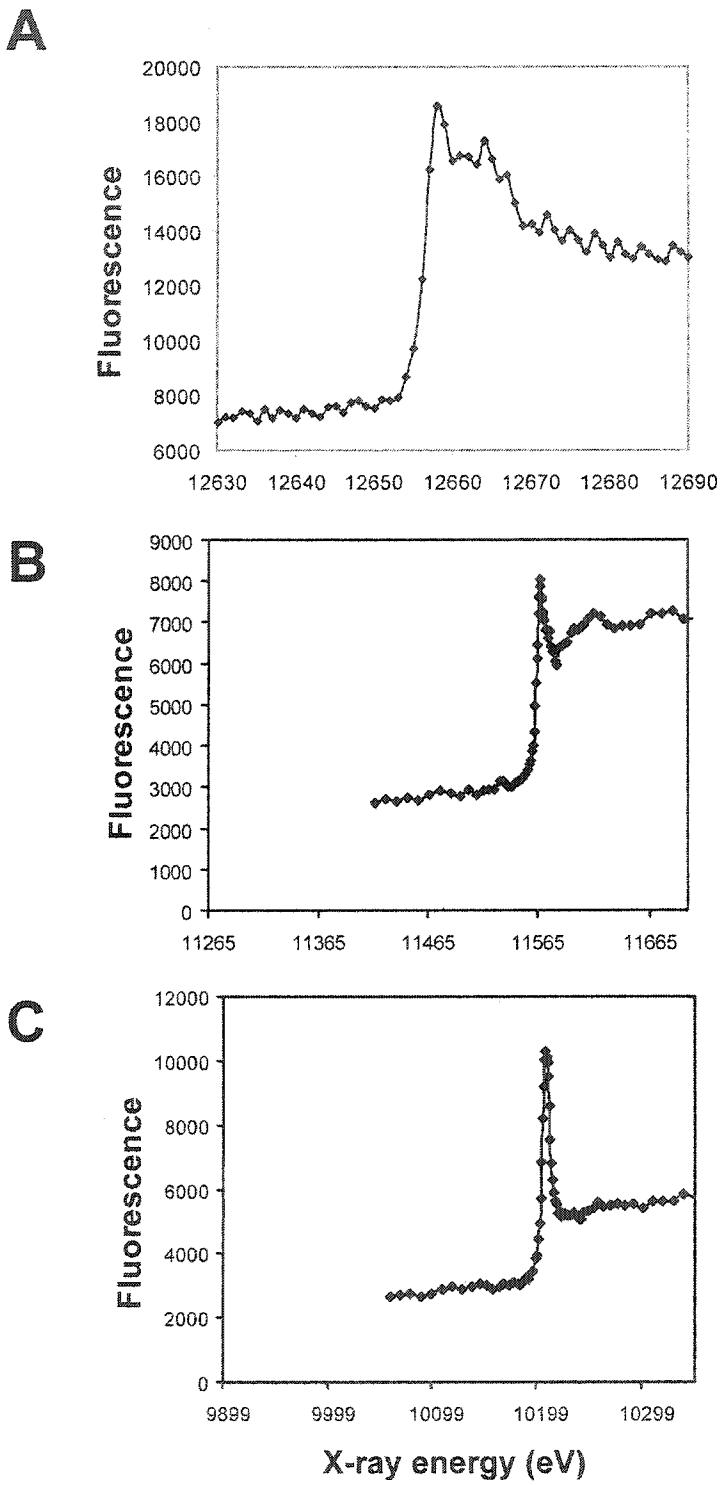

Figure 3. X ray Fluorescence spectrum of heavy atom derivative crystal. **A)** Se, **B)** Pt, **C)** W atom aborption spectrum measured as X-ray fluorescence at beamline ALS 502.

Table 2. Data collection statistics

	Native protein crystal		Heavy atom derivative protein crystal									
Protein	NAP (1-417)	NAP (74-417)	NAP (1-417)									
Heavy atom			Se [a]			W [b]		Pt [c]			Pt [d]	
Wavelength (Å)	1.1	1.1	0.9796	0.9795	0.9643	1.214	1.253	1.072	1.100		1.072	1.1005
Space group	$P4_32_12$	$P4_32_12$	$P4_32_12$			$P4_32_12$		$P4_32_12$			$P4_32_12$	
Unit cell dimension (Å)	a = b = 86.7 c = 176.1		a = b = 86.9 c = 176.6			a =b = 86.4 c = 178		a = b = 84.9 c = 179.3			a = b = 85.8 c = 177.56	
Resolution range (Å)	50-3.0	50-3.2	50-3.0			50-3.1		50-3.7			50-3.25	
Mosacity	0.619	0.6	0.488			0.5		0.418			0.493	
Completeness (%) [e]	99.3 (93.4)	98.6 (86.6)	99.8 (98.3)	98.3 (94.3)	96.9 (81.4)	99.7 (99.5)	99.8 (99.9)	99.7 (99)	99.5 (99)		99.9 (99)	99.8 (99.0)
Rmerge [e f]	0.061 (0.2)	0.079 (0.37)	0.055 (0.145)	0.059 (0.179)	0.05 (0.198)	0.103 (0.35)	0.071 (0.298)	0.056 (0.408)	0.042 (0.389)		0.079 (0.307)	0.061 (0.285)
I / σ (I) [e]	24.3 (3.7)	22.7 (3.9)	29.9 (4.7)	27.9 (3.3)	28.7 (3.9)	14.6 (2.6)	18.4 (3.1)	19.4 (2.9)	16.9 (1.8)		13 (1.9)	10.5 (1.8)
No. of heavy atom sites			2			2		2			2	
Figure of merit[g]			0.46			0.48		0.47			0.48	
Refinement Resolution range Residue built R R free(10% of DATA)	50 – 3.2 240 38 39											

[a] Selenomethionine, [b] Ammonium tetrathio tungstate, [c] Dichloroethlene diamine platinum, [d] Di-mu-ido bis (ethylenediamine) di platinum
[e] Values in parentheses refer to data in the highest resolution shell.
[f] $R_{merge} = \Sigma \mid I_h - \langle I_h \rangle \mid / \Sigma I_h$, where I_h is the mean of the measurements for a single hkl.
[g] Figure of merit was calculated by CNS.

diffraction (MAD) data set collected from a single Se-Met crystal. We also identified the heavy atom peaks from platinum (Pt) and tungsten (W). It became clear at this stage that the screw operation was $P4_3$ and not $P4_1$; thus, the space group was determined to be $P4_32_12$. The electron density map calculated from Se or Pt -MAD phase showed clear features of α-helices and revealed most of the loops connecting them (Fig. 4). To calculate experimental density map, the "SOLVE" and "CNS" program are used [Brunger et al., 1998; Terwilliger, 2004]. Polyalanine chains were initially fitted into the visible secondary structure density map using the program "O" [Jones et al., 1991]. In the electron density map, the SeMet MAD map shows better helix structure and the platinum MAD map gives better strands. By comparing the electron density maps of those three different MAD results, the initial backbone was fitted and connected. As the partial structure of NAP-1 was traced, the refinement of the model was started. The refinement was carried out by the program "CNS" [Brunger et al., 1998]. The combination of several specific refinement methods was applied to refine the model of NAP-1. We, then, replaced the alanine with the sequence of the protein.

4.4.D Structure description - NAP-1 has 417 amino acid residues, and the crystal structure of NAP-1 provides the structural information of the NAP-1 core domain (residue number from 74 to 365). In the present study, three of the crystals were prepared from the full-length (1 to 417), N-terminal truncated (74 to 417), and NC-terminal truncated (74 to 365) proteins. No electron density corresponding to the N-terminal segment or C-terminal segment was visible in any of the maps. Tests of the supposedly full-length protein indicated that it had

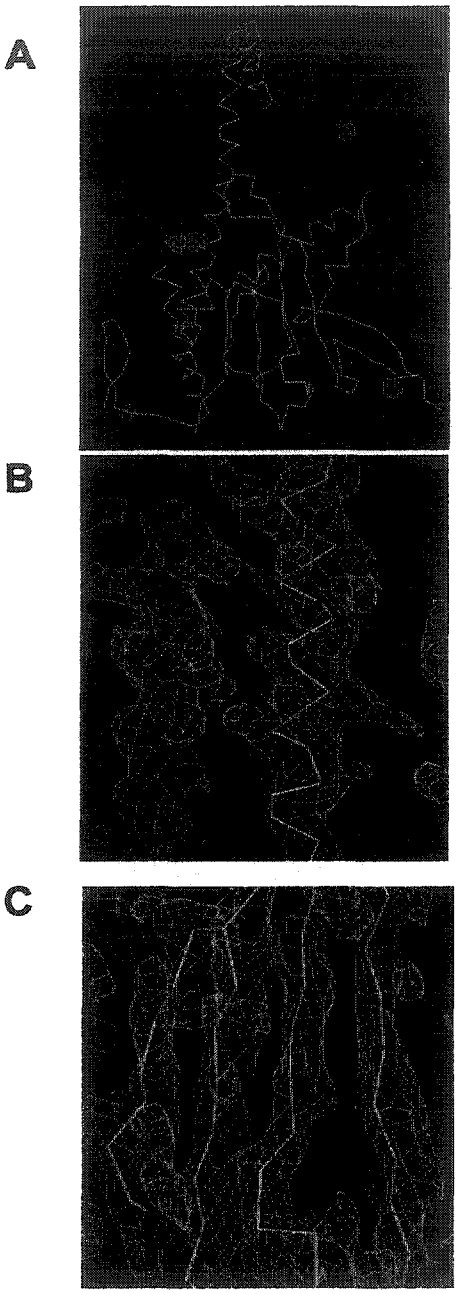

Figure 4. The initial electron density map without refinement.
The experimental density map was calculated by the program "solve" and "CNS". Anomalous difference (Se) fourier map is shown in (A). It shows clearly α-helix and β strands structure at Se (B) and at Pt (C) MAD phasing map. The maps contoured at the 10 σ (A) and 1 σ (B and C) level. The α-carbon trace of the refined NAP-1 is shown as a stick representation.

not lost the N- or C-terminal segment during either storage or crystallization. The combined observations suggest that the N and C-terminal segment are normally disordered, which agrees well with the results of in vitro studies [McBryant et al., 2003] [Fujii-Nakata et al., 1992]. The core domain (residue number 74 to 365) that we observed in this study is the essential domain for histone binding and nucleosome assembly reaction [McBryant et al., 2003] [Fujii-Nakata et al., 1992] .

In the NAP-1 protein crystals, NAP-1 monomer structure was identified as the asymmetric unit (ASU), and the crystallographic 2-fold symmetry generates a homodimer (Fig. 5). This observation is consistent with solution studies [McBryant and Peersen, 2004b]. When calculating the buried surface area between NAP-1 monomers in the present structure, a value of 3054 $Å^2$ is found. This number is much higher than the 'threshold (1600 $Å^2$)' given in Janin [Bahadur et al., 2004; Janin, 1997] for non-specific protein-protein interactions that are due simply to crystal packing effects.

The molecular 2-fold axis coincides with one crystallographic 2-fold axis. This symmetry operation aligns the two monomers in an antiparallel orientation so that the N-terminal helix of one monomer packs against that of the second monomer. The dimeric NAP-1 has an overall ellipsoidal shape and approximate dimensions of 75 × 57 × 32 Å. This structure consists mainly of a long helix and four β-strands. The structure of dimeric NAP-1 can be divided into two domains. The central domain consists of two antiparallel helices. The central helix spans a total

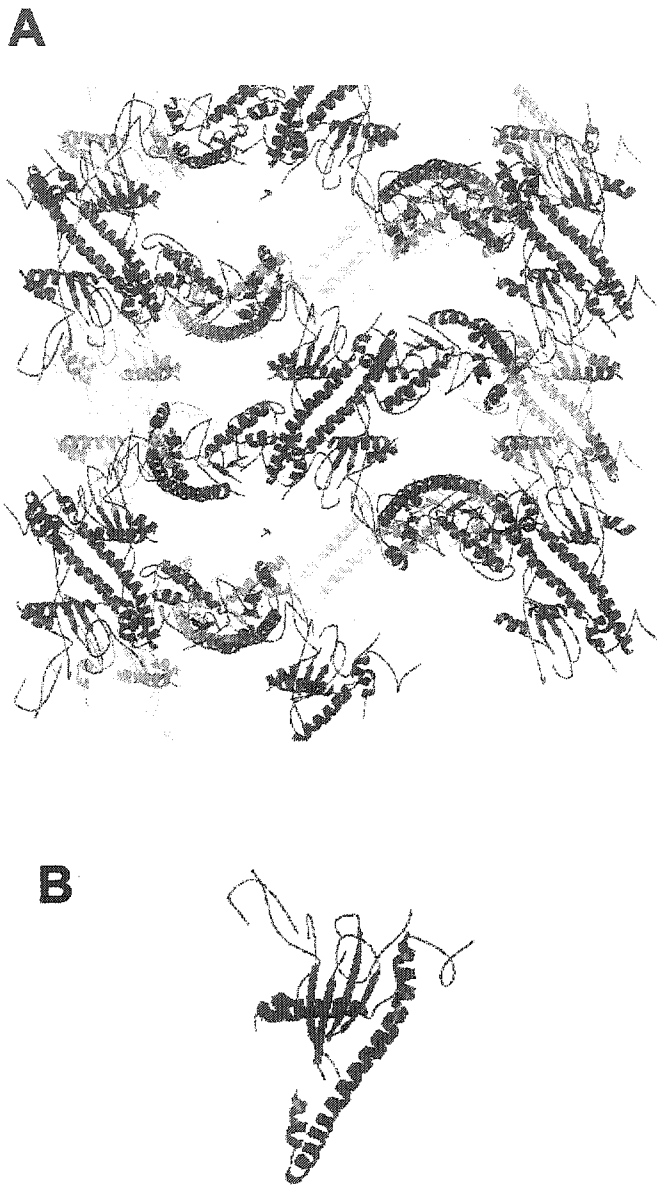

Figure 5. The crystal packing and NAP-1 structure within the asymmetric unit. The crystal packing of yNAP-1 (A) and overall fold of yNAP-1 monomer at the current stage of refinement (B) are shown.

of 48 amino acids and a distance of approximately 69 Å. The unique feature of this structure is the presence of a non-coiled coil dimerization motif in which each monomer contributes a long α-helix that participates in a pair in the dimer, and loop domains wrapping around adjacent helices (Fig. 6). Two adjacent helices are slightly curved in the middle so that the antiparallel bends by a few degrees (26° and 32°) making a "sigmoid helix motif". The side domain of the NAP-1 is composed of four β strands. The second part of the substructure, a four-stranded antiparallel beta-sheet, is relatively concave and is covered on one side by helices (Fig. 6). The β-sheet domain from each NAP-1 monomer does not contribute to the dimer interface formation. The lower part of the antiparallel β-sheet domain is the histone fold-like (HFL) domain, helix-loop-helix structural motif (1.5 Å r.m.s. difference, see Fig. 7). This has a very stable interface with the antiparallel β-sheet domain. Such interactions could perhaps provide the stability of the antiparallel β-sheet domain. The cavity below the antiparallel β-sheet domain may provide the binding site for other proteins. Although we have not identified the histone-binding site of yNAP-1 yet, this possibility is attractive since the histone fold-like domain exists in this cavity.

We compared the NAP-1 structure with the known histone chaperone protein structures (Fig. 8). The results show that the anti-parallel β-strand domain of the NAP1 is topologically similar to other histone chaperones such as nucleoplasmin (pdb access code 1kfj), ASF-1 (pdb access code 1roc), CAF-1 (homology model, see Fig. 9) and Hira (homology model), which are involved in histone binding and nucleosome assembly.

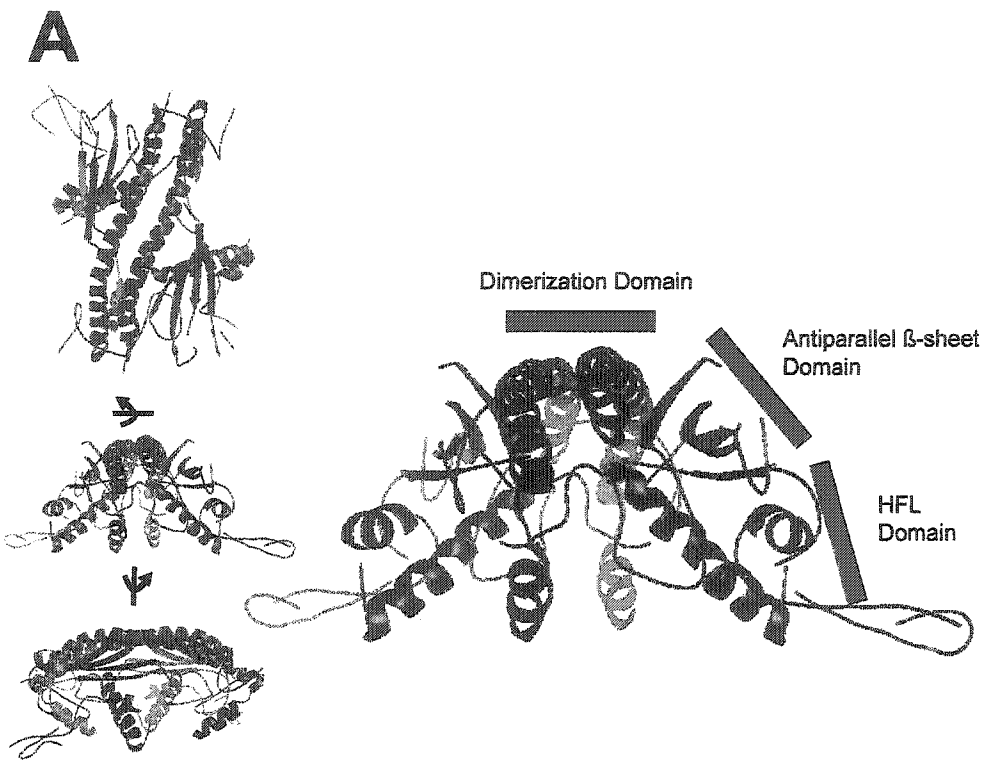

B

1 MSDPIRTKPK SSMQIDNAPT PHNTPASVLN PSYLKNGNPV RAQAQEQDDK IGTINEEDIL

61 ANQPLLLQSI QDRLGSLVGQ DSGYVGGLPK NVKEKLLSLK TLQSELFEVE KEFQVEMFEL

121 ENKFLQKYKP IWEQRSRIIS GQEQPKPEQI AKGQEIVESL NETELLVDEE EKAQNDSEEE

181 QVKGIPSFWL TALENLPIVC DTITDRDAEV LEYLQDIGLE YLTDGRPGFK LLFRFDSSAN

241 PFFTNDILCK TYFYQKELGY SGDFIYDHAE GCEISWKDNA HNVTVDLEMR KQRNKTTKQV

301 RTIEKITPIE SFFNFFDPPK IQNEDQDEEL EEDLEERLAL DYSIGEQLKD KLIPRAVDWF

361 TGAALEFEFE EDEEEADEDE DEEEDDDHGL EDDDGESAEE QDDFAGRPEQ APECKQS

Figure 6. Structure of yeast NAP-1. A) Ribbon diagram. Figures were made using PyMol. **B)** Amino acid sequence. The sequence of *S. cerevisiae* NAP-1 is shown with secondary structure elements.

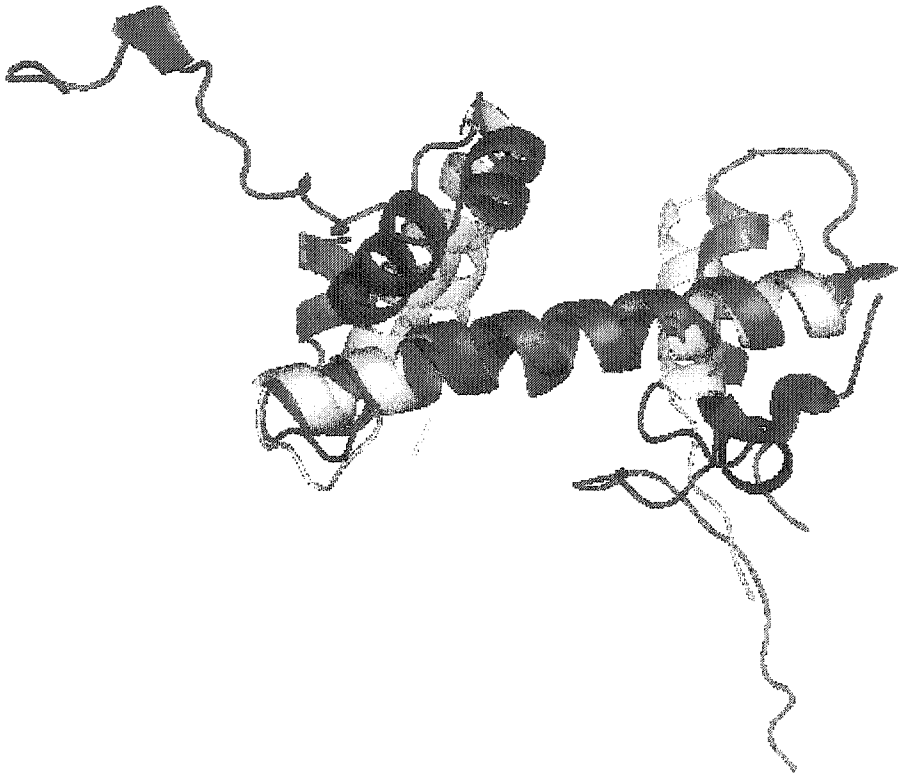

Figure 7. Superposition of histone fold like (HFL) domain and histones (H2A and H2B). Figure shows the superimposition of 3 peptides. Histone fold like domain of yNAP-1, histone H2A, and histone H2B shown in blue, red, and yellow, respectively. The superimposition and r.m.s.d were calculated by LSQMAN.

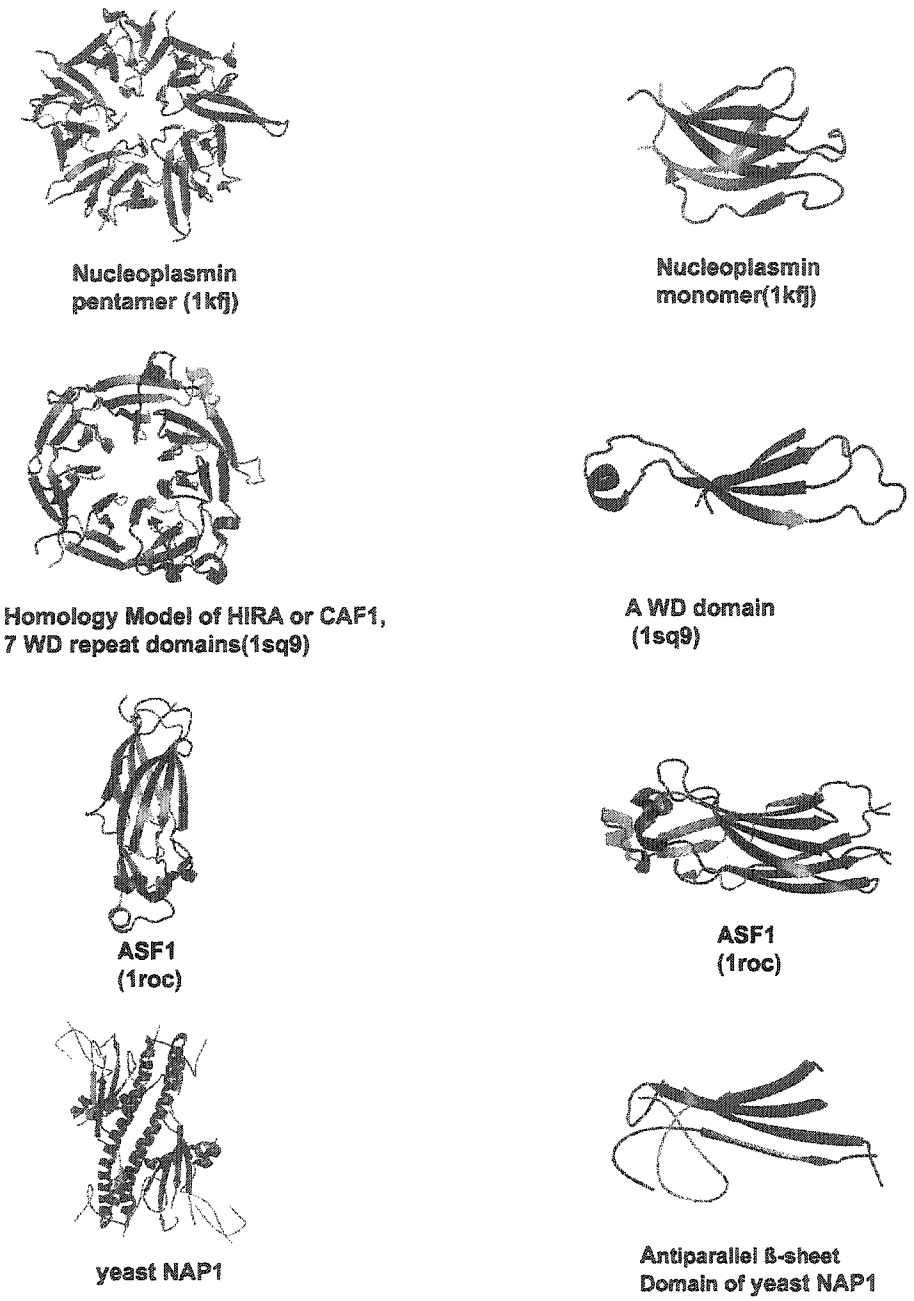

Figure 8. Structure of histone chaperones and concaved antiparallel beta-sheet motif within histone chaperones. pdb access codes are indicated.

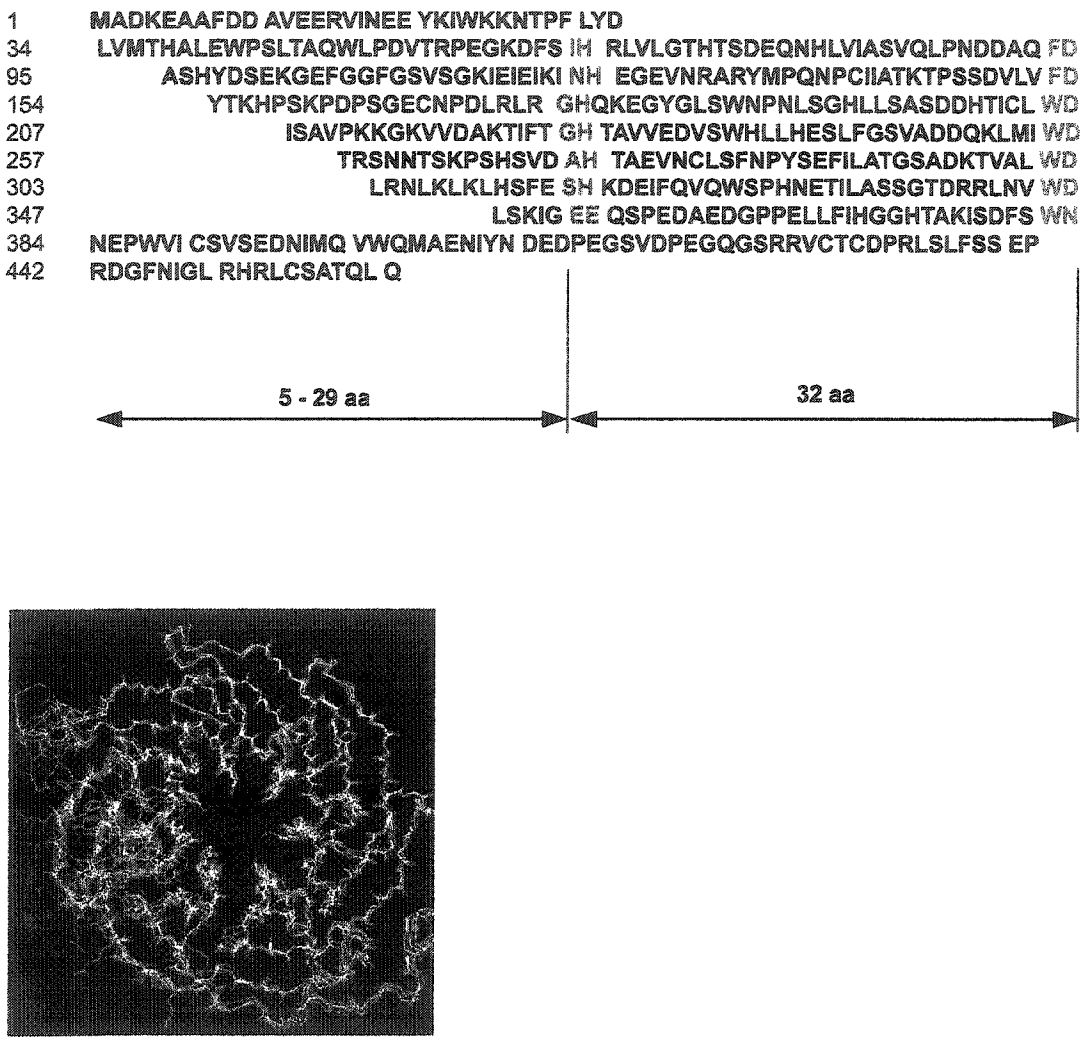

Figure 9. The Homology model of CAF-1 p55. Most of the conserved features involved in the WD repeat proteins are identified in the WD repeats of CAF1, p55. The characteristics are tryptophan-aspartate (WD) of each repeat, an aspartic acid residue six position N-terminal to the WD that is position in 85% of the WD repeats [Garcia-Higuera et al., 1998], glycine and histidine in GH motif, and serine(or threonine) residues of the WD repeat, which forms inter- and intra blade hydrogen bonds [Martínez-Balbás et al., 1998]. CAF-1 p55 protein homology-model was generated using SWISS-MODEL [Schwede et al., 2003].

The antiparallel β sheet domain of the NAP-1 structure and the currently available structures of histone chaperones (or homology model of CAF1 p55) are compared in table 2. The homology-model of CAF-1 p55 protein was generated using SWISS-MODEL depending on the amino acid sequence (Fig. 9) [Schwede et al., 2003]. The anti-parallel β sheet domain of NAP-1 was used in this measurement. The results revealed that there are moderate structural deviations (r.m.s.d from 1.7 to 2.2 Å) among the nucleosome chaperones. The most similar to NAP-1 is ASF-1, in which 48 % of the residues match with an r.m.s. difference of 1.677Å using a 3.5 Å cut-off. This comparison shows that all histone chaperones share the common structural motif, antiparallel β-sheet, although these do not structurally align precisely.

A search for proteins structurally homologous to NAP-1 was done using the Dali database [Holm and Sander, 1994; Holm and Sander, 1998]. The results revealed no information on the potential structural fold of the NAP-1. None of the histone chaperones were identified as a homology model. The variation in length of β-strands and the pronounced difference between sequence-based sequence alignments and structure-based sequence alignments of the "concave β-strands domain" explain why ASF-1 or nucleoplasmin were not identified as a homologous structures, although NAP1 is topologically similar to other histone chaperones such as nucleoplasmin, ASF-1, CAF-1 or Hira.

We finished the replacement of the alanines with the real sequence of the protein. However, high free R was observed (~39%). Possible explanations are that the main-chain tracing could be wrong, some part of the side chains are not

Table 2. Structural comparisons

	NAP-1[a]	Nucleoplasmin	ASF-1	WD domain of CAF-1
NAP-1	**59**[a]	2.2 Å	1.7 Å	1.7 Å
Nucleoplasmin	29 (49%)	**74**	1.9 Å	1.5 Å
ASF-1	48 (81%)	31 (42%)	**161**	1.7 Å
WD domain of CAF-1	29 (49%)	24 (32%)	35 (22%)	**41**

Numbers at top right (blue) are r.m.s. differences obtained using a cut-off of 3.5 Å in the superposition in "LSQMAN". Numbers at bottom left (red) are the number of residues matching (with % amino acid sequence identity in parentheses). And those on the diagonal (black) are the number of residues in the structures being compared.
[a] the anti-parallel β strands domain of yNAP-1 is used.

really correct, or the overall structure within the crystal is locally (or globally) disordered, even though we can see the electron density from experimental maps. We are cautious about proposing specific atomic contacts based upon this crude model although the initial model was finished. Specific locations of some of the side chains are still obvious because of locally weak experimental electron density map. Precisely determining the histone-binding geometry and locating the side chains, which are not currently apparent, will be the priority for our future experiments. In this chapter, we will only discuss the global structure of NAP-1.

4.5 Discussion

The entire NAP-1 dimer molecule has 2-fold rotational symmetry. The monomer consists mainly of four β-strands and long α-helices. The structure shows tight interaction between two monomers. Of the total acessable surface area of each NAP1 monomer (18269 $Å^2$), 16.7% (3054 $Å^2$) is in the buried region. The helix of each monomer only contributes to the dimer interface formation. Concave β-strands like those in NAP-1 were found in some functionally related proteins. A Dali database search [Holm and Sander, 1994; Holm and Sander, 1998] did not reveal any known protein structures significantly similar to the NAP1 structure. When NAP-1 and other histone chaperones are compared, a similar structural pattern, antiparallel strands, is observed, although these are not completely aligned structures, and no sequence similarity among the histone chaperone proteins has been detected thus far. Many proteins involved in histone binding or nucleosome assembly contain a highly modular structure,

which seems to provide a scaffold for protein-protein interaction. This structural similarity, despite the absence of overall sequence homology, may be based on the conservation of function, and the variation in overall sequence may contribute to an oligomerization behavior providing different roles in chromatin assembly.

The functional form of many proteins is oligomeric, with the most common being a dimeric structure. In general, dimeris or oligomeris may have an advantage over the monomers. Dimerization of a protein, generally, provides an enlarged interaction surface increasing the potential for protein-protein or protein-DNA interactions, relative to the monomer. Also, it is a more efficient means of enlarging the interaction surface than increasing the size of the protein within the monomer. Oligomerization also functions to increase the local concentration. As a functional regulation method, the monomer-to-dimer transition itself can be a regulated process. Additionally, a dimeric protein may have a more dynamic structure than a monomeric protein of twice the size.

In stable homo-dimeric proteins (Fig. 10), several different types have been suggested, dependent on the conformation of the dimerization motif and types of denaturation transition: domain swapping dimers, non-domain swapping dimers, two state dimer denaturation, and three state dimer denaturation [Xu et al., 1998]. Many proteins can form a dimer or higher oligomer by exchanging an identical structural domain; eq, "domain swapping" [Gouldson et al., 1998; Spinelli et al., 1998; Xu et al., 1998]. A dimeric protein evolves by the interchange or swap of parts between two monomeric proteins.

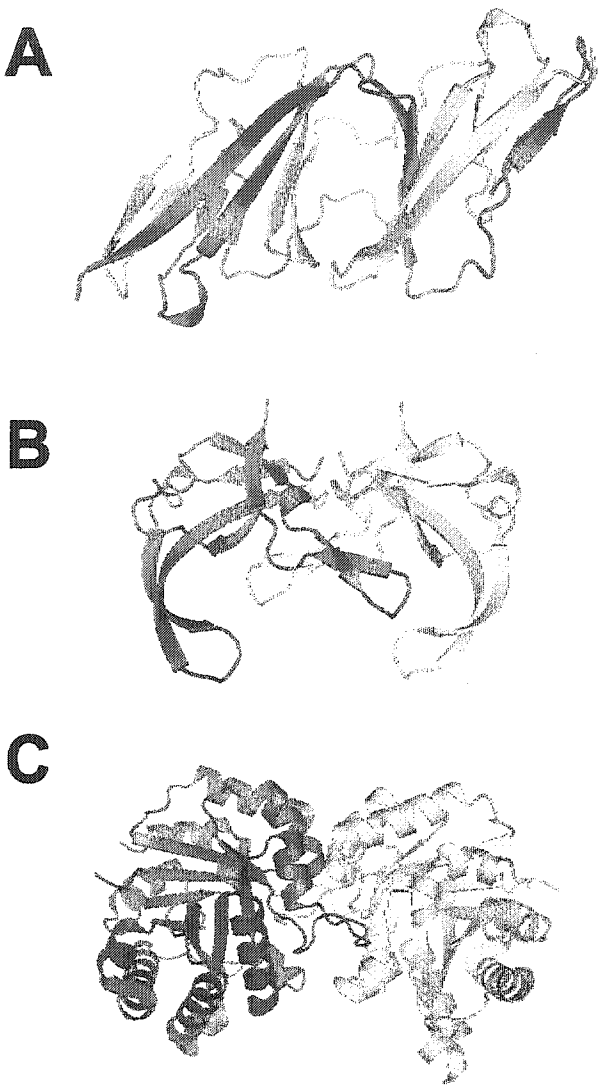

Figure 10. Structural examples of homo-dimers. Two chains are differentiated using yellow and red colors. **A)** Domain swapping dimer (pdb access code 1cdc, cell adhesion molecule CD2), **B)** non-domain swaping and 2-state dimer denaturation (pdb access code 2gvb, the single-stranded DNA binding protein encoded by gene V of the bacteriophage M13), **C)** non-domain swaping and 3-state dimer denaturation (pdb access code 1tim, Triose Phosphate Isomerase).

In the NAP-1 structure, we could not find any evidence of domain swapping. The second type, interlocked interfaces, are composed of subunits that adopt much of their folded structure only after forming the complex. In general, two chains intertwined (coiled-coil) or large flat interfaces (parallel or anti-parallel helices) within non-compact monomers is observed in 2 transition state dimer proteins. There is no compact monomer structure. The native dimer state and denatured monomer state are only detected from the equilibrium denaturation experiment. A recent report reveals that yNAP-1 is classified as a 2-transition state dimer [McBryant and Peersen, 2004b]. From the equilibrium denaturation experiment, McBryant and Peersen only observed the stable NAP-1 dimer and denatured NAP-1 monomer state. While, 3 state transition dimers have flat small interfaces with a compact monomer domain. Because of stable monomer domain, the native dimer, the stable monomer, and the denatured monomer state can be detected from the equilibrium denaturation experiment. Most interfaces are formed between globular subunits.

The coiled-coil or helix bundle, a ubiquitous protein motif, is often used to control oligomerization (Fig. 11). The coiled-coil is found in many types of proteins, such as transcription factors (leucine zipper), viral fusion peptides, SNARE complexes, certain tRNA synthetases and tropomyosin [Lin and Scheller, 1997; Schumacher et al., 2000; Takeda et al., 2003]. Most coiled-coil sequences contain heptad repeats. The coiled-coil is formed by component helices coming together to bury their hydrophobic residues that twist around the

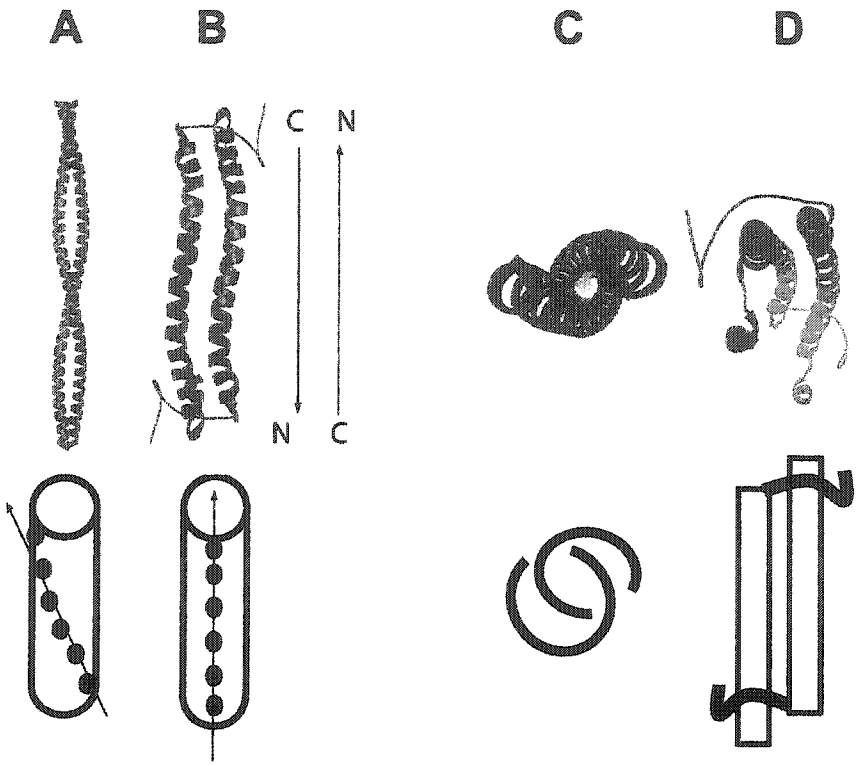

Figure 11. Coiled-coil and noncoiled-coil dimerization motif. **A** and **C)** coiled-coil dimerization motif (pdb access code 1d7m). **B** and **D)** noncoiled-coil dimerization motif of NAP-1. Hydrophobic residues around the helix are represented as dots.

helix (represented as dots in Fig. 11) [Burkhard et al., 2001]. As the hydrophobic residues twist around each helix, the helices also twist to coil around each other, burying the hydrophobic residues and forming a supercoil (Seen in Fig. 11). Non-intertwined chain structures are mostly found in membrane proteins [Lemmon et al., 1994; Russ and Engelman, 2000], or a multi-stranded helix bundle complex to increase the interface area, making a stable oligomeric structure. NAP-1 has a novel dimerization fold having antiparallel noncoiled-coil helices. In NAP-1 case, loop domains wrap around adjacent helices to stabilize the dimer structure (Fig. 11). This helix loop - helix loop (HL-HL) dimer conformation may provide the stability of overall structure (Fig. 11).

It has been thought that there is no sequence homology, no characteristic sequence, and no characteristic structural motif among the histone chaperones although numerous molecules that can bind histone and facilitate chromatin assembly *in vitro* have been identified as histone chaperones. However, recent atomic structural information for two histone chaperones, nucleoplasmin, and ASF-1 [Daganzo et al., 2003; Dutta et al., 2001], provide new insight for histone chaperones. While the othe two do not form the same oligomerized state, the concave antiparallel beta sheet architecture occurs in all these atomic structures. From the NAP-1 structure, we also identified a similar structural motif. More interestingly, we can also expect similar architecture from other histone chaperone proteins containing WD repeat domain such as CAF-1 or HIRA [Kirov et al., 1998; Martínez-Balbás et al., 1998]. There is not any experimental evidence that the concave β-strands domain in the histone chaperones functions

to assist in the binding of the histones. The concave β-strands domain may be the structural unit of protein-protein binding motif.

It is believed that the WD repeats in a protein may provide multiple interfaces for interactions with other proteins, which are also found in histone chaperones [Kirov et al., 1998; Martínez-Balbás et al., 1998]. The WD repeat proteins are found in diverse biological processes such as signal transduction, RNA processing, gene expression, vesicular trafficking, and cell division [Neer et al., 1994]. All WD repeat proteins have been proposed to fold into beta propeller- like structures. Most of the conserved features involved in the WD repeat proteins are identified in the WD repeats of CAF1 p55 (Fig. 9). These highly conserved sequences of WD repeat protein make it very likely that they all have a typical propeller structure, providing docking sites for multiple complexes. WD repeat domain within some of the histone chaperones functions a histone-binding site [Verreault et al., 1996] and also may bind chromatin assembly factors [Martinez-Balbas et al., 1998], histone acetyltransferases [Verreault, 1998] and histone deacetylases [Ahmad et al., 2003]. The presence of concave antiparallel beta-sheets in WD repeat proteins suggests that this motif might be the common characteristic of protein-protein interaction motif (Fig. 8, 9 and 12).

Fig. 12 shows the specialization of oligomerization state for unique function. Even though they all share a similar building block, various oligomerized structures may provide specialized functions; homo-pentamer or decamer in nucleoplasmin, homo-dimer (or multi homo-dimer) in NAP1, monomer in ASF1, and seven-repeat but slightly different motif within the monomer structure of

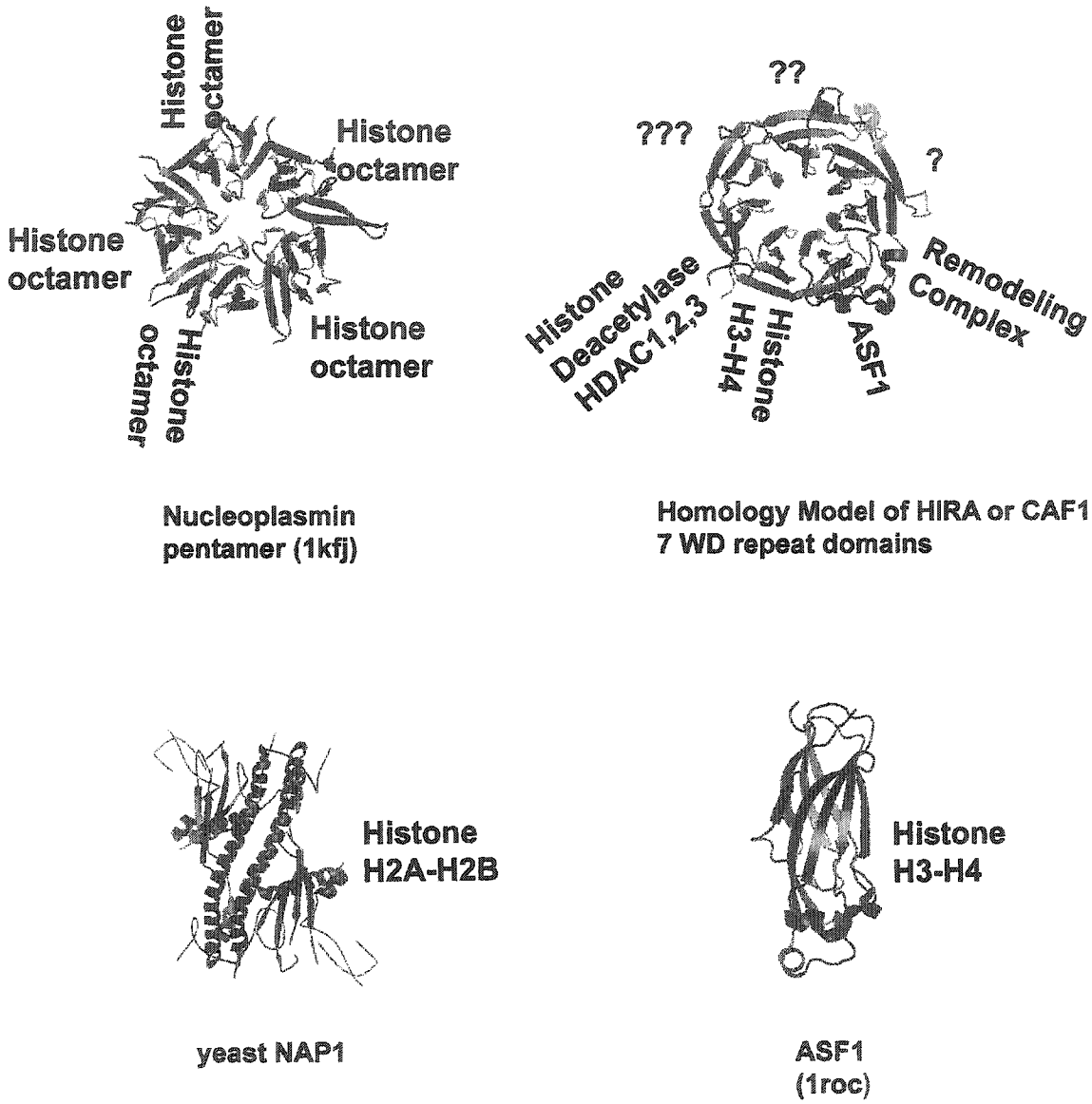

Figure 12. The specialization of oligomarization state for unique function of histone chaperones.

CAF-1 or HIRA. The different oligomerization states of histone chaperones may suggest that functional diversity requires having various oligomerized forms. In the case of CAF-1 or HIRA, multi-repeat domains within a single peptide are required for binding of multiple partners. In contrast, to serve as storage for single type of protein, a homooligomer of identical subunits, like nucleoplasmin, may be the more efficient way to increase the local concentration (Fig. 8 and 12). The monomer of ASF1 may function as a histone H3-H4 donor. A stable dimer structure within NAP-1 suggests a high affinity for the target protein or histone H2A-H2B dimer specificity.

Although the final refinement of NAP-1 structure is not complete, this structural information may allow us to understand the function of histone chaperones. The structure of yeast NAP-1, as described in the present study, is the first for a member of the nucleosome assembly protein (NAP) family and therefore serves as a model for characterization of this group of proteins. Topologically, the structural elements, as determined in the current crystal structure, show similarities to proteins involved as histone chaperones. However, the arrangement of the dimer within yeast NAP-1 structure results in a new protein fold with unique features.

4.6 Acknowledgements

We thank Steven J. McBryant for providing truncated yeast NAP-1plasmids, and Paul Scherrer in Institute of Rigaku for help in data collection using a rotating chromium anode.

Chapter 5

Crystallization and preliminary X-ray diffraction analysis of Nucleosome Assembly Protein 1 (NAP-1) with histone complex

5.1 Abstract

Various nucleosome assembly protein 1 (NAP-1) - histones complexes have been purified and crystallized. The NAP-1 co-crystal with histone H2A belongs to space group $P4_22_12$, with unit-cell parameters a = b =125, c=147 Å that is different from NAP-1 alone, and contains one dimeric NAP-1 molecule in the asymmetric unit. NAP-1 protein is a homodimer in the crystal structure, which is consistent with solution studies [McBryant and Peersen, 2004b]. A complete data set was collected to 3.3 Å resolution using a synchrotron radiation source. The three-dimensional structure of the NAP1-H2A complex will provide an understanding of the interaction between a histone chaperone and histones in the chromatin assembly process. Attempts are being made to improve the electron density using the non-crystallographic symmetry. Model building and refinement are in progress in order to reveal the structure of the NAP1-histone complex.

5.2 Introduction

The basic unit of DNA packaging in eukaryotic chromatin is the nucleosome. DNA is wrapped around a central histone octamer within the nucleosome [Luger et al., 1997a]. The four core histones H2A, H2B, H3, and H4 associate as H2A-H2B dimers and H3/H4 tetramers to then form the histone octamer. The structural units of the octamer are stabilized by the interaction between the histone fold motifs. The histone fold motif has been defined as an extended helix-loop-helix domain [Arents and Moudrianakis, 1995]. Histones are among the most highly conserved proteins known. The histone fold is the most conserved region of each histone, with ~ 100% sequence identity observed between different species in some cases [Sullivan et al., 2002]. This fold motif is also found in a number of non-histone proteins that are involved in protein-protein and protein-DNA interactions, for example TAF (TATA box binding protein-associated factors), CBF (the CCAAT-binding factor), archaeal DNA-binding proteins [Decanniere et al., 2000; Maity and de Crombrugghe, 1998; Xie et al., 1996].

Histone chaperones are by definition histone-binding proteins. The H3-H4 histone complex appears to be associated with p48, a subunit of the chromatin assembly factor 1 (CAF-1) [Verreault et al., 1996]. In oocytes of *Xenopus laevis*, the H3-H4 tetramer is found in complex with N1/N2 [Kleinschmidt et al., 1985; Kleinschmidt et al., 1990]. Whereas the H2A-H2B dimer associats with the chaperone nucleoplasmin in oocytes of *Xenopus laevis*, and nucleosome assembly protein 1 (NAP-1) co-precipitates with histone H2A-H2B from

Drosophila embryos [Ito et al., 1996a]. Similarly, human NAP-1 co-precipitates from HeLa cytoplasmic extract with H2A [Chang et al., 1997]. Using native gel electrophoresis, complex formation between the H2A-H2B dimer and yeast NAP-1 was tested *in vitro* [Park et al., 2004a]. Yeast NAP-1 exhibits no species-specific preference for H2A-H2B dimers interacting equally well with yeast, mouse, Xenopus, and Drosophila histones [Park et al., 2004a]. Similarly, H2A-H2B dimers containing any of the currently available histone variants (H2A.Z, macroH2A, and H2A Bbd) are bound equally well [Park et al., 2004a]. Also NAP-1 bind H3-H4 tetramer or globular domain of H2A-H2B dimer *in vitro* [McBryant et al., 2003]. These results suggest that NAP-1 mainly recognizes a structural domain, the histone dimer-fold motif [McBryant et al., 2003].

Here we report the purification, crystallization and x-ray diffraction analysis of yeast NAP-1 with various histone complexes. We utilized the NAP-1 protein without its acidic stretch (365-417). This protein fragment is fully functional but lacks the non-specific interaction with positively charged proteins seen with the full length NAP1 [McBryant et al., 2003].

5.3 Experimental Procedures

Preparation of proteins and crystallization – Full-length yeast nucleosome assembly protein 1 (yNAP-1) and truncated yNAP-1 proteins were purified as described [McBryant et al., 2003]. Recombinant *Xenopus laevis* histone proteins [Luger et al., 1997b] were produced in bacteria and purified as we described

before [Dyer et al., 2004]. The electrophoresis mobility shift assay (EMSA) method was used to detect the complex formation of yNAP-1 with histones [McBryant et al., 2003]. A size-exclusion column (HiLoad 16/60 Superdex 200 HR prep grade gel filtration column (Pharmacia)) was used to purify the NAP-1 with histone complex.

The crystals of NAP-1 with histone H2A complex were obtained by the hanging drop vapor diffusion method: 1.5 µl protein solution (10mg/ml in 20 mM Tris-HCl (pH 7.5)) were mixed with 1.5 µl of reservoir solution containing 40% MPD (2-methyl 2,4-pentanediol), and equilibrated against the reservoir solution at 4^0C.

Data collection and structure determination – In-house diffraction data, mostly limited to a resolution of 4 - 3.5 Å were collected, on a Rigaku rotating anode generator (Cu-Kα radiation, λ=1.5418 Å) under cryoprotectant conditions. 20% MPD solution was used as a cryo protectant. Synchrotron data were collected at beamline ALS 5.0.2. The crystal diffracted to 3.3 Å. Data analysis and reduction were performed with HKL2000 software [Otwinowski and Minor, 1997]. The space group ($P4_22_12$) and cell dimensions (a = b = 125, and c = 147 Å) were determined.

Using the final model of NAP-1, we attempted to solve the NAP-1 with histone H2A complex structure. NAP-1 monomer was used as a search model. Two molecules were located in the asymmetric unit (ASU). This was followed by rigid body refinement (resolution 20-3.3 Å) that allowed the two molecules to move

independently. The structure model was refined against a native dataset using CNS [Brunger et al., 1998]. Graphical presentations were prepared using PYMOL [DeLano, 2002]. The accessible surface area for the complex was calculated using CCP4 program "AREAIMOL" [Lee and Richards, 1971].

5.4 Results and Discussion

Purified NAP-1 / histone complexes were concentrated to 15 mg/ml, using centricon centrifugal filter devices with 10KDa cutoff membranes (Amicon Bioseparations (Millipore), Bedford, MA, USA). Figures 1 and 2 show the purity of yNAP-1 and yNAP-1 / histone complexes. To prepare NAP-1 with H2A-H2B dimer (or histone H2A) complex crystals, multiple screens for crystallization conditions were tested using the hanging drop method. Initial crystallization trials were performed using commercial screening kits including Hampton research crystal screen, Natrix, and Emerald biostructures Wizard. Crystal screening for NAP-1 (74-365) with H2A (1-106, 1-112, or 13-118) - H2B (27-122) are in progress (Fig.3 and table 1). To find optimal crystallization conditions, the screen consisting of varying concentrations of salt, varying concentrations of yNAP-1 / H2A-H2B dimer complex, and varying temperature was set up. Full-length yNAP-1 / H2A-H2B dimer complex did not crystallize at all. From these results, it appears that the full-length NAP-1 protein is too flexible or exhibits multiple conformational states to crystallize. From truncated yNAP-1 proteins (residue from 74 to 417 and from 74 to 365

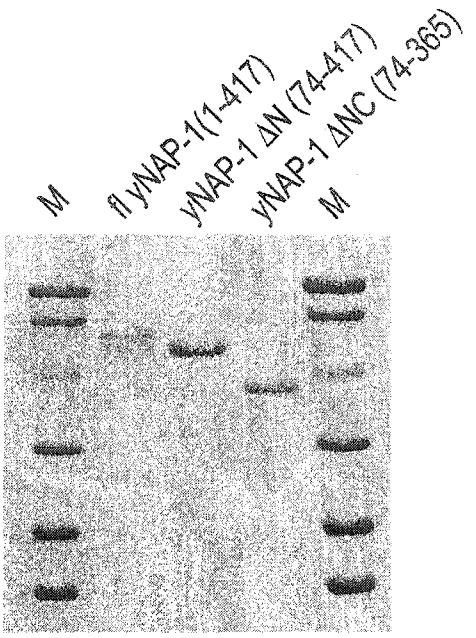

Figure 1: SDS-PAGE of NAP-1 proteins. Lane 2-4: full length NAP1, N-terminal truncated NAP-1, N and C-terminal truncated NAP-1 Lane 1 and 5: protein marker (M) 14.5, 21.5, 31, 45, 66.2, and 94.4 kDa.

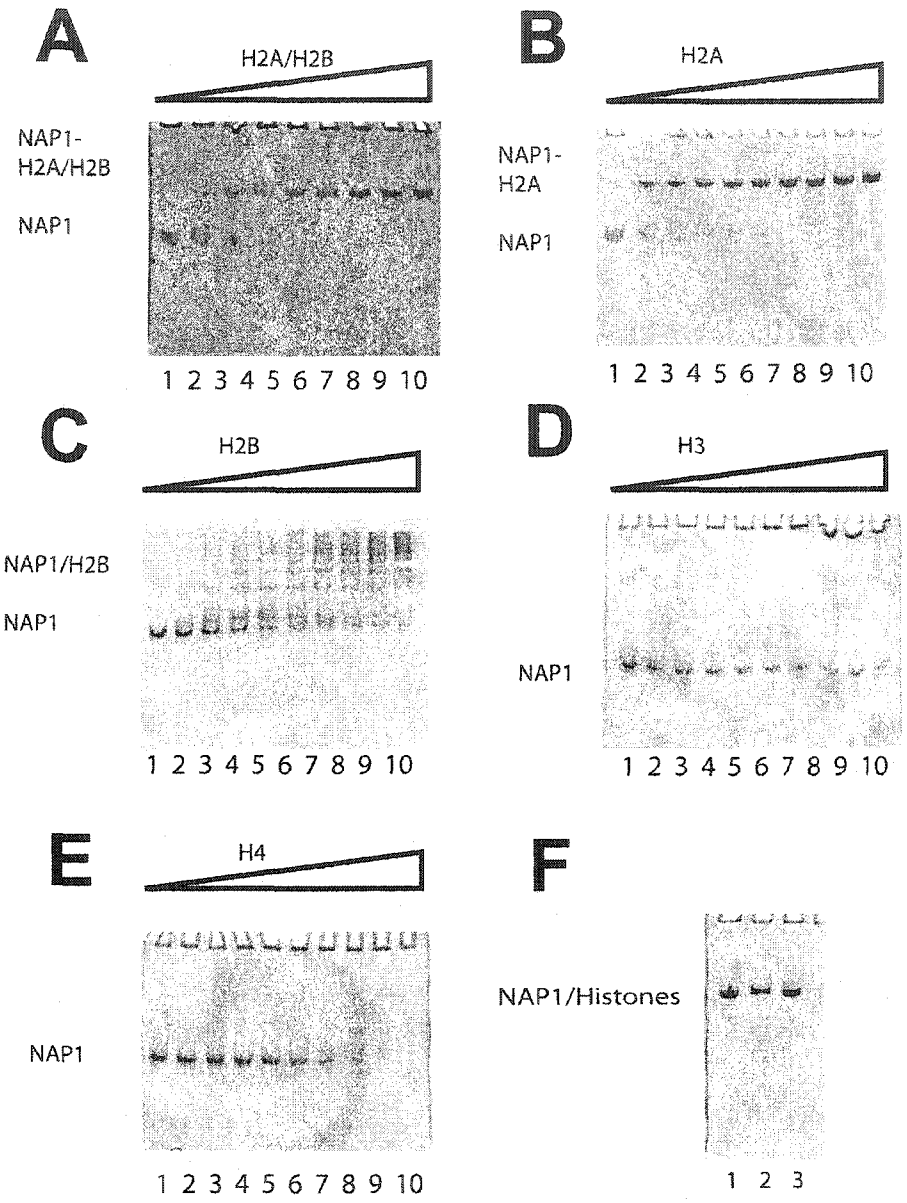

Figure 2. NAP-1 / histone complexes. 10 µM yNAP-1 dimer was incubated in the presence of *Xenopus laevis* (H2A-H2B) dimer **(A)** (lane 1- 10: 0 to 10 µM) or histones H2A **(B)**, H2B **(C)**, H3 **(D)**, H4 **(E)** (lane 1- 10: 0 to 20µM). Samples were incubated at 4 °C for 10 hours and complex formation was analyzed by native PAGE. The position of yNAP-1 / histone complex and yNAP-1 are indicated. **(F)** A complex of yNAP-1 with (H2A-H2B) dimer, H2A (1-106), or H2A (1-112) was purified by size exclusion column (lane 1-3). Under these conditions, no free yNAP-1 is present.

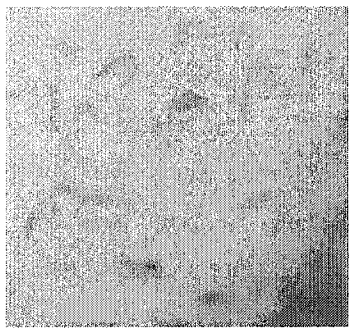

NAP(74-417)/ H2A(13-118)-H2B(27-122) complex

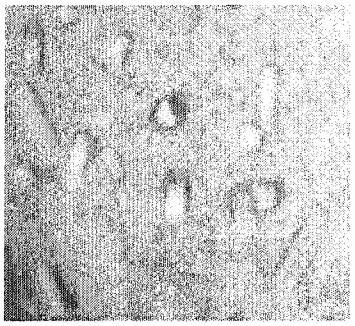

NAP(74-365)/ H2A(13-118)-H2B(27-122) complex

NAP(74-365)/ H2A(1-106) complex

Figure 3. The crystals of NAP-1 / histone complex. 10% PEG 2000 MME, 20% PEG 550 MME, or 20% MPD was used for NAP(74-417/H2A(13-118)-H2B(27-122), NAP(74-365)/H2A(13-118)-H2B(27-122), or NAP(74-365)/H2A(1-106) complex crystals.

of yNAP-1 proteins) with truncated histone dimer, crystals were obtained from several different conditions. Crystallization solutions for the complexes were different from those for yNAP-1 alone. yNAP1 with H2A/H2B protein in crystals was detected by electrophoresis. We tested the initial diffraction at room temperature using a conventional capillary mounting. These crystals did not diffract to more than 10 Å resolution. To improve the results, we proceeded to screen for conditions that allow us to collect data under cryogenic temperature. The diffraction quality was not much changed. We believed that changing the crystal packing using different kinds of crystallization conditions or different histone proteins might improve the data quality. We also screened several different truncations of histones or histone H2A-H2B dimers for NAP-1 with histone complex (table 1).

In order to optimize the crystallization conditions, we used salts as the additive. First, we determined the maximum concentration of salt at which the NAP-1 with histone complex form was maintained, using FRET between tryptophan from NAP-1 and CPM from histone (Fig 4, this method was optimized in Chapter 3). The best-diffracting crystals were found from truncated NAP-1 (residue number from 74 to 365) with histone H2A (1-106 or 1-112) complex in 18-22% MPD condition. Crystals grew to their full size in about 4-5 weeks. A single crystal was cryoprotected in a solution containing 20% MPD. A native data set was collected to 3.3 Å resolution. After indexing and density integration, systematic absences indicate that the crystal belongs to the tetragonal space group $P4_22_12$. The unit cell parameters are a = b = 125, c= 147 Å. A data set

Table 1. The crystals of NAP-1 with histones

Proteins		Crystal formation	Diffraction Data (ALS 5.0.2)	Space group, Unit cell (a, b, c)
NAP1	Histone			
NAP1 (1-417)		Yes	3.0 Å	$P4_32_12$, a=b=86.7 Å, c=176.1 Å
NAP1 (74-417)		Yes	3.0 Å	$P4_32_12$, a=b=86.7 Å, c=176.1 Å
NAP1 (74-365)		Yes	No diffraction (In progress)	
NAP1 (1-417)	Full length H2A/H2B	No crystal		
	H2A (13-118)/H2B (27-122)	No crystal		
NAP1 (74-417)	Full length H2A/H2B	No crystal		
	H2A (13-118)/H2B (27-122)	Yes	No diffraction (In progress)	
	H2A (1-112)/H2B (27-122)	Yes	No diffraction (In progress)	
	H2A (1-106)/H2B (27-122)	Yes	No diffraction (In progress)	
NAP1 (74-365)	Full length H2A/H2B	No crystal		
	H2A (13-118)/H2B (27-122)	Yes	~9 Å (In progress)	
	H2A (1-112)/H2B (27-122)	Yes	No diffraction (In progress)	
	H2A (1-106)/H2B (27-122)	Yes	~ 9 Å (In progress)	
	Full length H2A	Yes (Not reproducible)		
	H2A (13-118)	No crystal		
	H2A (1-112)	Yes	3.3 Å	$P4_22_12$, a=b=124 Å, c=147 Å
	H2A (1-106)	Yes	3.3 Å	$P4_22_12$, a=b=124 Å, c=147 Å

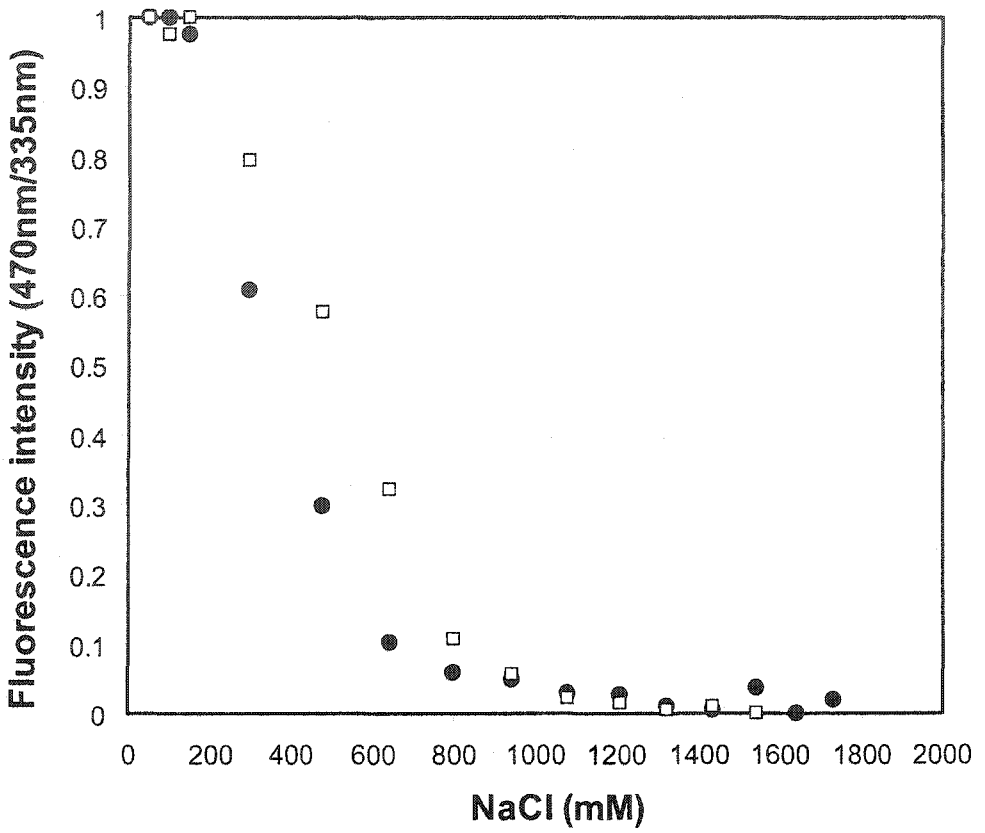

Figure 4. The salt-induced dissociation of NAP-1 with H2A-H2B dimer complex. 10μM yNAP-1dimer was incubated with 10μM fluorescently labeled (H2A-H2B CPM) dimer. Under these conditions, no free yNAP-1 is observed. Tryptophan was excited at 300nm, and fluorescence of the complex was monitored. NAP-1 (1-417) with fluorescently labeled (H2A-H2B CPM) dimer complex (□) or NAP-1 (74-365) with fluorescently labeled (H2A-H2B CPM) dimer complex (●) was dissociated by increasing amount of salt concentration. Ratios of fluorescence intensities (470 nm/335 nm, Acceptor/Donor) are calculated and then normalized data are ploted.

essentially complete to 3.3 Å resolution was collected using a synchrotron radiation source (ALS 5.0.2). A total of 507750 diffraction intensities were collected to 3.3 Å; they were merged into 43707 unique reflections using HKL2000. The data set is 99% complete up to 3.3 Å resolution, with I/σ(I) above 3, and a merging R factor for symmetry-related reflection of 7.7%. Crystal data and data collection statistics are given in table 2.

The crystals have two molecules of NAP-1 in the asymmetric unit. The NAP-1 monomer was used as the search model in molecular replacement calculations using CNS [Brunger et al., 1998]. 2Fo-Fc and Fo-Fc type electron density maps were calculated and displayed at 3.3 Å resolution by "O" [Jones et al., 1991]. All of the residues seen in the model of NAP-1 were visible in this map. However, considerable uncertainty remained about the position of the histone H2A. Although the electron density map was considerably improved relative to the previous map after finding the second NAP-1 monomer within the ASU, the density still was not well enough defined to locate histone H2A.

We were unable to find the solution from cross rotation and translation search using histone H2A structure (pdb access code 1aoi). The simple explanation is that the structure of the histone H2A in the NAP-1 / H2A complex may not be the same as that of the histone H2A in the nucleosome structure. It is also possible that H2A is not well positioned within the crystal structure or may be heterogeneously located with NAP-1.

Table 2. Data collection statistics

	Native protein crystal
Protein	NAP (74-365) / H2A (1-106)
Wavelength (Å)	1.0
Space group	$P4_22_12$
Unit cell dimension (Å)	a = b = 125.3 c = 146.9
Resolution range (Å)	30-3.3
Mosacity	0.34
Completeness (%) [a]	99.6 (97.5)
Rmerge [a b]	0.077 (0.38)
I / σ (I) [a]	22.7 (3.5)

[a] Values in parentheses refer to data in the highest resolution shell.
[b] $R_{merge} = \Sigma \mid I_h - \langle I_h \rangle \mid / \Sigma I_h$, where I_h is the mean of the measurements for a single hkl.

Two monomers, which make up a dimer with two-fold symmetry, were located. The dimer structure of NAP-1 was used as the initial model for refinement. The current R and R free Values are 43 and 45 %, respectively, in the 30-3.3 Å resolution range. Further refinement is in progress.

At the present stage of refinement, the NAP-1 / histone H2A complex structure reveals an expected fold consisting of two repeating units, each containing the helix and four beta-strands that we observed from NAP-1 structure alone. The entire molecule has 2-fold rotational symmetry (Fig. 5). The two monomers of NAP-1 in a symmetric unit form a homodimer in an anti-parallel fashion. The topology of the polypeptide fold is identical in each monomer; the structure of the dimer is symmetric. The dimer structure is stabilized by a loop domain. The two long helices in the dimer do not form a canonical coiled-coil but instead lie nearly in the same plane. The helix in the distal monomer continues unbroken for 14 turns that is ~ 69 Å. The concave β domains are ~59 residues in length, and have 4 β strands. The mainly anti-parallel four-stranded β strand motif is bent to form a concave shape. All the connections between the β strands are turns or small loops.

We reported previously that yNAP-1 exhibits no species-specific preference for H2A-H2B dimer, the structured region of the H2A-H2B dimers is recognized by yNAP-1, and that the histone-fold motif can be the main binding site for yNAP-1 [Park et al., 2004a]. yNAP-1 can strongly bind H3-H4 tetramer or tailless histones *in vitro* [McBryant et al., 2003]. This suggests that histone-fold domain is an important domain for NAP-1 binding. In the crystal packing, we could

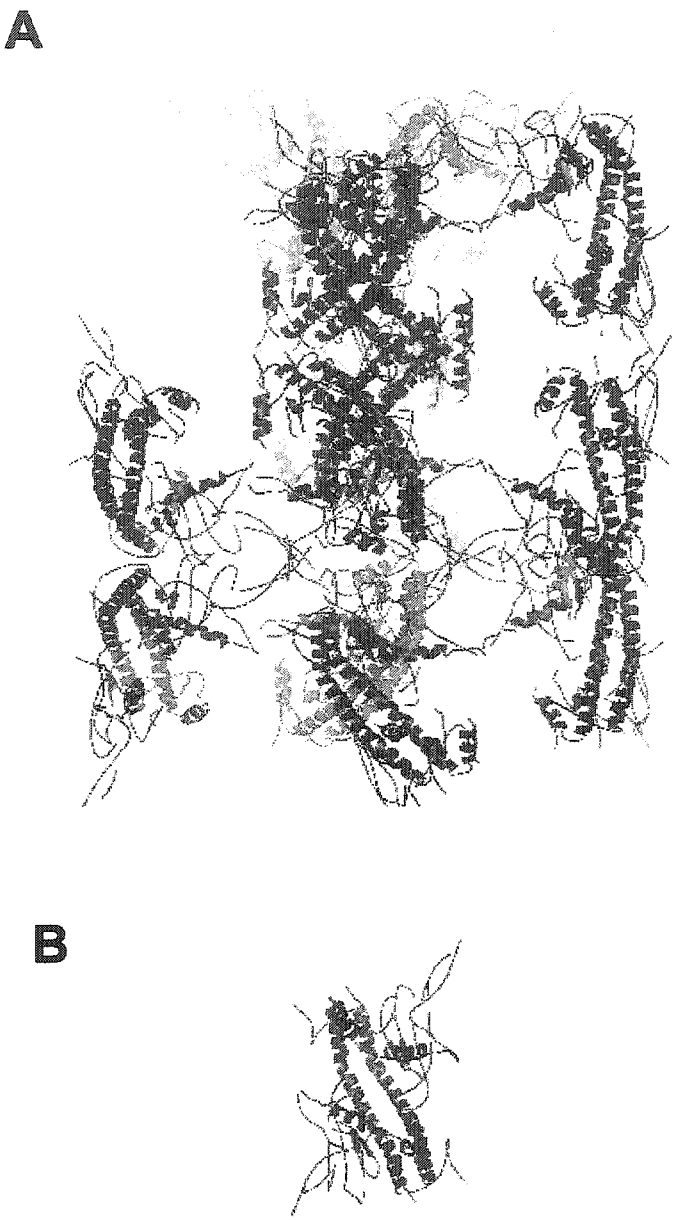

Figure 5. The crystal packting and NAP-1 dimer structure within the asymmetric unit. The crystal packing of yNAP-1 dimer (A) and overall fold of yNAP-1 dimer at the current stage of refinement (B) are shown.

observe the room for histones around yNAP-1 (Fig. 5). While continuing refinement using the currently available data set, efforts are also currently under way to modify the crystallization conditions and to make H2A or H2B histone fold domain alone for new NAP-1 with histone complexes to produce crystal that diffract better.

Chapter 6

Contributions to other Publications

1. Muthurajan UM, Park YJ, Edayathumangalam RS, Suto RK, Chakravarthy S, Dyer PN, Luger K. 2003 Structure and dynamics of nucleosomal DNA.Biopolymers. Apr; 68(4): 547-56.

In this paper, I introduced a new FRET method as a technique to study nucleosome stability and dynamics. We also summarize the recent structural studies of nucleosome core particles (both published and unpublished) that concern the structure and dynamics of nucleosomal DNA, and the nature of protein-DNA interactions. Current mechanisms for chromatin remodeling and nucleosome sliding are discussed in light of new structural evidence.

2. McBryant SJ, Park YJ, Abernathy SM, Laybourn PJ, Nyborg JK, Luger K. 2003. Preferential binding of the histone (H3-H4)2 tetramer by NAP1 is mediated by the amino-terminal histone tails. J Biol Chem. Nov 7; 278(45): 44574-83.

In this paper, we demonstrate that yNAP1 binds to one histone-fold domain, thus specifying the stoichiometry of the complexes formed with the histone dimer

and tetramer. I participated in the preliminary study of NAP1 with histone complex formation. Using EMSA, we could detect the yNAP1 complexes with the histones and determine the stoichiometry.

3. Bao Y, Konesky K, Park YJ, Rosu S, Dyer PN, Rangasamy D, Tremethick DJ, Laybourn PJ and Luger K. 2004. Nucleosomes containing the histone variant H2A.Bbd organize only 118 base pairs of DNA. EMBO J.

From this study, we found that Bbd-NCP had a more relaxed structure in which only 118 bp of DNA is protected against digestion with micrococcal nuclease. The Bbd docking domain is largely responsible for this behavior, as shown by domain-swap experiments. I participated in initial FRET study for H2A.Bbd containing nucleosome. We found that that the distance between the DNA ends is increased significantly.

Chapter 7

Perspective and Future direction

The work presented in this dissertation is focused on understanding the role of histone chaperones in the dynamic behavior of nucleosome. The overall results of the first part of the thesis (chapter 2) support the hypothesis that dynamic processes in the nucleosome can be modulated by the replacement of major histones with their variants, affecting nucleosome structure and function. Using fluorescence resonance energy transfer, we compared the structural transitions of a histone variant (H2A.Z) containing nucleosome and a canonical nucleosome in response to increasing ionic strength. We have shown that the (H2A-H2B) dimer dissociation from the $(H3\text{-}H4)_2$ tetramer – DNA complex was significantly stabilized in nucleosomes containing histone variant H2A.Z. The data presented in chapter 2 may help to explain that the stability of nucleosome core particle can be modulated by incorporation of histone variant.

In chapter 3, we demonstrated the yeast NAP-1-mediated histone variant exchange mechanism. First, complex formation between the H2A-H2B dimer and NAP-1 was tested using native gel electrophoresis. NAP-1 exhibits no species-specific preference for H2A-H2B dimers. Similarly, H2A-H2B dimers containing

any of the histone variants are bound equally well. Using fluorescence resonance energy transfer (FRET) and gel shift assays, we showed that the addition of NAP-1 to NCP leads to H2A-H2B dimer dissociation from NCP, changes in the position of NCP are synchronized with the dissociation of histone H2A-H2B dimer, and, under these dynamic conditions, NAP-1 can exchange the histone variant H2A.Z-H2B dimer.

To better understand the role of NAP-1, we determined the x-ray crystal structure (chapter 4). The dimeric NAP-1 has an overall ellipsoidal shape. This structure consists mainly with four β-strands and α-helix dimerization motif. Histone chaperone proteins share the similar structural motif, four antiparalle β-strands, observed from currently available structures of histone chaperones. The results resented in this dissertation provide a number of testable hypotheses that can be applied in further work using new structures.

Time-dependent experiments are now required. As preliminary results, I measured the time for dissociation of H2A-H2B dimer from nucleosome core particle which is induced by NAP-1 using gel shift assay and formation of NAP-1 with H2A-H2B dimer complex using FRET. There is currently an effort under way to do the kinetic experiments (J. V. Chodaparambil, K Luger Lab). These data will provide more specific information about H2A-H2B dimer dissociation or complex formation. The dynamic exchange of histone dimers within the nucleosome needs to be measured also.

Another hypothesis that needs to be tested is whether posttranslational

modifications such as phosphorylaton and polyglutamylation (see chapter 1 and 3) can regulate the function of NAP-1. In chapter 3, we reported that the C-terminal acidic region is responsible for the histone H2A-H2B dimer dissociation from the nucleosome core particle. Polyglutamylation will occur at the same C-terminal domain. At least two different polyglutamylation sites are identified from HeLa cells so far [Regnard et al., 2000]. If modification occurs, the number of acidic amino acid residues within C-terminal domain will be changed from 30 (55% of the total residues) up to 50 (67% of the total residues) in the case of yeast NAP-1.

One of the interesting observations is that higher eukaryotes are more affected by loss of individual histone chaperones than are budding yeast. In yeast *S. cerevisiae*, deletion of *NAP-1* causes no significant phenotypes, yeast disrupted for CAF-1 have no growth defects, and ASF1 mutants are viable in yeast [Tyler et al., 1999]. ASF1 in *Drosophila*, NAP-1 in *Drosophila* or in mouse is an essential gene product [Tyler et al., 1999]. One possible explanation is that there may be functional redundancy among the individual histone chaperones NAP-1, ASF1, CAF-1 or additional unidentified histone chaperones *in vivo*. As another possibility, the ability of yeast to survive without individual histone chaperone may show that yeast has a more open chromatin structure than higher eukaryotes. Together, it suggests that histone chaperones may be involve in the regulation of chromatin structure in higher eukaryotes.

References

Adams, C.R. and Kamakaka, R.T. (1999) Chromatin assembly: biochemical identities and genetic redundancy. *Curr Opin Genet Dev*, **9**, 185-190.

Adkins, M.W., Howar, S.R. and Tyler, J.K. (2004) Chromatin Disassembly Mediated by the Histone Chaperone Asf1 Is Essential for Transcriptional Activation of the Yeast PHO5 and PHO8 Genes. *Mol Cell*, **14**, 657-666.

Ahmad, A., Takami, Y. and Nakayama, T. (2003) WD dipeptide motifs and LXXLL motif of chicken HIRA are necessary for transcription repression and the latter motif is essential for interaction with histone deacetylase-2 in vivo. *Biochem Biophys Res Commun*, **312**, 1266-1272.

Ahmad, K. and Henikoff, S. (2002) The histone variant H3.3 marks active chromatin by replication- independent nucleosome assembly. *Mol Cell*, **9**, 1191-1200.

Akey, C.W. and Luger, K. (2003) Histone chaperones and nucleosome assembly. *Curr Opin Struct Biol*, **13**, 6-14.

Allis, C.D., Glover, C.V., Bowen, J.K. and Gorovsky, M.A. (1980) Histone variants specific to the transcriptionally active, amitotically dividing macronucleus of the unicellular eucaryote, Tetrahymena thermophila. *Cell*, **20**, 609-617.

Altman, R. and Kellogg, D. (1997) Control of mitotic events by Nap1 and the Gin4 kinase. *J Cell Biol*, **138**, 119-130.

Anderson, J.D. and Widom, J. (2000) Sequence and position-dependence of the equilibrium accessibility of nucleosomal DNA target sites. *J Mol Biol*, **296**, 979-987.

Annunziato, A.T. and Seale, R.L. (1983) Histone deacetylation is required for the maturation of newly replicated chromatin. *J Biol Chem*, **258**, 12675-12684.

Arents, G. and Moudrianakis, E.N. (1995) The histone fold: a ubiquitous architectural motif utilized in DNA compaction and protein dimerization. *Proc Natl Acad Sci U S A*, **92**, 11170-11174.

Asahara, H., Tartare-Deckert, S., Nakagawa, T., Ikehara, T., Hirose, F., Hunter, T., Ito, T. and Montminy, M. (2002) Dual roles of p300 in chromatin assembly and transcriptional activation in cooperation with nucleosome assembly protein 1 in vitro. *Mol Cell Biol*, **22**, 2974-2983.

Ausio, J. and Abbott, D.W. (2002) The many tales of a tail: carboxyl-terminal tail heterogeneity specializes histone H2A variants for defined chromatin function. *Biochemistry*, **41**, 5945-5949.

Baake, M., Doenecke, D. and Albig, W. (2001) Characterisation of nuclear localisation signals of the four human core histones. *J Cell Biochem*, **81**, 333-346.

Baer, B.W. and Rhodes, D. (1983) Eukaryotic RNA polymerase II binds to nucleosome cores from transcribed genes. *Nature*, **301**, 482-488.

Bahadur, R.P., Chakrabarti, P., Rodier, F. and Janin, J. (2004) A dissection of specific and non-specific protein-protein interfaces. *J Mol Biol*, **336**, 943-955.

Banuelos, S., Hierro, A., Arizmendi, J.M., Montoya, G., Prado, A. and Muga, A. (2003) Activation mechanism of the nuclear chaperone nucleoplasmin: role of the core domain. *J Mol Biol*, **334**, 585-593.

Bao, Y., Konesky, K., Park, Y.J., Rosu, S., Dyer, P.N., Rangasamy, D., Tremethick, D.J., Laybourn, P.J. and Luger, K. (2004) Nucleosomes containing the histone variant H2A.Bbd organize only 118 base pairs of DNA. *Embo J.*

Barratt, M.J., Hazzalin, C.A., Zhelev, N. and Mahadevan, L.C. (1994) A mitogen- and anisomycin-stimulated kinase phosphorylates HMG-14 in its basic amino-terminal domain in vivo and on isolated mononucleosomes. *Embo J*, **13**, 4524-4535.

Bauer, U.M., Daujat, S., Nielsen, S.J., Nightingale, K. and Kouzarides, T. (2002) Methylation at arginine 17 of histone H3 is linked to gene activation. *EMBO Rep*, **3**, 39-44.

Becker, P.B. and Horz, W. (2002) ATP-dependent nucleosome remodeling. *Annu Rev Biochem*, **71**, 247-273.

Belotserkovskaya, R., Oh, S., Bondarenko, V.A., Orphanides, G., Studitsky, V.M. and Reinberg, D. (2003) FACT facilitates transcription-dependent nucleosome alteration. *Science*, **301**, 1090-1093.

Boeger, H., Griesenbeck, J., Strattan, J.S. and Kornberg, R.D. (2004) Removal of promoter nucleosomes by disassembly rather than sliding in vivo. *Mol Cell*, **14**, 667-673.

Brunger, A.T., Adams, P.D., Clore, G.M., DeLano, W.L., Gros, P., Grosse-Kunstleve, R.W., Jiang, J.S., Kuszewski, J., Nilges, M., Pannu, N.S., Read, R.J., Rice, L.M., Simonson, T. and Warren, G.L. (1998) Crystallography & NMR system: A new software suite for macromolecular structure determination. *Acta Crystallogr D Biol Crystallogr*, **54 (Pt 5)**, 905-921.

Bruno, M., Flaus, A. and Owen-Hughes, T. (2004) Site-specific attachment of

reporter compounds to recombinant histones. *Methods Enzymol*, **375**, 211-228.

Bruno, M., Flaus, A., Stockdale, C., Rencurel, C., Ferreira, H. and Owen-Hughes, T. (2003) Histone H2A/H2B dimer exchange by ATP-dependent chromatin remodeling activities. *Mol Cell*, **12**, 1599-1606.

Burkhard, P., Stetefeld, J. and Strelkov, S.V. (2001) Coiled coils: a highly versatile protein folding motif. *Trends Cell Biol*, **11**, 82-88.

Burton, D.R., Butler, M.J., Hyde, J.E., Phillips, D., Skidmore, C.J. and Walker, I.O. (1978) The interaction of core histones with DNA: equilibrium binding studies. *Nucleic Acids Res*, **5**, 3643-3663.

Celeste, A., Fernandez-Capetillo, O., Kruhlak, M.J., Pilch, D.R., Staudt, D.W., Lee, A., Bonner, R.F., Bonner, W.M. and Nussenzweig, A. (2003) Histone H2AX phosphorylation is dispensable for the initial recognition of DNA breaks. *Nat Cell Biol*, **5**, 675-679.

Chadwick, B.P. and Willard, H.F. (2001) A novel chromatin protein, distantly related to histone H2A, is largely excluded from the inactive X chromosome. *J Cell Biol*, **152**, 375-384.

Chang, L., Loranger, S.S., Mizzen, C., Ernst, S.G., Allis, C.D. and Annunziato, A.T. (1997) Histones in transit: cytosolic histone complexes and diacetylation of H4 during nucleosome assembly in human cells. *Biochemistry*, **36**, 469-480.

Chen, H., Li, B. and Workman, J.L. (1994) A histone-binding protein, nucleoplasmin, stimulates transcription factor binding to nucleosomes and factor-induced nucleosome disassembly. *Embo J*, **13**, 380-390.

Chung, D.G. and Lewis, P.N. (1986) Internal architecture of the core nucleosome: fluorescence energy transfer studies at methionine-84 of histone H4. *Biochemistry*, **25**, 5036-5042.

Clarkson, M.J., Wells, J.R., Gibson, F., Saint, R. and Tremethick, D.J. (1999) Regions of variant histone His2AvD required for Drosophila development. *Nature*, **399**, 694-697.

Clayton, A.L. and Mahadevan, L.C. (2003) MAP kinase-mediated phosphoacetylation of histone H3 and inducible gene regulation. *FEBS Lett*, **546**, 51-58.

Costanzi, C. and Pehrson, J.R. (1998) Histone macroH2A1 is concentrated in the inactive X chromosome of female mammals. *Nature*, **393**.

Cote, J., Peterson, C.L. and Workman, J.L. (1998) Perturbation of nucleosome

core structure by the SWI/SNF complex persists after its detachment, enhancing subsequent transcription factor binding. *Proc Natl Acad Sci U S A*, **95**, 4947-4952.

Cote, J., Quinn, J., Workman, J.L. and Peterson, C.L. (1994) Stimulation of GAL4 derivative binding to nucleosomal DNA by the yeast SWI/SNF complex. *Science*, **265**, 53-60.

Daganzo, S.M., Erzberger, J.P., Lam, W.M., Skordalakes, E., Zhang, R., Franco, A.A., Brill, S.J., Adams, P.D., Berger, J.M. and Kaufman, P.D. (2003) Structure and function of the conserved core of histone deposition protein Asf1. *Curr Biol*, **13**, 2148-2158.

Davey, C.A., Sargent, D.F., Luger, K., Maeder, A.W. and Richmond, T.J. (2002) Solvent mediated interactions in the structure of the nucleosome core particle at 1.9 a resolution. *J Mol Biol*, **319**, 1097-1113.

Davie, J.R. and Murphy, L.C. (1990) Level of ubiquitinated histone H2B in chromatin is coupled to ongoing transcription. *Biochemistry*, **29**, 4752-4757.

Debreczeni, J.E., Bunkoczi, G., Girmann, B. and Sheldrick, G.M. (2003) In-house phase determination of the lima bean trypsin inhibitor: a low-resolution sulfur-SAD case. *Acta Crystallogr D Biol Crystallogr*, **59**, 393-395.

Decanniere, K., Babu, A.M., Sandman, K., Reeve, J.N. and Heinemann, U. (2000) Crystal structures of recombinant histones HMfA and HMfB from the hyperthermophilic archaeon Methanothermus fervidus. *J Mol Biol*, **303**, 35-47.

DeLano, W.L. (2002) ***The PyMOL User's Manual***. DeLano Scientific, San Carlos, CA, USA.

DeSilva, H., Lee, K. and Osley, M.A. (1998) Functional Dissection of Yeast Hir1p, a WD Repeat-Containing Transcriptional Corepressor. *Genetics*, **148**, 657-668.

Dhillon, N. and Kamakaka, R.T. (2000) A Histone Variant, Htz1p, and a Sir1p-like Protein, Esc2p, Mediate Silencing at HMR. *Mol Cell*, **6**, 769-780.

Dong, F., Hansen, J.C. and van Holde, K.E. (1990) DNA and protein determinants of nucleosome positioning on sea urchin 5S rRNA gene sequences in vitro. *Proc Natl Acad Sci U S A*, **87**, 5724-5728.

Dutta, S., Akey, I.V., Dingwall, C., Hartman, K.L., Laue, T., Nolte, R.T., Head, J.F. and Akey, C.W. (2001) The crystal structure of nucleoplasmin-core: implications for histone binding and nucleosome assembly. *Mol Cell*, **8**, 841-853.

Dyer, P.N., Edayathumangalam, R.S., White, C.L., Bao, Y., Chakravarthy, S., Muthurajan, U.M. and Luger, K. (2004) Reconstitution of nucleosome core particles from recombinant histones and DNA. *Methods Enzymol*, **375**, 23-44.

Eickbush, T.H. and Moudrianakis, E.N. (1978) The histone core complex: an octamer assembled by two sets of protein-protein interactions. *Biochemistry*, **17**, 4955-4964.

Eshaghpour, H., Dieterich, A.E., Cantor, C.R. and Crothers, D.M. (1980) Singlet-singlet energy transfer studies of the internal organization of nucleosomes. *Biochemistry*, **19**, 1797-1805.

Fairclough, R.H. and Cantor, C.R. (1978) Singlet-Singlet Energy Transfer to Study Macromolecular Assembly. *Meth. Enzymol.*, **48**, 347-379.

Fan, J.Y., Gordon, F., Luger, K., Hansen, J.C. and Tremethick, D.J. (2002a) The essential histone variant H2A.Z regulates the equilibrium between different chromatin conformational states. *Nat Struct Biol*, **19**, 172-176.

Fan, J.Y., Gordon, F., Luger, K., Hansen, J.C. and Tremethick, D.J. (2002b) The essential histone variant H2A.Z regulates the equilibrium between different chromatin conformational states. *Nat Struct Biol*, **9**, 172-176.

Feng, Q., Wang, H., Ng, H.H., Erdjument-Bromage, H., Tempst, P., Struhl, K. and Zhang, Y. (2002) Methylation of H3-Lysine 79 Is Mediated by a New Family of HMTases without a SET Domain. *Curr Biol*, **12**, 1052-1058.

Flaus, A., Luger, K., Tan, S. and Richmond, T.J. (1996) Mapping nucleosome position at single base-pair resolution by using site-directed hydroxyl radicals. *Proc Natl Acad Sci U S A*, **93**, 1370-1375.

Flaus, A. and Owen-Hughes, T. (2001) Mechanisms for ATP-dependent chromatin remodelling. *Curr Opin Genet Dev*, **11**, 148-154.

Fujii Nakata, T., Ishimi, Y., Okuda, A. and Kikuchi, A. (1992) Functional analysis of nucleosome assembly protein, NAP-1. The negatively charged COOH-terminal region is not necessary for the intrinsic assembly activity. *J Biol Chem*, **267**, 20980-20986.

Fujii-Nakata, T., Ishimi, Y., Okuda, A. and Kikuchi, A. (1992) Functional analysis of nucleosome assembly protein, NAP-1. The negatively charged COOH-terminal region is not necessary for the intrinsic assembly activity. *J Biol Chem*, **267**, 20980-20986.

Fyodorov, D.V. and Kadonaga, J.T. (2003) Chromatin assembly in vitro with purified recombinant ACF and NAP-1. *Methods Enzymol*, **371**, 499-515.

Gaillard, P.H., Martini, E.M., Kaufman, P.D., Stillman, B., Moustacchi, E. and Almouzni, G. (1996) Chromatin assembly coupled to DNA repair: a new role for chromatin assembly factor I. *Cell*, **86**, 887-896.

Garcia Ramirez, M., Rocchini, C. and Ausio, J. (1995) Modulation of chromatin folding by histone acetylation. *J Biol Chem*, **270**, 17923-17928.

Garcia-Higuera, I., Gaitatzes, C., Smith, T.F. and Neer, E.J. (1998) Folding a WD repeat propeller. Role of highly conserved aspartic acid residues in the G protein beta subunit and Sec13. *J Biol Chem*, **273**, 9041-9049.

Garman, E. and Murray, J.W. (2003) Heavy-atom derivatization. *Acta Crystallogr D Biol Crystallogr*, **59**, 1903-1913.

Gasser, R., Koller, T. and Sogo, J.M. (1996) The stability of nucleosomes at the replication fork. *J Mol Biol*, **258**, 224-239.

Geiman, T.M. and Robertson, K.D. (2002) Chromatin remodeling, histone modifications, and DNA methylation-how does it all fit together? *J Cell Biochem*, **87**, 117-125.

Gorlich, D. and Kutay, U. (1999) Transport between the cell nucleus and the cytoplasm. *Annu Rev Cell Dev Biol*, **15**, 607-660.

Gottesfeld, J.M. and Luger, K. (2001) Energetics and Affinity of the Histone Octamer for Defined DNA Sequences. *Biochemistry*, **40**, 10927-10933.

Gouldson, P.R., Snell, C.R., Bywater, R.P., Higgs, C. and Reynolds, C.A. (1998) Domain swapping in G-protein coupled receptor dimers. *Protein Eng*, **11**, 1181-1193.

Grant, P.A. (2001) A tale of histone modifications. *Genome Biol*, **2**, REVIEWS0003.

Haushalter, K.A. and Kadonaga, J.T. (2003) Chromatin assembly by DNA-translocating motors. *Nat Rev Mol Cell Biol*, **4**, 613-620.

He, H. and Lehming, N. (2003) Global effects of histone modifications. *Brief Funct Genomic Proteomic*, **2**, 234-243.

Hendrickson, W.A., Horton, J.R. and LeMaster, D.M. (1990) Selenomethionyl proteins produced for analysis by multiwavelength anomalous diffraction (MAD): a vehicle for direct determination of three-dimensional structure. *Embo J*, **9**, 1665-1672.

Hendzel, M.J., Wei, Y., Mancini, M.A., Van Hooser, A., Ranalli, T., Brinkley, B.R., Bazett-Jones, D.P. and Allis, C.D. (1997) Mitosis-specific phosphorylation of histone H3 initiates primarily within pericentromeric heterochromatin

during G2 and spreads in an ordered fashion coincident with mitotic chromosome condensation. *Chromosoma*, **106**, 348-360.

Holm, L. and Sander, C. (1994) The FSSP database of structurally aligned protein fold families. *Nucleic Acids Res*, **22**, 3600-3609.

Holm, L. and Sander, C. (1998) Touring protein fold space with Dali/FSSP. *Nucleic Acids Res*, **26**, 316-319.

Ishimi, Y., Hirosumi, J., Sato, W., Sugasawa, K., Yokota, S., Hanaoka, F. and Yamada, M. (1984) Purification and initial characterization of a protein which facilitates assembly of nucleosome-like structure from mammalian cells. *Eur J Biochem*, **142**, 431-439.

Ishimi, Y. and Kikuchi, A. (1991) Identification and molecular cloning of yeast homolog of nucleosome assembly protein I which facilitates nucleosome assembly in vitro. *J Biol Chem*, **266**, 7025-7029.

Ishimi, Y., Kojima, M., Yamada, M. and Hanaoka, F. (1987) Binding mode of nucleosome-assembly protein (AP-I) and histones. *Eur J Biochem*, **162**, 19-24.

Ishimi, Y., Yasuda, H., Hirosumi, J., Hanaoka, F. and Yamada, M. (1983) A protein which facilitates assembly of nucleosome-like structures in vitro in mammalian cells. *J Biochem (Tokyo)*, **94**, 735-744.

Ito, T., Bulger, M., Kobayashi, R. and Kadonaga, J.T. (1996a) Drosophila NAP-1 is a core histone chaperone that functions in ATP-facilitated assembly of regularly spaced nucleosomal arrays. *Mol Cell Biol*, **16**, 3112-3124.

Ito, T., Bulger, M., Pazin, M.J., Kobayashi, R. and Kadonaga, J.T. (1997) ACF, an ISWI-containing and ATP-utilizing chromatin assembly and remodeling factor. *Cell*, **90**, 145-155.

Ito, T., Ikehara, T., Nakagawa, T., Kraus, W.L. and Muramatsu, M. (2000) p300-mediated acetylation facilitates the transfer of histone H2A-H2B dimers from nucleosomes to a histone chaperone. *Genes Dev*, **14**, 1899-1907.

Ito, T., Tyler, J.K., Bulger, M., Kobayashi, R. and Kadonaga, J.T. (1996b) ATP-facilitated chromatin assembly with a nucleoplasmin-like protein from Drosophila melanogaster. *J Biol Chem*, **271**, 25041-25048.

Jackson, V. (1990) In vivo studies on the dynamics of histone-DNA interaction: evidence for nucleosome dissolution during replication and transcription and a low level of dissolution independent of both. *Biochemistry*, **29**, 719-731.

Janicki, S.M., Tsukamoto, T., Salghetti, S.E., Tansey, W.P., Sachidanandam, R.,

Prasanth, K.V., Ried, T., Shav-Tal, Y., Bertrand, E., Singer, R.H. and Spector, D.L. (2004) From silencing to gene expression: real-time analysis in single cells. *Cell*, **116**, 683-698.

Janin, J. (1997) Specific versus non-specific contacts in protein crystals. *Nat Struct Biol*, **4**, 973-974.

Jason, L.J., Moore, S.C., Lewis, J.D., Lindsey, G. and Ausio, J. (2002) Histone ubiquitination: a tagging tail unfolds? *Bioessays*, **24**, 166-174.

Jones, T.A., Zou, J.Y., Cowan, S.W. and Kjelgaard, M. (1991) Improved methods for building protein models in electron density maps and the location of errors in these models. *Acta Cryst*, **A47**, 110-119.

Kawase, H., Okuwaki, M., Miyaji, M., Ohba, R., Handa, H., Ishimi, Y., Fujii-Nakata, T., Kikuchi, A. and Nagata, K. (1996) NAP-I is a functional homologue of TAF-I that is required for replication and transcription of the adenovirus genome in a chromatin-like structure. *Genes Cells*, **1**, 1045-1056.

Kellogg, D.R. and Murray, A.W. (1995) NAP1 acts with Clb1 to perform mitotic functions and to suppress polar bud growth in budding yeast. *J Cell Biol*, **130**, 675-685.

Khorasanizadeh, S. (2004) The nucleosome: from genomic organization to genomic regulation. *Cell*, **116**, 259-272.

Kimura, H. and Cook, P.R. (2001) Kinetics of core histones in living human cells: little exchange of H3 and H4 and some rapid exchange of H2B. *J Cell Biol*, **153**, 1341-1353.

Kireeva, M.L., Walter, W., Tchernajenko, V., Bondarenko, V., Kashlev, M. and Studitsky, V.M. (2002) Nucleosome Remodeling Induced by RNA Polymerase II. Loss of the H2A/H2B Dimer during Transcription. *Mol Cell*, **9**, 541-552.

Kirov, N., Shtilbans, A. and Rushlow, C. (1998) Isolation and characterization of a new gene encoding a member of the HIRA family of proteins from drosophila melanogaster. *Gene*, **212**, 323-332.

Kleinschmidt, J.A., Fortkamp, E., Krohne, G., Zentgraf, H. and Franke, W.W. (1985) Co-existence of two different types of soluble histone complexes in nuclei of Xenopus laevis oocytes. *J Biol Chem*, **260**, 1166-1176.

Kleinschmidt, J.A., Seiter, A. and Zentgraf, H. (1990) Nucleosome assembly in vitro: separate histone transfer and synergistic interaction of native histone complexes purified from nuclei of Xenopus laevis oocytes. *Embo J*, **9**, 1309-1318.

Kobor, M.S., Venkatasubrahmanyam, S., Meneghini, M.D., Gin, J.W., Jennings, J.L., Link, A.J., Madhani, H.D. and Rine, J. (2004) A Protein Complex Containing the Conserved Swi2/Snf2-Related ATPase Swr1p Deposits Histone Variant H2A.Z into Euchromatin. *PLoS Biol*, **2**, E131.

Korber, P. and Horz, W. (2004) SWRred not shaken; mixing the histones. *Cell*, **117**, 5-7.

Kornberg, R.D. and Lorch, Y. (1991) Irresistible force meets immovable object: transcription and the nucleosome. *Cell*, **67**, 833-836.

Krogan, N.J., Keogh, M.C., Datta, N., Sawa, C., Ryan, O.W., Ding, H., Haw, R.A., Pootoolal, J., Tong, A., Canadien, V., Richards, D.P., Wu, X., Emili, A., Hughes, T.R., Buratowski, S. and Greenblatt, J.F. (2003) A Snf2 family ATPase complex required for recruitment of the histone H2A variant Htz1. *Mol Cell*, **12**, 1565-1576.

Krude, T. (1999) Chromatin assembly during DNA replication in somatic cells. *Eur J Biochem*, **263**, 1-5.

Krude, T. and Keller, C. (2001) Chromatin assembly during S phase: contributions from histone deposition, DNA replication and the cell division cycle. *Cell Mol Life Sci*, **58**, 665-672.

Langst, G. and Becker, P.B. (2001) Nucleosome mobilization and positioning by ISWI-containing chromatin- remodeling factors. *J Cell Sci*, **114**, 2561-2568.

Lankenau, S., Barnickel, T., Marhold, J., Lyko, F., Mechler, B.M. and Lankenau, D.H. (2003) Knockout targeting of the Drosophila nap1 gene and examination of DNA repair tracts in the recombination products. *Genetics*, **163**, 611-623.

Laskey, R.A., Honda, B.M., Mills, A.D. and Finch, J.T. (1978) Nucleosomes are assembled by an acidic protein which binds histones and transfers them to DNA. *Nature*, **275**, 416-420.

Laskey, R.A., Mills, A.D., Philpott, A., Leno, G.H., Dilworth, S.M. and Dingwall, C. (1993) The role of nucleoplasmin in chromatin assembly and disassembly. *Philos Trans R Soc Lond B Biol Sci*, **339**, 263-269.

Leach, T.J., Mazzeo, M., Chotkowski, H.L., Madigan, J.P., Wotring, M.G. and Glaser, R.L. (2000) Histone H2A.Z is widely but nonrandomly distributed in chromosomes of Drosophila melanogaster. *J Biol Chem*, **275**, 23267-23272.

Lee, B. and Richards, F.M. (1971) The interpretation of protein structures: estimation of static accessibility. *J Mol Biol*, **55**, 379-400.

Lee, K.P., Baxter, H.J., Guillemette, J.G., Lawford, H.G. and Lewis, P.N. (1982) Structural studies on yeast nucleosomes. *Can J Biochem*, **60**, 379-388.

Lemmon, M.A., Treutlein, H.R., Adams, P.D., Brunger, A.T. and Engelman, D.M. (1994) A dimerization motif for transmembrane alpha-helices. *Nat Struct Biol*, **1**, 157-163.

Levchenko, V. and Jackson, V. (2004) Histone release during transcription: NAP1 forms a complex with H2A and H2B and facilitates a topologically dependent release of H3 and H4 from the nucleosome. *Biochemistry*, **43**, 2359-2372.

Li, M., Strand, D., Krehan, A., Pyerin, W., Heid, H., Neumann, B. and Mechler, B.M. (1999) Casein kinase 2 binds and phosphorylates the nucleosome assembly protein-1 (NAP1) in Drosophila melanogaster. *J Mol Biol*, **293**, 1067-1084.

Lin, R.C. and Scheller, R.H. (1997) Structural organization of the synaptic exocytosis core complex. *Neuron*, **19**, 1087-1094.

Lorain, S., Demczuk, S., Lamour, V., Toth, S., Aurias, A., Roe, B.A. and Lipinski, M. (1996) Structural Organization of the WD repeat protein-encoding gene HIRA in the DiGeorge syndrome critical region of human chromosome 22. *Genome Res*, **6**, 43-50.

Louters, L. and Chalkley, R. (1984) In vitro exchange of nucleosomal histones H2a and H2b. *Biochemistry*, **23**, 547-552.

Louters, L. and Chalkley, R. (1985) Exchange of histones H1, H2A, and H2B in vivo. *Biochemistry*, **24**, 3080-3085.

Loyola, A. and Almouzni, G. (2004) Histone chaperones, a supporting role in the limelight. *Biochim Biophys Acta*, **1677**, 3-11.

Luger, K., Maeder, A.W., Richmond, R.K., Sargent, D.F. and Richmond, T.J. (1997a) Crystal structure of the nucleosome core particle at 2.8 Å resolution. *Nature*, **389**, 251-259.

Luger, K., Rechsteiner, T.J., Flaus, A.J., Waye, M.M. and Richmond, T.J. (1997b) Characterization of nucleosome core particles containing histone proteins made in bacteria. *J Mol Biol*, **272**, 301-311.

Luger, K., Rechsteiner, T.J. and Richmond, T.J. (1999) Preparation of nucleosome core particle from recombinant histones. *Methods Enzymol*, **304**, 3-19.

Luger, K. and Richmond, T.J. (1998a) DNA binding within the nucleosome core. *Current Opinion in Structural Biology*, **8**, 33-40.

Luger, K. and Richmond, T.J. (1998b) The histone tails of the nucleosome. *Curr Opin Genet Dev*, **8**, 140-146.

Madigan, J.P., Chotkowski, H.L. and Glaser, R.L. (2002) DNA double-strand break-induced phosphorylation of Drosophila histone variant H2Av helps prevent radiation-induced apoptosis. *Nucleic Acids Res*, **30**, 3698-3705.

Maity, S.N. and de Crombrugghe, B. (1998) Role of the CCAAT-binding protein CBF/NF-Y in transcription. *Trends Biochem Sci*, **23**, 174-178.

Malik, H.S. and Henikoff, S. (2003) Phylogenomics of the nucleosome. *Nat Struct Biol*, **10**, 882-891.

Marheineke, K. and Krude, T. (1998) Nucleosome Assembly Activity and Intracellular Localization of Human CAF-1 Changes during the Cell Division Cycle. *J Biol Chem*, **273**, 15279-15286.

Martinez-Balbas, M.A., Tsukiyama, T., Gdula, D. and Wu, C. (1998) Drosophila NURF-55, a WD repeat protein involved in histone metabolism. *Proc Natl Acad Sci U S A*, **95**, 132-137.

Martínez-Balbás, M.A., Tsukiyama, T., Gdula, D. and Wu, C. (1998) Drosophila NURF-55, a WD repeat protein involved in histone metabolism. *PNAS*, **95**, 132-137.

McBryant, S.J., Park, Y.J., Abernathy, S.M., Laybourn, P.J., Nyborg, J.K. and Luger, K. (2003) Preferential binding of the histone (H3-H4)2 tetramer by NAP1 is mediated by the amino-terminal histone tails. *J Biol Chem*, **278**, 44574-44583.

McBryant, S.J. and Peersen, O.B. (2004a) Self-Association of the Yeast Nucleosome Assembly Protein 1. *Biochemistry*, **In Press**.

McBryant, S.J. and Peersen, O.B. (2004b) Self-association of the yeast nucleosome assembly protein 1. *Biochemistry*, **43**, 10592-10599.

McQuibban, G.A., Commisso-Cappelli, C.N. and Lewis, P.N. (1998) Assembly, Remodeling, and Histone Binding Capabilities of Yeast Nucleosome Assembly Protein 1. *Biol Chem*, **273**, 6582-6590.

Meneghini, M.D., Wu, M. and Madhani, H.D. (2003) Conserved histone variant H2A.Z protects euchromatin from the ectopic spread of silent heterochromatin. *Cell*, **112**, 725-736.

Miyaji-Yamaguchi, M., Kato, K., Nakano, R., Akashi, T., Kikuchi, A. and Nagata, K. (2003) Involvement of nucleocytoplasmic shuttling of yeast Nap1 in mitotic progression. *Mol Cell Biol*, **23**, 6672-6684.

Mizuguchi, G., Shen, X., Landry, J., Wu, W.H., Sen, S. and Wu, C. (2004) ATP-driven exchange of histone H2AZ variant catalyzed by SWR1 chromatin remodeling complex. *Science*, **303**, 343-348.

Moore, S.C., Jason, L. and Ausio, J. (2002) The elusive structural role of ubiquitinated histones. *Biochem Cell Biol*, **80**, 311-319.

Mosammaparast, N., Ewart, C.S. and Pemberton, L.F. (2002) A role for nucleosome assembly protein 1 in the nuclear transport of histones H2A and H2B. *Embo J*, **21**, 6527-6538.

Mosammaparast, N., Jackson, K.R., Guo, Y., Brame, C.J., Shabanowitz, J., Hunt, D.F. and Pemberton, L.F. (2001) Nuclear import of histone H2A and H2B is mediated by a network of karyopherins. *J Cell Biol*, **153**, 251-262.

Mueller, R.D., Yasuda, H., Hatch, C.L., Bonner, W.M. and Bradbury, E.M. (1985) Identification of ubiquitinated histones 2A and 2B in Physarum polycephalum. Disappearance of these proteins at metaphase and reappearance at anaphase. *J Biol Chem*, **260**, 5147-5153.

Muhlhausser, P., Muller, E.C., Otto, A. and Kutay, U. (2001) Multiple pathways contribute to nuclear import of core histones. *EMBO Rep*, **2**, 690-696.

Muthurajan, U.M., Park, Y.J., Edayathumangalam, R.S., Suto, R.K., Chakravarthy, S., Dyer, P.N. and Luger, K. (2003) Structure and dynamics of nucleosomal DNA. *Biopolymers*, **68**, 547-556.

Nacheva, G.A., Guschin, D.Y., Preobrazhenskaya, O.V., Karpov, V.L., Ebralidse, K.K. and Mirzabekov, A.D. (1989) Change in the pattern of histone binding to DNA upon transcriptional activation. *Cell*, **58**, 27-36.

Nakagawa, T., Bulger, M., Muramatsu, M. and Ito, T. (2001) Multistep chromatin assembly on supercoiled plasmid DNA by nucleosome assembly protein-1 and ATP-utilizing chromatin assembly and remodeling factor. *J Biol Chem*, **276**, 27384-27391.

Neer, E.J., Schmidt, C.J., Nambudripad, R. and Smith, T.F. (1994) The ancient regulatory-protein family of WD-repeat proteins. *Nature*, **371**, 297-300.

Ohkuni, K., Shirahige, K. and Kikuchi, A. (2003) Genome-wide expression analysis of NAP1 in Saccharomyces cerevisiae. *Biochem Biophys Res Commun*, **306**, 5-9.

Olsen, J.G., Flensburg, C., Olsen, O., Bricogne, G. and Henriksen, A. (2004) Solving the structure of the bubble protein using the anomalous sulfur signal from single-crystal in-house Cu Kalpha diffraction data only. *Acta Crystallogr D Biol Crystallogr*, **60**, 250-255.

Oohara, I. and Wada, A. (1987a) Spectroscopic studies on histone-DNA interactions. I. The interaction of histone (H2A, H2B) dimer with DNA: DNA sequence dependence. *J Mol Biol*, **196**, 389-397.

Oohara, I. and Wada, A. (1987b) Spectroscopic studies on histone-DNA interactions. II. Three transitions in nucleosomes resolved by salt-titration. *J Mol Biol*, **196**, 399-411.

Otwinowski, Z. and Minor, W. (1997) *Processing of X-ray diffraction data collected in oscillation mode*. Academic Press, New York.

Park, Y.J., Chodaparambil, J.V., Bao, Y., McBryant, S.J. and Luger, K. (2004a) Nucleosome assembly protein 1 exchanges histone H2A-H2B dimers and assists nucleosome sliding. *J Biol Chem*.

Park, Y.J., Dyer, P.N., Tremethick, D.J. and Luger, K. (2004b) A New Fluorescence Resonance Energy Transfer Approach Demonstrates That the Histone Variant H2AZ Stabilizes the Histone Octamer within the Nucleosome. *J Biol Chem*, **279**, 24274-24282.

Paull, T.T., Rogakou, E.P., Yamazaki, V., Kirchgessner, C.U., Gellert, M. and Bonner, W.M. (2000) A critical role for histone H2AX in recruitment of repair factors to nuclear foci after DNA damage. *Curr Biol*, **10**, 886-895.

Pehrson, J.R. and Fried, V.A. (1992) MacroH2A, a core histone containing a large nonhistone region. *Science*, **257**, 1398-1400.

Peterson, C.L. (2002) Chromatin remodeling enzymes: taming the machines. Third in review series on chromatin dynamics. *EMBO Rep*, **3**, 319-322.

Phillips, J.D., Whitby, F.G., Warby, C.A., Labbe, P., Yang, C., Pflugrath, J.W., Ferrara, J.D., Robinson, H., Kushner, J.P. and Hill, C.P. (2004) Crystal structure of the oxygen-dependant coproporphyrinogen oxidase (Hem13p) of Saccharomyces cerevisiae. *J Biol Chem*, **279**, 38960-38968.

Polach, K.J. and Widom, J. (1995) Mechanism of protein access to specific DNA sequences in chromatin: a dynamic equilibrium model for gene regulation. *J Mol Biol*, **254**, 130-149.

Polach, K.J. and Widom, J. (1996) A model for the cooperative binding of eukaryotic regulatory proteins to nucleosomal target sites. *J Mol Biol*, **258**, 800-812.

Puhl, H.L. and Behe, M.J. (1993) Structure of nucleosomal DNA at high salt concentration as probed by hydroxyl radical. *J Mol Biol*, **229**, 827-832.

Quintini, G., Treuner, K., Gruss, C. and Knippers, R. (1996) Role of amino-terminal histone domains in chromatin replication. *Mol Cell Biol*, **16**, 2888-

2897.

Rangasamy, D., Berven, L., Ridgway, P. and Tremethick, D.J. (2003) Pericentric heterochromatin becomes enriched with H2A.Z during early mammalian development. *Embo J*, **22**, 1599-1607.

Rasmussen, S.R., Larsen, M.R. and Rasmussen, S.E. (1991) Covalent immobilization of DNA onto polystyrene microwells: the molecules are only bound at the 5' end. *Anal Biochem*, **198**, 138-142.

Redon, C., Pilch, D., Rogakou, E., Sedelnikova, O., Newrock, K. and Bonner, W. (2002) Histone H2A variants H2AX and H2AZ. *Curr Opin Genet Dev*, **12**, 162-169.

Regnard, C., Desbruyeres, E., Huet, J.C., Beauvallet, C., Pernollet, J.C. and Edde, B. (2000) Polyglutamylation of nucleosome assembly proteins. *J Biol Chem*, **275**, 15969-15976.

Regnard, C., Fesquet, D., Janke, C., Boucher, D., Desbruyeres, E., Koulakoff, A., Insina, C., Travo, P. and Edde, B. (2003) Characterisation of PGs1, a subunit of a protein complex co-purifying with tubulin polyglutamylase. *J Cell Sci*, **116**, 4181-4190.

Rehtanz, M., Schmidt, H.M., Warthorst, U. and Steger, G. (2004) Direct interaction between nucleosome assembly protein 1 and the papillomavirus E2 proteins involved in activation of transcription. *Mol Cell Biol*, **24**, 2153-2168.

Reinke, H. and Horz, W. (2003) Histones are first hyperacetylated and then lose contact with the activated PHO5 promoter. *Mol Cell*, **11**, 1599-1607.

Rhoades, A.R., Ruone, S. and Formosa, T. (2004) Structural features of nucleosomes reorganized by yeast FACT and its HMG box component, Nhp6. *Mol Cell Biol.*, **24**, 3907-3917.

Richmond, T.J., Searles, M.A. and Simpson, R.T. (1988) Crystals of a nucleosome core particle containing defined sequence DNA. *J Mol Biol*, **199**, 161-170.

Robzyk, K., Recht, J. and Osley, M.A. (2000) Rad6-dependent ubiquitination of histone H2B in yeast. *Science*, **287**, 501-504.

Rodriguez, P., Munroe, D., Prawitt, D., Chu, L.L., Bric, E., Kim, J., Reid, L.H., Davies, C., Nakagama, H., Loebbert, R., Winterpacht, A., Petruzzi, M.J., Higgins, M.J., Nowak, N., Evans, G., Shows, T., Weissman, B.E., Zabel, B., Housman, D.E. and Pelletier, J. (1997) Functional characterization of human nucleosome assembly protein-2 (NAP1L4) suggests a role as a histone chaperone. *Genomics*, **44**, 253-265.

Rodriguez, P., Pelletier, J., Price, G.B. and Zannis-Hadjopoulos, M. (2000) NAP-2: histone chaperone function and phosphorylation state through the cell cycle. *J Mol Biol*, **298**, 225-238.

Rundlett, S.E., Carmen, A.A., Suka, N., Turner, B.M. and Grunstein, M. (1998) Transcriptional repression by UME6 involves deacetylation of lysine 5 of histone H4 by RPD3. *Nature*, **392**, 831-835.

Russ, W.P. and Engelman, D.M. (2000) The GxxxG motif: a framework for transmembrane helix-helix association. *J Mol Biol*, **296**, 911-919.

Samso, M. and Daban, J.R. (1993) Unfolded structure and reactivity of nucleosome core DNA-histone H2A,H2B complexes in solution as studied by synchrotron radiation X-ray scattering. *Biochemistry*, **32**, 4609-4614.

Santisteban, M.S., Kalashnikova, T. and Smith, M.M. (2000) Histone H2A.Z regulats transcription and is partially redundant with nucleosome remodeling complexes. *Cell*, **103**, 411-422.

Scamps, C., Lorain, S., Lamour, V. and Lipinski, M. (1996) The HIR protein family: isolation and characterization of a complete murine cDNA. *Biochim Biophys Acta*, **1306**, 5-8.

Schmidt-Zachmann, M.S., Hugle-Dorr, B. and Franke, W.W. (1987) A constitutive nucleolar protein identified as a member of the nucleoplasmin family. *Embo J*, **6**, 1881-1890.

Schuermann, J.P. and Tanner, J.J. (2003) MRSAD: using anomalous dispersion from S atoms collected at Cu Kalpha wavelength in molecular-replacement structure determination. *Acta Crystallogr D Biol Crystallogr*, **59**, 1731-1736.

Schumacher, M.A., Goodman, R.H. and Brennan, R.G. (2000) The structure of a CREB bZIPmiddle dotSomatostatin CRE complex reveals the basis for selective dimerization and divalent cation-enhanced DNA binding [In Process Citation]. *J Biol Chem*, **275**, 35242-35247.

Schwede, T., Kopp, J., Guex, N. and Peitsch, M.C. (2003) SWISS-MODEL: An automated protein homology-modeling server. *Nucleic Acids Res*, **31**, 3381-3385.

Shen, H.H., Huang, A.M., Hoheisel, J. and Tsai, S.F. (2001) Identification and characterization of a SET/NAP protein encoded by a brain-specific gene, MB20. *Genomics*, **71**, 21-33.

Shibahara, K. and Stillman, B. (1999) Replication-dependent marking of DNA by PCNA facilitates CAF-1-coupled inheritance of chromatin. *Cell*, **96**, 575-585.

Shibahara, K., Verreault, A. and Stillman, B. (2000) The N-terminal domains of histones H3 and H4 are not necessary for chromatin assembly factor-1-mediated nucleosome assembly onto replicated DNA in vitro. *Proc Natl Acad Sci U S A*, **97**, 7766-7771.

Shikama, N., Chan, H.M., Krstic-Demonacos, M., Smith, L., Lee, C.W., Cairns, W. and La Thangue, N.B. (2000) Functional interaction between nucleosome assembly proteins and p300/CREB-binding protein family coactivators. *Mol Cell Biol*, **20**, 8933-8943.

Shimizu, Y., Akashi, T., Okuda, A., Kikuchi, A. and Fukui, K. (2000) NBP1 (Nap1 binding protein 1), an essential gene for G2/M transition of Saccharomyces cerevisiae, encodes a protein of distinct sub-nuclear localization. *Gene*, **246**, 395-404.

Simpson, R.T. and Stafford, D.W. (1983) Structural features of a phased nucleosome core particle. *Proc Natl Acad Sci U S A*, **80**, 51-55.

Simpson, R.T., Thoma, F. and Brubaker, J.M. (1985) Chromatin reconstituted from tandemly repeated cloned DNA fragments and core histones: a model system for study of higher order structure. *Cell*, **42**, 799-808.

Sobel, R.E., Cook, R.G., Perry, C.A., Annunziato, A.T. and Allis, C.D. (1995) Conservation of deposition-related acetylation sites in newly synthesized histones H3 and H4. *Proc Natl Acad Sci U S A*, **92**, 1237-1241.

Spinelli, S., Ramoni, R., Grolli, S., Bonicel, J., Cambillau, C. and Tegoni, M. (1998) The structure of the monomeric porcine odorant binding protein sheds light on the domain swapping mechanism. *Biochemistry*, **37**, 7913-7918.

Steer, W.M., Abu-Daya, A., Brickwood, S.J., Mumford, K.L., Jordanaires, N., Mitchell, J., Robinson, C., Thorne, A.W. and Guille, M.J. (2003) Xenopus nucleosome assembly protein becomes tissue-restricted during development and can alter the expression of specific genes. *Mech Dev*, **120**, 1045-1057.

Sullivan, S., Sink, D.W., Trout, K.L., Makalowska, I., Taylor, P.M., Baxevanis, A.D. and Landsman, D. (2002) The Histone Database. *Nucleic Acids Res*, **30**, 341-342.

Suto, R.K., Clarkson, M.J., Tremethick, D.J. and Luger, K. (2000) Crystal structure of a nucleosome core particle containing the variant histone H2A.Z. *Nat Struct Biol*, **7**, 1121-1124.

Suto, R.K., Edayathumangalam, R.S., White, C.L., Melander, C., Gottesfeld, J.M., Dervan, P.B. and Luger, K. (2003) Crystal Structures of Nucleosome Core Particles in Complex with Minor Groove DNA-binding Ligands. *J Mol*

Biol, **326**, 371-380.

Takeda, S., Yamashita, A., Maeda, K. and Maeda, Y. (2003) Structure of the core domain of human cardiac troponin in the Ca(2+)-saturated form. *Nature*, **424**, 35-41.

Terwilliger, T. (2004) SOLVE and RESOLVE: automated structure solution, density modification and model building. *J Synchrotron Radiat*, **11**, 49-52.

Thomson, J.A., Shirley, B.A., Grimsley, G.R. and Pace, C.N. (1989) Conformational stability and mechanism of folding of ribonuclease T1. *J Biol Chem*, **264**, 11614-11620.

Tong, A.H., Lesage, G., Bader, G.D., Ding, H., Xu, H., Xin, X., Young, J., Berriz, G.F., Brost, R.L., Chang, M., Chen, Y., Cheng, X., Chua, G., Friesen, H., Goldberg, D.S., Haynes, J., Humphries, C., He, G., Hussein, S., Ke, L., Krogan, N., Li, Z., Levinson, J.N., Lu, H., Menard, P., Munyana, C., Parsons, A.B., Ryan, O., Tonikian, R., Roberts, T., Sdicu, A.M., Shapiro, J., Sheikh, B., Suter, B., Wong, S.L., Zhang, L.V., Zhu, H., Burd, C.G., Munro, S., Sander, C., Rine, J., Greenblatt, J., Peter, M., Bretscher, A., Bell, G., Roth, F.P., Brown, G.W., Andrews, B., Bussey, H. and Boone, C. (2004) Global mapping of the yeast genetic interaction network. *Science*, **303**, 808-813.

Tse, C., Sera, T., Wolffe, A.P. and Hansen, J.C. (1998) Disruption of higher-order folding by core histone acetylation dramatically enhances transcription of nucleosomal arrays by RNA polymerase III. *Mol Cell Biol*, **18**, 4629-4638.

Tyler, J.K. (2002) Chromatin assembly. *Eur J Biochem*, **269**, 2268-2274.

Tyler, J.K., Adams, C.R., Chen, S.R., Kobayashi, R., Kamakaka, R.T. and Kadonaga, J.T. (1999) The RCAF complex mediates chromatin assembly during DNA replication and repair. *Nature*, **402**, 555-560.

Tyler, J.K., Bulger, M., Kamakaka, R.T., Kobayashi, R. and Kadonaga, J.T. (1996) The p55 subunit of Drosophila chromatin assembly factor 1 is homologous to a histone deacetylase-associated protein. *Mol Cell Biol*, **16**, 6149-6159.

Tyler, J.K., Collins, K.A., Prasad-Sinha, J., Amiott, E., Bulger, M., Harte, P.J., Kobayashi, R. and Kadonaga, J.T. (2001) Interaction between the Drosophila CAF-1 and ASF1 chromatin assembly factors. *Mol Cell Biol*, **21**, 6574-6584.

Umehara, T., Chimura, T., Ichikawa, N. and Horikoshi, M. (2002) Polyanionic stretch-deleted histone chaperone cia1/Asf1p is functional both in vivo and in vitro. *Genes Cells*, **7**, 59-73.

Umehara, T. and Horikoshi, M. (2003) Transcription initiation factor IID-interactive histone chaperone CIA-II implicated in mammalian spermatogenesis. *J Biol Chem*, **278**, 35660-35667.

Van Holde, K.E. (1988) *Chromatin*. Springer-Verlag, New York.

Van Hooser, A., Goodrich, D.W., Allis, C.D., Brinkley, B.R. and Mancini, M.A. (1998) Histone H3 phosphorylation is required for the initiation, but not maintenance, of mammalian chromosome condensation. *J Cell Sci*, **111 (Pt 23)**, 3497-3506.

Verreault, A., Kaufman, P.D., Kobayashi, R. and Stillman, B. (1996) Nucleosome assembly by a complex of CAF-1 and acetylated histones H3/H4. *Cell*, **87**, 95-104.

Verreault, A., Kaufman, P. D., Kobayashi, R., and Stillman, B. (1998) Nucleosomal DNA regulates the core-histone-binding subunit of the human hat1 acetyltransferase. *Curr. Biol.*, **15**, 96-108.

Walter, P.P., Owen-Hughes, T.A., Cote, J. and Workman, J.L. (1995) Stimulation of transcription factor binding and histone displacement by nucleosome assembly protein 1 and nucleoplasmin requires disruption of the histone octamer. *Mol Cell Biol*, **15**, 6178-6187.

Wei, Y., Mizzen, C.A., Cook, R.G., Gorovsky, M.A. and Allis, C.D. (1998) Phosphorylation of histone H3 at serine 10 is correlated with chromosome condensation during mitosis and meiosis in Tetrahymena. *Proc Natl Acad Sci U S A*, **95**, 7480-7484.

White, C.L., Suto, R.K. and Luger, K. (2001) Structure of the yeast nucleosome core particle reveals fundamental changes in internucleosome interactions. *Embo J*, **20**, 5207-5218.

Whitehouse, I., Flaus, A., Cairns, B.R., White, M.F., Workman, J.L. and Owen-Hughes, T. (1999) Nucleosome mobilization catalysed by the yeast SWI/SNF complex [In Process Citation]. *Nature*, **400**, 784-787.

Wilhelm, M.L. and Wilhelm, F.X. (1980) Conformation of nucleosome core particles and chromatin in high salt concentration. *Biochemistry*, **19**, 4327-4331.

Woodcock, C.L. and Dimitrov, S. (2001) Higher-order structure of chromatin and chromosomes. *Curr Opin Genet Dev*, **11**, 130-135.

Workman, J.L. and Kingston, R.E. (1998) Alteration of nucleosome structure as a mechanism of transcriptional regulation. *Annu Rev Biochem*, **67**, 545-579.

Wu, P. and Brand, L. (1994) Resonance energy transfer: methods and

applications. *Anal Biochem*, **218**, 1-13.

Xie, X., Kokubo, T., Cohen, S.L., Mirza, U.A., Hoffmann, A., Chait, B.T., Roeder, R.G., Nakatani, Y. and Burley, S.K. (1996) Structural similarity between TAFs and the heterotetrameric core of the histone octamer [see comments]. *Nature*, **380**, 316-322.

Xu, D., Tsai, C.J. and Nussinov, R. (1998) Mechanism and evolution of protein dimerization. *Protein Sci*, **7**, 533-544.

Yager, T.D., McMurray, C.T. and van Holde, K.E. (1989) Salt-induced release of DNA from nucleosome core particles. *Biochemistry*, **28**, 2271-2281.

Yang, C., Pflugrath, J.W., Courville, D.A., Stence, C.N. and Ferrara, J.D. (2003) Away from the edge: SAD phasing from the sulfur anomalous signal measured in-house with chromium radiation. *Acta Crystallogr D Biol Crystallogr*, **59**, 1943-1957.